Random Medium Access Decision-Based Cooperative Spectrum Sensing for Cognitive Radio Vehicular Ad-hoc Networks

by

Ahmed Mohamed Abdelsalam Ahmed

A thesis submitted in partial fulfillment of the requirements for the Ph.D. degree in Electrical and Computer Engineering

School of Electrical Engineering and Computer Science
Faculty of Engineering
University of Ottawa

Abstract

In this thesis, the performance of decision-based Cooperative Spectrum Sensing (CSS) using random medium access sequential reporting assuming an imperfect reporting channel shared with a primary user is studied. Random medium access reporting using unacknowledged transmissions is the case of vehicular networks using IEEE 802.11p. This entails, as opposed to scheduled medium access, a non-negligible probability of collision and a variable reporting phase duration. Sequential reporting can reduce the reporting phase duration by employing different early termination schemes where the Fusion Centre (FC) terminates the reporting process once it receives enough evidence about the primary user status. A reduced reporting phase duration for a given detection accuracy performance enhances the overall network throughput. A centralized CSS scheme, where energy detection is employed at the secondary users, and hard-decision fusion is employed at the FC, is considered in this thesis. The objective is then to derive closed-form expressions for the overall probabilities of detection and false alarm at the FC as well as the average reporting phase duration. Analysis is performed first for the simple OR decision fusion rule, at the FC, and then generalized to the K-out-of-M decision fusion rule. Two early termination schemes are investigated for sequential reporting and then a heuristic energy-based reporting priority scheme is proposed. The proposed energy-based reporting scheme gives higher priority to secondary users more capable of detecting the primary user to access the common reporting channel. The proposed reporting scheme is compared to a base or control scheme where all secondary users have the same reporting priority.

Acknowledgements

Firstly, I would like to express my sincere gratitude to my advisor Prof. Hussein T. Mouftah for his continuous support, motivation, and immense knowledge through my PhD. studies. His practical guidance and valuable contributions were crucial in all the time of research and writing of my thesis. My deepest appreciations also go to Dr. Ala Abu Alkheir for his continuous support, mentoring, and insightful technical discussions that were a great help for me to continue this thesis. I thank my colleagues in our research group for stimulating discussions, encouragements, and a great fun throughout the years that we spent together in the lab.

Last but not the least, I wish to thank my family, especially my mother, my brother, my wife and kids for their tremendous support, encouragement and love that inspired me throughout writing this thesis and in my life in general.

Dedication

To the loving memory of my late father Mohamed Abd El-Salam Ahmed, my mother Mervat Badie, my brother Mohamed, my wife Samar, and my children Maryam, Aisha, and Mohamed.

Table of Contents

List of Figures

List of Symbols

$c_{\max}$	Maximum window size for random medium access
$d_{i,j}$	Distance between nodes i and j
d_k	Local binary decision for SU R_k
$\hat{d}_k$	Decoded version of d_k at the FC
E_p	Transmit energy of the PU
E_k	Transmit energy of SU R_k
ET_i	Early termination rule i
$\mathcal{H}_0$	Hypotheses PU is idle
$\mathcal{H}_1$	Hypotheses PU is active
P_{fa}	Local probability of false alarm
$P_{d,k}$	Local probability of detection for SU R_k
$P_{e,k\|\mathcal{H}_j}$	Decoding error probability for SU's k report given $\mathcal{H}_j$ is true
Q	The spectral efficiency
Q_d	Overall probability of detection at the FC
Q_{fa}	Overall probability of false alarm at the FC
R_0	Fusion Center (FC)
R_k	Secondary User (SU) k
t_s	Sensing period in seconds
u	Number of sensing samples divided by 2
W	Channel bandwidth in Hz
γ_{th}	Outage threshold at SUs
$\overline{\gamma}_{i,j}$	Average received SNR over channel between nodes i and j

$\Gamma(\cdot)$	Gamma function
$\Gamma(\cdot, \cdot)$	Upper incomplete Gamma function
Θ_n	Decision metric at the FC after the n^{th} time-slot
Θ_{th}	Decision threshold at the FC
λ	Energy detection local decision threshold
ν	Path loss exponent
ρ_p	Transmit Signal to Noise Ratio (SNR) of Primary User (PU)
ρ_k	Transmit SNR of SU R_k
σ^2	Variance of the Additive White Gaussian Noise (AWGN)
ϕ_k	Local energy estimate for SU R_k
ψ_k	Received SNR ($\mathcal{H}_0$) or SINR ($\mathcal{H}_1$)
$\Omega_{i,j}$	Average channel gain between nodes i and j

List of Abbreviations

ACSS	Asynchronous Cooperative Spectrum Sensing
AGM	Arithmetic-to-Geometric Mean
APs	Access Points
BPSK	Binary Phase Shift Keying
BSS	Basic Service Set
CAF	Cyclic Autocorrelation Function
CCC	Common Control Channel
CCH	Control CHannel
CDF	Cumulative Distribution Function
CFF	Collusive False Feedback attack
CP	Collision Penalty
CR	Cognitive Radio
CR-MAC	Cognitive Radio Medium ACcess
CRN	Cognitive Radio Network
CR-VANET or CRV	Cognitive Radio Vehicular Ad hoc NETwork
CSD	Cyclo-Stationary Detection
CSS	Cooperative Spectrum Sensing
CTS	Clear to Send
DCF	Distributed Coordination Function
DoS	Denial of Service
DP	Dirichlet Process
DSRC	Dedicated Short Range Communications
ED	Energy detection

EGC	Equal Gain Combining
EI	Energy Information
ET	Early Termination
EVD	EigenValue-based Detection
FC	Fusion Centre
FCC	Federal Communication Commission
GPS	Global Positioning Systems
HCSS-STC	Hybrid Cooperative Spectrum Sensing based on Spatial Temporal Correlation
HDF	Hard-Decision-Fusion
HMM	Hidden Markov Model
HOSD	Higher-Order Statistics Detection
HSU	Honest Secondary User
ICT	Information and Communication Technologies
IoT	Internet of Things
ISSDF	Insistent Spectrum Sensing Data Falsification attack
ITS	Intelligent Transportation Systems
LE	Largest Eigenvalue
LRMR-RCSS	Low-Rank Matrix Recovery Robust Cooperative Spectrum Sensing
MC	Matrix Completion
MFD	Matched Filter Detection
MLR	Maximum Likelihood Ratio
MMD	Maximum Mean Discrepancy
MME	Maximum-Minimum Eigenvalue
MSU	Malicious Secondary User
OAS	Oracle-Approximating Shrinkage estimator
OFDM	Orthogonal Frequency Division Multiplexing
OHF	Over Head Free Protocol
OMP	Orthogonal Matching Pursuit

PDF	Probability Density Function
PMF	Probability Mass Function
PUE	Primary User Emulation attack
PU	Primary User
REM	Radio Environment Map
ROC	Receiver Operation Characteristics
RSSI	Received Signal Strength Indicator
RSU	Road Side Unit
RTS	Request To Send
RV	Reputation Value
SADB	Spectrum Availability Database
SAE	Spectrum Availability Entries
SDF	Soft-Decision-Fusion
SDR	Software Defined Radio
SINR	Signal to Interference plus Noise Ratio
SNR	Signal-to-Noise-Ratio
SOP	Spectrum OPportunities
SP-CAF	Symmetry Property of the Cyclic Autocorrelation Function
SPRT	Sequential Probability Ratio Test
S-RTS	Sensing data and Request To Send
SSDF	Spectrum Sensing Data Falsification attack
SSP	Spectrum Sensing Provider
SU	Secondary User
TDMA	Time Division Medium Access
TVWS	TeleVision White Space
VSU	Vehicular Secondary User
VANET	Vehicular Ad hoc NETwork
WAVE	Wireless Access in a Vehicular Environment
WGC	Weighted Gain Combining

WLRMR-RCSS	Weighted Low-Rank Matrix Recovery Robust Cooperative Spectrum Sensing
WRANs	Wireless Regional Area Networks

Chapter 1

Introduction

Modern vehicles are increasingly getting equipped with Global Positioning System (GPS), navigation systems, a multitude of environmental awareness sensors, in addition to advanced multimedia systems. Research and deployment of Intelligent Transportation Systems (ITS) utilize vehicles as floating sensors and a primary source of traffic control measurements, and makes use of Information and Communication Technologies (ICT) to reduce road congestion costs, and to improve the safety, reliability, quality, and efficiency of the transportation system. The objective is to create an ICT-based transport environment that can exploit recent advances in communications and electronics to connect vehicles to both the transportation infrastructure and to other vehicles, which enables a number of new services and applications [Eze10].

Vehicular Ad hoc NETworks (VANETs) are one of the most promising, and challenging areas in ITS. A number of cooperative vehicular applications have already been implemented and evaluated in realistic urban environments with a view to improving drivers' safety and traffic monitoring (e.g., adaptive cruise control, enhanced driver awareness, collision avoidance, traffic control systems, network management, cooperative freight, fleet management, and cooperative traffic information and monitoring systems). Practical systems have been created by a Honda and Volkswagen-led consortium, the Car-2-Car Communication Consortium (C2C-CC). These systems and solutions are the result of massive investments made by several developed nations, such as the United States, Japan, South

Korea, Singapore, Hong Kong, and the European Union in the field of ITS. For example, in Europe, the European Commission's Directorate-General for Mobility and Transport is investing billions of Euros for the adoption of ICT-based solutions in the transport sector. The CVIS project , the COOPERS project (CO-OPerative SystEms for Intelligent Road Safety), Pre-DRIVE C2X project, and the European Field Operational Test on active safety systems (EuroFOT) are some of the most developed examples of such systems [SRB14, DFCB13].

A radio spectrum scarcity problem is looming on the horizon for ITSs for several reasons. First, the number of wireless-enabled vehicles is expected to increase considerably in the future. Second, vehicular communication applications are expected to grow in a number of areas, beside road safety, reliability, and transport efficiency, and include common entertainment applications (e.g., gaming and video) and information applications (e.g., driver assistance through real-time feeds on traffic, weather, and visual inputs from external cameras) [DFDMCB12]. Many of these applications need strict bandwidth and/or limited delay requirements to function properly. This high demand for spectrum is especially anticipated in urban environments, particularly during peak traffic hours. Third, federal agencies, in the United States for example, have been recently subjected to strong pressure from major industry players (e.g., Qualcomm, Cisco) to release a part of the 5.9 GHz band for more general usages such as WiFi. Hence, these bands could be jointly used by both ITSs and other applications. For these and other reasons there is a need; for adoption of novel techniques and approaches to address this looming spectrum scarcity problem in VANETs, and to allow for efficient use of radio spectrum resources.

Spectrum scarcity is a growing concern in telecommunications in general and not just VANETs. This situation has arisen due to the fixed spectrum allocation policy used by many governments that leads to over utilization of some frequency bands and sporadic use of other frequency bands (like the DTV bands). Cognitive Radio (CR) technology is a key solution to enable more efficient spectrum usage through the implementation of opportunistic spectrum sharing. Examples include IEEE 802.22 Wireless Regional Area Networks (WRANs) that uses CR on TV bands in rural areas, and the IEEE 802.16h

(Improved Coexistence Mechanisms for License-Exempt Operation) that is working on efficient resource allocation and interference management over shared spectrum bands. This motivated the interest in analyzing how the CR concept could be applied to the vehicular environment with the goal of increasing the available bandwidth to address this looming spectrum scarcity problem.

A Cognitive Radio Vehicular Ad hoc NETwork (CR-VANET or CRV) is composed of communicating vehicles and Road Side Units (RSUs) with reconfigurable Software Defined Radio (SDR) devices and intelligent CR functionalities, that enables network nodes to reconfigure all the aspects of radio control including the operating spectrum frequencies, and the transmitted power levels, among others. Consequently, vehicles will need to detect vacant spectrum with high reliability in order to use it as Secondary Users (SUs) and vacate it upon the return of Primary Users (PUs) for whom the spectrum is allocated. CR-VANETs; however, cannot be considered a mere application of the CR technology to VANETs, as they have some unique characteristics that must be accounted for and assumptions that can be exploited. For example, the spectrum management process is more involved as it becomes a function of vehicular mobility in addition to the activity of PUs' where a vehicle may experience several PUs along its trajectory. On the other hand, constrained and predictable, in nature, vehicular mobility can be exploited for better information about available spectrum. By example, vehicles can cooperate to inform other vehicles about Spectrum OPportunities (SOP) at future locations along their path [DFCB10a]. In the remainder of this chapter we discuss the motivation behind the thesis as set out in Section 1.1, followed by the research objectives and contributions noted in Sections 1.2, and 1.3 respectively. Finally, the thesis outline is given in Section 1.4.

1.1 Motivation

Quick and accurate detection of SOPs as well as returning PUs is crucial in a CR-VANET. However, the vehicular environment is characterized with high mobility and propagation obstructions (e.g., buildings and bridges) that cause several channel impairments such as shadowing, multipath fading, and Doppler shifts that reduce the accuracy of detecting PUs, that must be protected, and increase the probability of false alarms. Cooperative Spectrum Sensing (CSS), is a powerful means of enhancing the spectrum awareness of CR terminals by virtue of spatial diversity. CSS is well studied in the Cognitive Radio (CR) literature [YA09, ALB11]. Dispersed CR vehicles, say K terminals, each perform local spectrum sensing, and then share their sensing outcomes among each other or with a central Fusion Centre (FC) for the purpose of reaching a better decision about the status of the examined channel [BLZ09]. The duration of this collaborative endeavor is proportional to the sensing accuracy, but also causes a proportional loss in the network throughput. This tradeoff between sensing accuracy and throughput loss is referred to as sensing-throughput tradeoff [LZPH08].

The CSS process consists of three consecutive stages, local spectrum sensing, reporting, and decision (data) fusion. Most works on CSS assume scheduled reporting in a round-robin manner. This requires pre-allocation of time-slots to reporting CR terminals in a Time Division Medium Access (TDMA) fashion. In a vehicular network however, vehicles travel across adjacent cells and hence the pre-allocation or scheduling of reporting has to be repeated continuously. The result is therefore a significant increase in control traffic to prepare the vehicles' reporting schedule in each cell. Furthermore, in a vehicular network using IEEE 802.11p, terminals access the Common Control Channel (CCC) using random medium access which is more practical, lacks the need for tight vehicles' synchronization, and more suitable for the varying number of vehicles in a given cell.

The reporting stage is the least studied aspect of CSS. Therefore, we are interested in CSS based on random medium access using unacknowledged transmissions, (e.g., the case of vehicular networks using IEEE802.11p). In such networks, terminals use random back-offs to avoid collision with other terminals. Once a back-off counter expires, the corresponding terminal performs clear channel assessment. If the channel is found empty, the terminal transmits its decision, otherwise, it chooses another back-off counter and repeats the same process. It is important to analyze the impact of random medium access on the performance of CSS in CR-VANETs. That performance is reflected by the detection and false alarm probabilities as well as the average reporting time as a function of the medium access process. Such analysis also will be useful in devising random medium access schemes with lower average reporting time without sacrificing detection accuracy accounting for the sensing-throughput tradeoff discussed earlier.

1.2 Objectives

A cooperative spectrum sensing process consists of three consecutive stages, local spectrum sensing, reporting, and decision (data) fusion. In this thesis, we consider the problem of agile cooperative spectrum sensing in CR-VANETs. More specifically, we study the performance of several decision reporting strategies based on random medium access using unacknowledged transmissions, (e.g., the case of vehicular networks using IEEE802.11p). Terminals use random back-offs to avoid colliding with each other; hence, causing an additional delay. Our objective is to derive closed form expressions for the average reporting time in addition to the probabilities of detection and false alarm. Then verify these equations with intensive computer simulations. The final goal is to devise a sequential decision making version wherein the base station will be terminating the process once it receives sufficient evidence about the status of the channel. In doing so, a higher priority access category is assigned to CR terminals that are more capable in detecting the PU to access the reporting channel. This reduces the reporting phase duration without sacrificing the accuracy of detection, i.e. protecting the PU.

1.3 Contributions

The contributions of this thesis are as follows:

- Closed form expressions are derived for the detection and false alarm probabilities as well as the average reporting time as explicit functions of the contention window size. We assume the absence of a dedicated reporting channel, and hence, reports are transmitted over a shared channel resulting in non-negligible decoding errors.

- Two sequential reporting with early termination schemes are devised to reduce the reporting phase duration and hence increase network throughput.

- We introduced an Energy-based Heuristic Reporting Priority Scheme using both sequential decision reporting mechanisms. The Energy-based heuristic reporting priority scheme favours SUs more capable of detecting the PU in reporting to the FC. We compare energy-based sequential reporting scheme to a base or control scheme where all SUs have equal reporting priority.

1.4 Thesis Outline

This thesis is organized as follows. In Chapter 2, we present a literature review of CSS techniques devised for CR-VANETs. Chapter 3 introduces decision-based cooperative spectrum sensing using random medium access reporting, the simple OR decision fusion rule, and a fixed contention window. In Chapter 4, we generalize this analysis to the K-out-of-M decision rule, and investigate two sequential reporting schemes with the objective of reducing the decision reporting duration, and hence increase network throughput. In Chapter 5, we introduce an Energy-based Heuristic Reporting Priority Scheme which favours CR terminals more capable of detecting the PU in reporting to the FC. Conclusions and future work are discussed in Chapter 6.

Chapter 2

Cooperative Spectrum Sensing for Cognitive Radio Vehicular Ad Hoc Networks: State-of-the-Art

2.1 Introduction

Intelligent Transportation Systems (ITS) aim to improve transport safety, reduce road accidents, and offer infotainment services. In response, the US Federal Communication Commission (FCC) allocated 75 MHz of spectrum in the 5.9 GHz band (i.e., 5.85-5.925 GHz) to support vehicular communications. Cognitive Radio (CR)-assisted Vehicular Ad-hoc NETworks (CR-VANET) utilize Cognitive Radio (CR) technology to increase Spectrum OPportunities (SOPs) for vehicular communications when the allocated 75 MHz cannot meet the high spectrum demands due to the increasing number of connected vehicles foreseen in the future [SA18, EZLE18a]. It is predicted that 75% of vehicles will come with built-in Internet of Things (IoT) connectivity by 2020 where CR-VANETs represent one of the frameworks to build CR-based IoT systems [Gre16, AAAT19]. CR-VANETs are expected to play a significant role in the development and implementation of various smart city applications [GSMJ18]. For example, vehicles with CR capability are sought-of to support delay-tolerant data transportation, necessary for various smart city applications, as opportunistic data carriers to transport data from its collection points to its places of consumption [YHM+17, MTC17, DZCF17, DLC+18].

Spectrum awareness is the cornerstone for the operation of a CR-VANET. Vehicles will need to identify Spectrum Opportunities (SOPs) quickly and accurately. Spectrum awareness can be achieved through sending queries to a spectrum databases and/or through spectrum sensing. Database queries by CR vehicles are expected to be more frequent due to high vehicle mobility and they will require Internet access. On the other hand, spectrum sensing lends more control to individual vehicles. However, in a vehicular environment mobility as well as surrounding infrastructure, like buildings and bridges, cause several channel impairments such as shadowing, multi-path fading, and Doppler shifts that significantly reduces PU detection accuracy and increases the probability of a false alarm [DFCB11a]. Cooperative Spectrum Sensing (CSS) is used to leverage cooperation among CR vehicles in order to exploit spatial and temporal diversity in the spectrum sensing process and thus allowing for higher PU protection and reduced false alarms.

Several CSS techniques have been proposed for general Cognitive Radio Networks (CRNs). However, many of these techniques cannot be applied directly to CR-VANETs due to their unique characteristics. More specifically, the lifetime of SOPs is not merely a function of PUs' activity, but also the mobility of vehicles. Moreover, a vehicle may encounter several PUs along its path, and hence collecting PUs activity statistics by an individual vehicle is of less benefit than in general CRNs. Furthermore, a vehicle's neighbours will change more dynamically than in a CRN. These aspects, along with others, fuel the need for more frequent spectrum sensing, and hence higher control and coordination communication overhead. On the positive side, vehicles' mobility are restricted by road topology and the path of each vehicle is predictable, thus encouraging the utilization of cooperation and prediction techniques. For example, a vehicle can obtain future knowledge of SOPs along its path through cooperation with its neighbours to reduce delay and control traffic.

This chapter reviews state-of-the-art CSS techniques proposed in the literature for CR-VANETs. The different techniques are discussed in terms of architecture, local-sensing methods used by individual vehicles, soft vs. hard sensing reports, the data fusion algorithm, and the assumptions made about the reporting mechanism used to exchange sensing reports. In terms of architecture, a CSS technique can be centralized, where vehicles report to a BS or a RSU that is responsible for the decision fusion process, or distributed where vehicles exchange reports amongst themselves and make spectrum decisions individually, or a hybrid where vehicles make individual decisions with assistance from a BS or a RSU. The reporting channel, necessary for exchanging sensing reports between RSUs and vehicles and amongst vehicles is often assumed ideal in the literature. However, some of the proposed work investigate the impact of an imperfect reporting channel. Furthermore, it is usually assumed that dedicated reporting channels exist between each vehicle and the RSU in range. Some work, however, assume the use of Wireless Acces in Vehicular Environments (WAVE)/Dedicated Short Range Communications (DSRC) Common Control Channel (CCH) for reporting purposes using random access according to the IEEE 802.11p PHY/MAC layers. With regards to data fusion, it is important to differentiate between Hard-Decision-Fusion (HDF) and Soft-Decision-Fusion (SDF). In general SDF leads to higher sensing accuracy but at a reporting overhead cost. Either way, we also discuss the fusion algorithm employed by the CSS technique. For example,the OR rule or the K-out-of-M rule in the case of HDF techniques, and Equal Gain Combining (EGC) vs Weighted Gain Combining (WGC) for SDF techniques. How weights for WGC are calculated is also investigated in this chapter. Some open research issues and future directions are then discussed, namely possible security threats to CSS in a CR-VANET and possible mitigation techniques, as well as more on the overhead necessary for control and coordination. While secure CSS have been considered in the literature for general CRNs, the vehicular environment brings about additional security challenges that will be discussed in this chapter. The remainder of this chapter is organized as follows: Section 2.2 provides an overview of CSS techniques for CR-VANETs. Security issues are then discussed in Section 2.3. Section 2.4 include open research issues and future directions pertaining to CSS in CR-VANETs. Finally, we present our conclusions in Section 2.5.

2.2 Cooperative Spectrum Sensing

A CSS scheme is comprised of three main steps, namely local sensing, reporting, and decision making. Local sensing schemes are assessed in terms of their detection accuracy as well as their agility, (i.e., sensing speed). Energy detection (ED) [DAS07] is the most commonly used local sensing method due to its simplicity and ease of implementation. ED does not require prior knowledge of the PUs' signals, but it needs to estimate the noise power at the SU's receiver and hence its performance deteriorates significantly at low Signal-to-Noise-Ratio (SNR) environments [YA09]. Other local sensing techniques include Matched Filter Detection (MFD) [CMB04], Cyclo-Stationary Detection (CSD) [GS08], EigenValue-based Detection (EVD) [GT90], and Higher-Order Statistics Detection (HOSD) [GT90]. MFD offers higher detection accuracy but requires prior knowledge of the PU transmit signals, achieved through periodic pilot signals transmitted by the PU to enable coherent detection by the SUs. This entails explicit cooperation between the primary and the secondary systems [CMB04]. CSD, on the other hand, does not require prior knowledge of the PUs signals while offering better performance than ED in the low SNR region by exploiting the periodic statistics, (e.g., the modulation type of the PUs' signals). EVD also is robust to the noise uncertainty problem, encountered by ED, but also is computationally intensive as it needs to perform eigenvalue decomposition. HOSD use higher-order statistics, third-order cumulant of the received signal to combat Gaussian noise effect, to separate noise from received signals even at extremely low SNR regions. However, HOSD requires a large number of samples to obtain an accurate estimate of relevant statistics lending it to be impractical due to high sensing time. The authors in [HCK11], aim to reduce the sensing time needed of HOSD by employing a Sequential Probability Ratio Test (SPRT), where the third-order cumulant is calculated for a new block of samples only if needed.

Vehicular Secondary Users (VSUs) report their sensing results to each other or to a central FC which can be a RSU or a cluster head. Sensing results reported can be local decisions, (i.e., hard-decisions), and local decision metrics, (i.e., soft-decisions), such as local energy values. In the literature, it is mostly assumed that reporting is carried over ideal dedicated channels. Some works assume dedicated orthogonal channels between VSUs and the FC, but consider channel impairments such as noise and fading. Other works use the WAVE/DSRC CCH using IEEE 802.11p PHY/MAC layers for random multiple access. Fusion or aggregation of sensing reports is carried on at the centralized FC, in the centralized case, or at individual VSUs, in the distributed case. Some hybrid techniques are found in the literature where a centralized FC receives sensing reports from VSUs and distributes estimates of channels availability probabilities to VSUs, while the final decision is made by individual VSUs. Fig. 2.1 shows the basic architecture for centralized and distributed CSS techniques.

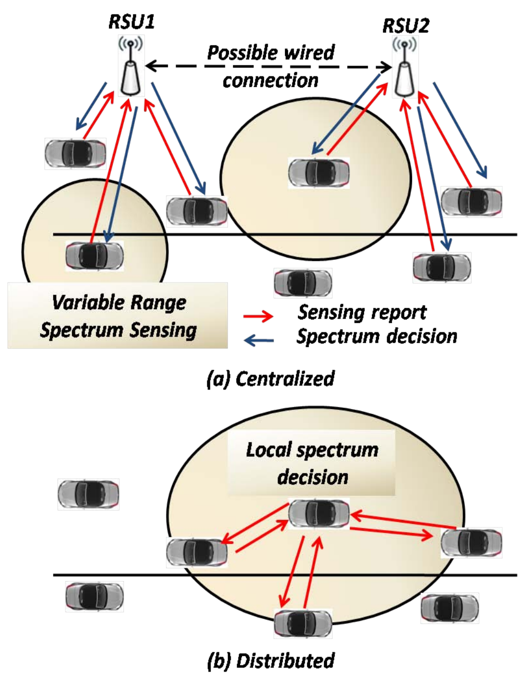

Figure 2.1: Cooperative Spectrum Sensing Architecture

In this chapter we classify CSS techniques proposed for CR-VANETs into detection and predication techniques. Detection techniques represent the basic effort of a group of CR vehicles to determine whether a channel is busy or idle. All channels in this class are treated equally when searching for a SOP. Prediction techniques, on the other hand, employ sensing statistics to calculate a channel's probability of being available. Channels, in a multi-channel network, are then ordered according to their probability of availability.

VSUs utilize this information to expedite the detection of SOPs. Even though detection techniques can be thought of as a special case of the more general class of prediction techniques, we treat them separately to illustrate the impact of the CSS technique on the process of searching for a SOP. In the following, we discuss CSS techniques proposed in the literature for each class in terms of their architecture (centralized vs. distributed), local sensing technique employed, type of decision fusion used, and reporting channel assumptions.

2.2.1 Detection Techniques

Detection techniques can be centralized, distributed. or hybrid. Local sensing techniques employed at the individual VSUs include Energy-based Detection (ED), EigenValue-based Detection (EVD), and Maximum Likelihood Ratio (MLR) detection. Sensing reports sent to the FC or exchanged among vehicles can be Soft or Hard reports, and hence data fusion can be Soft Data Fusion (SDF) or Hard Decision Fusion (HDF). Most of the work in the literature assumes ideal dedicated reporting channels between each vehicle and the FC. However, some authors consider fading reporting channels, while others consider multiple random access to a single reporting channel using the WAVE/DSRC IEEE 802.11p PHY/MAC layer.

Centralized Detection Techniques

The performance of CSS performance in a vehicular environment is investigated in [BIV+11] for sensing pilot tone signals transmitted from i) a RSU and ii) radios located on other vehicles using Energy-based Detection (ED). The authors' goal is to characterize the detection speed and reliability of simple hard and soft ED CSS for the vehicular environment. They show cooperation reduces sensing time by a factor of five in an AWGN channel, and even more significantly for a fading and shadowing environment. However, the authors assumed ideal dedicated reporting channels. The performance of centralized CSS using ED local sensing and HDF is investigated in [QH15, QHNT18], assuming temporally correlated Rayleigh fading sensing channels, as well as binary symmetric dedicated reporting channels in [QH15] and temporally correlated Rayleigh fading dedicated reporting channels in [QHNT18]. These works illustrate the influence of the reporting channel conditions over the decision made by the FC, as well as the opportunity to exploit temporal diversity at each vehicle due to its high mobility in addition to the benefits of spatial diversity.

Furthermore, another centralized ED-based HDF CSS technique designed around IEEE 802.11p called Over Head Free (OHF) protocol is proposed in [EKM18]. The purpose of OHF is to address the considerable amount of time dissipated in channel exploration, since each vehicle has to sequentially sense all available channels as well as the time needed to obtain a Radio Environment Map (REM) to be broadcast by the FC if all vehicles need to report their sensing results. OHF divides time into frames, each is divided into four phases: local sensing, reporting, REM broadcast, and data transmission. In the local sensing phase each vehicle randomly selects, with equal probability, a channel to sense to distribute the sensing load over cooperating vehicles. Reporting to the RSU, (i.e., FC), is done over 802.11p CCH, where the reporting phase is further divided into a number of equal-duration contention slots equal to the number of channels, where only vehicles that chose to sense channel i contend to report to the FC during contention slot i. A contention slot is divided further into a back-off interval and a report transmission interval. The back-off interval is composed of CW mini-slots. Each contending vehicle chooses a random counter, listens to the CCH, and reports only if the CCH is idle until its counter expires. Remaining vehicles contending during a given contention slot will drop their reports. Therefore, OHF sacrifices spatial diversity in its channel exploration endeavour for reduced reporting time. This is justified by the authors for a dense vehicular network in a rural scenario where vehicles' sensing results are highly correlated, noise levels and shadowing effects are relativity low, and hidden terminals almost do not exist. The RSU produces its REM after the reporting phase is over to indicate which channels can be used by the vehicles in its road segment, where vehicles may commence data transmission upon receiving the REM. The result is a reduction in the time needed to obtain the REM compared to IEEE 802.11p based CR-VANETs, an increase in network throughput, and a reduction in PU outage which can be controlled through the contention window size.

Another centralized CSS scheme using Maximum Likelihood Ratio (MLR) local detection and OR-rule HDF at the FC is investigated in [XHZG12, XJLW13] for wide-band spectrum detection in Orthogonal Frequency Division Multiplexing (OFDM)-based overlay CR-VANET. MLR, similar to ED, uses an estimate of the channel SNR which is related to the noise variance. MLR has an adaptive detection threshold that can be changed with received Signal-to-Noise-Ratio (SNR). The scheme's performance is evaluated in terms of global detection probability and corresponding Receiver Operation Characteristics (ROC) performances considering the fading of sensing and reporting channels as well as inter-user error rates.

A Centralized detection CSS technique employing ED local sensing and EGC-SDF is investigated in [QH14], assuming ideal reporting channels with negligible delay. ED-EGC-SDF also is used for a dense CR-VANET in [ZGFL16]. In a dense-traffic network, the authors drop the assumption of independence across reports from different VSUs, as neighbouring vehicles are more likely to experience a higher degree of spatial and temporal correlation [DFCB11b]. The selection of cooperating VSUs is hence crucial, hence the authors compare two VSUs-selection algorithms, random vs. distance based, in terms of sensing capacity of the network. The authors also derive expressions for the detection and false alarm probabilities based on a mobility model derived from trajectory data set obtained from traffic simulators for specific roads in the U.S. Another distance-based correlation-aware VSU selection and weight assignment CSS technique, also using ED-EGC-SDF, is proposed in [LZG17, LZG18] to select a limited number of uncorrelated VSUs having higher sensing reliability from a dense CR-VANET. Cooperating VSUs selection using a double-threshold optimization problem is proposed in [LSZ$^+$18] followed by a joint spatial-temporal correlation based CSS, also using ED-EGC-SDF, called Hybrid Cooperative Spectrum Sensing based on Spatial-Temporal Correlation (HCSS-STC). First threshold is a mobility stability threshold, where larger speed corresponds to lower mobility stability, while the second threshold is a probability of detection threshold for a given desired probability of false alarm. The optimization problem is both non-convex and non-linear, and hence solved using an exhaustive, or brute-force, search algorithm. After VSUs selection, the FC can proceed with EGC of sensing data from selected VSUs.

Previous sensing results from a VSU, for a certain length, are used as virtual VSUs and fused together with most recent results from the VSU in a linear matter. The weights used for previous sensing results are calculated according to the VSU location and the time at which each previous sensing result was obtained reflecting spatio-temporal correlations.

A number of authors considered WGC-SDF centralized CSS. For example, Asynchronous Cooperative Spectrum Sensing (ACSS) is proposed in [LXY+14]. Energy Information (EI) is tagged with location and time information, where these tags are used to assign weights to EI reports from VSUs during fusion factoring in spatial and temporal diversity. More specifically, the weights are calculated using an optimization problem to maximize the overall detection probability and minimize the overall probability of false alarm. The asynchronous feature of the proposed technique is justified by the high hardware requirements needed to synchronize all VSUs. This asynchronous feature entails that cooperation can only be received from VSUs that already performed their sensing, (i.e., using most recent and tagged EI). Moreover, the weights of WGC-ED-SDF in [DD16] reflect the spatial correlation between VSUs. In [YWMF17], an adaptive CSS technique is proposed where the RSU can request more sensing samples from a VSU if the average power of the received samples falls below a certain threshold, and the weight of samples received from a VSUs is equal to the received power. The authors show that WGC performs better than EGC in low SNR region.

EVD is investigated in multiple works in the literature. EVD-based techniques received a lot of attention as they do not require prior information on the transmitted signal, as in cyclostationary detection. EVD, also does not require knowledge or estimation of noise variance as in ED, where a slight error in the estimation of the noise variance may lead to a noticeable degradation of sensing performance. EVD uses a test statistic computed from the eigenvalues of the received signal covariance matrix. The detection performance of multiple eigenvalue based techniques is investigated in [GdSB13, AAdSAGAdA13, SBCA14]. These works consider an $M-$antenna VSU using local EVD, or equivalently M single-antenna VSUs each using local ED and EVD-fusion at the FC. The performance of the Arithmetic-to-Geometric Mean (AGM) EVD algorithm from [ZLLZ10] is investigated in [SBCA14].

The Nakagami-m fading model is used to characterize the sensing channels as it is empirically proven to be suitable model for the 5.9 GHz DSRC narrow-band allocated to VANET communications [CHS+07]. Meanwhile, [GdSB13, AAdSAGAdA13] investigate the performance of the Generalized Likelihood Ratio Test, Max-Min Eigenvalue Detection, and Maximum Eigenvalue Detection vs. ED. The same authors also consider a realistic implementation-oriented model of the VSU receiver-end, taking into account typical signal processing tasks performed by a CR before sending its collected samples to a FC. Such tasks include wide-band bandpass filtering, low-noise amplifying, down conversion, automatic gain control, lowpass filtering, analog-to-digital conversion, and white filtering. The authors also model the possibility of Impulsive Noise, typically caused by lightning or a vehicle's ignition system, using models from [Fer04, TS10, TSC11].

A centralized CSS using a Largest Eigenvalue (LE) detector, also a blind EVD technique, for local sensing and the HDF AND-rule at the FC is proposed in [KLC+17]. Each vehicle employs multiple receive antennas. The LE detector compares the largest eigenvalue of the received covariance matrix to a threshold to make the local decision. A centralized joint CSS and channel allocation scheme is proposed in [BSA+15] that uses a blind EVD-based local sensing technique called Symmetry Property of the Cyclic Autocorrelation Function (SP-CAF) [KNP12, SAN+14]. SP-CAF estimates the Cyclic Autocorrelation Function (CAF) of the received signal using an iterative compressed sensing tools, known as Orthogonal Matching Pursuit (OMP) [DMA97], that benefits from the sparseness property of the CAF function to guarantee relatively small sensing time. The authors show that three iterations of OMP are sufficient to decide on the symmetry of the vector. A channel is deemed busy if the CAF function has a symmetry feature. The SP-CAF detector can outperform ED in low SNR environments at a reasonable computation complexity [KNP12]. The objective of the joint scheme is to extend WAVE/DSRC CCH using CR and create maps of ISM bands to exploit as cognitive extensions across the roads. Local sensing, using SP-CAF, occurs during the SCH time slot and stored in the Vehicle's Spectrum Availability Database (SADB) as Spectrum Availability Entries (SAE). The road is divided into segments, each served by a RSU which contains a Central SADB (CSADB). At the end of a road segment or after a timeout a vehicle aggregates its SAEs and sends it to the RSU to update its CSADB. RSUs use collected data from passing vehicles to assign a quality grade between 0 and 1 for each (channel, cell) pair falling on their corresponding road segments. The accompanying channel assignment algorithm assigns an extension ISM band channel for a road segment using a heuristic algorithm that aims to reduce the number of switches in a road segment, and the variance in length for the sub-segments assigned to the same channel.

In order to reduce sensing time and control overhead, a CSS technique based on limited data sets for PU detection and a density-based clustering mechanism is proposed in [NS18] for a relatively low SNR environment. VSUs forward hard sensing results to their corresponding cluster heads, which use HDF OR-rule to aggregate received reports. Cluster heads forward aggregated results to the RSU, where the final sensing decision is performed using the logical AND rule, and then it is sent to the cluster heads that in turn inform VSUs. Individual VSUs use a blind cumulative spectrum sensing method proposed for small data sets based on the Maximum-Minimum Eigenvalue (MME) algorithm [ZL07], and the Oracle-Approximating Shrinkage (OAS) estimator [CWH11]. The decision metric used in the MME algorithm is the ratio of maximum and minimum eigenvalues of the sample covariance matrix. However, since the data set is limited, MME performance will be compromised. Hence, the OAS estimator is used to replace the eigenvalues from the sample covariance matrix with the eigenvalues from an estimated covariance matrix.

Distributed Detection Techniques

Distributed detection techniques delegate data fusion and spectrum decision duties to individual vehicles. Two iterative techniques are proposed in [LI10] and [WYB15], where vehicles exchange messages several times before converging on a spectrum decision. The first technique [LI10] uses belief propagation message passing for data fusion. A VSU sends a message to each of its neighbouring VSUs. This message represents the sending vehicle's belief about the state (busy or idle) of a channel at the receiving VSU. Note that each VSU has to send a separate message to each of its neighbours for each channel to sense, and hence we can see the high degree of communication overhead involved. After all iterations, a VSU can calculate its final belief about the channel that represents the marginalized probability of the channel state given the set of all local and received observations. The second technique is a weighted consensus-based CSS scheme [WYB15]. In each iteration, each VSU receives EI from its neighbours and calculates a new local EI to send in the next iteration. The weights used for EI received from neighbour VSUs represent a trust metric that is used to marginalize sensing reports from non-trustworthy VSUs. A VSU compares local EI with a designated threshold to conclude a final spectrum decision about a given channel. This is done after the difference between the new EI and a common consensus EI is less than or equal a given tolerance deviation.

Another distributed CSS and allocation framework, referred to as Cog-V2V, is proposed in [DFCB10b, DFCB11a] that allows vehicles to decide in advance the channels to use on future locations. This work introduces the concept of spectrum horizon that represents a vehicle's current segment in addition to a fixed number of future and past segments for which a VSU maintain spectrum information in a local data base. Licensed channels to be used opportunistically are periodically sensed for a full SCH period to update the local spectrum database. VSUs remain quiet and do not transmit data in the SCH period designated for sensing. Spectrum databases are exchanged, periodically as well, over the CCH. Note that, sensing and database broadcast periods are different. A weighted sum data fusion algorithm is used by each VSU to decide a schedule that specifies available channels for use during current and future road segments in the vehicle's spatial horizon. The weights used by a VSU to merge EI received from a neighbour vehicle may depend on the number of sensing samples collected by the neighbour or on the distance from the neighbour VSU. More specifically, a VSU that collected more sensing samples for a channel over a given road segment will have a higher weight, likewise a more distant neighbour will have a higher weight to enhance spatial diversity.

The authors in [LXY$^+$14], propose a distributed version of the centralized ACSS discussed above. Again, weights assigned to EI from neighbour vehicles are based upon the location and time information tags to reflect spatial and temporal correlation. Each VSU runs a frame-by-frame operation consisting of four major components: reservation through negotiation, sensing, exchanging, and transmission, where a VSU can only receive EI from its immediate neighbours that already performed their sensing. The authors in [AW17] propose another distributed CSS technique that uses an adaptive ED threshold and a robust voting mechanism for cooperative decision making. The ED threshold is chosen by each VSU to minimize the probability of misdetection using the Secant Method. VSUs use WAVE/DSRC CCH to exchange sensing reports with one-hop neighbours. Sensing results from neighbours are given weights according to two mechanisms: a proposed entropy-based weighting voting mechanism, where weights are determined according to received SNR, and an equal weight voting mechanism. The entropy-based voting mechanism has higher control overhead as opposed to the equal-weight voting mechanism, and hence the authors propose to switch between entropy-based voting for low traffic scenarios and equal weight voting for dense traffic scenario considering a tradeoff between computational cost/latency and accuracy.

Hybrid Detection Techniques

A two-stage hybrid CSS technique where individual vehicles perform final spectrum decision based on coordination instructions from a coordinator node is proposed in [WhH10]. The coordinator could be a RSU or a cluster head. The coordinator performs periodic coarse (fast) ED of licensed channels considered for opportunistic access. A VSU with data to transmit sends a request over the CCH to the coordinator specifying data transmission requirements such as tolerable delay and bandwidth. Upon receiving the request, the coordinator responds back with sensing instructions which include a number of channels that are likely to satisfy the VSU requirements. The VSU then has to perform its own fine sensing for each of the suggested channels until a SOP is detected. The VSU informs its neighbours as well as the coordinator of the detected SOP over the CCH, causing the VSU's intended receiver to sense the detected SOP to ensure its availability on the receiving side. The transmitting VSU waits for a reply from the intended receiver on the detected SOP. Note that the coordinator does not only periodically sense licensed channels but also keeps track of VSUs' access attempts which aids its coordinating capabilities.

The authors in [EZLE18b] developed a hybrid CSS and allocation scheme which allows VSUs to be aware of SOPs on their current and future positions. Local sensing is based on a three-state, (i.e., double threshold), ED from [EZL+15, JZL+16], where a licensed channel can be idle, (i.e., H_0), occupied by a PU, (i.e., H_1), or occupied by another VSU, (i.e., H_2). Using a double threshold reduces the probability of false alarm due to the gap between the two thresholds. A VSU can distinguish whether the spectrum channel is actually occupied by a PU or by another VSU using a distance estimation technique. The CSS scheme is slot-based, where a certain VSU provides one observation on a certain channel in a certain slot so that the total number of observations in all slots is equal to the total number of VSUs. The challenge is to determine the number of VSUs that should cooperate to sense a channel i during slot $i, \forall i = 1, 2, \cdots, N$. This problem is solved by the RSU in order to maximize the sum of probability that channel i is available when VSU V_i sense channel i for $i = 1, 2, \cdots, N$. The solution of this optimization problem is an assignment of sensing duties to all VSUs in the road segment over the set of licensed channels to be sensed. A low complexity solution is obtained through dynamic programming using the Viterbi algorithm [BD15]. The final sensing decision is determined by each VSU in a distributed manner using local sensing and overheard sensing reports from neighbours. Therefore, the RSU is responsible for distributing the sensing duties over the VSUs that are responsible for making the final decisions about the channel state. The authors then discuss integration of the proposed framework into the IEEE 802.11p protocol stack.

2.2.2 Prediction Techniques

Prediction techniques estimate channel availability in the future to expedite a vehicle's search for a SOP or to determine the amount of sensing reports needed to make a decision about the state of a given channel. A RSU or a cluster head usually provides VSUs with coordination instructions that represent channel availability probabilities or channel state predictions. A clustering scenario is proposed in [BDGD12], where the cluster head is responsible for data fusion and consequently spectrum decision. The cluster head also is responsible for channel allocation to requesting vehicles, (i.e., cluster members). The cluster head would like to reduce the time needed to allocate a licensed channel to a requesting CR vehicle. Normally, in each frame the cluster head has to wait for sensing reports from all cluster members before deciding on channel availability. Instead, the authors proposed a CSS prediction technique that utilize a Hidden Markov Model (HMM) to predict the state of a channel over subsequent time frames. This prediction, which is a probability, is then used to reduce the number of sensing reports needed by the cluster head to make a decision on channel availability.

A hybrid CSS prediction technique is proposed in [AQAA15] that utilizes channel availability probability estimates as coordination instructions to determine the order of channels to sense for both suburban and highway scenarios. RSUs are installed at proper distances on the sides of highways and vehicles are arranged in clusters in each direction. Each cluster has three coordinators: main coordinator, front coordinator, and back coordinator. The communication range of the main coordinator is divided into equal distance segments. Coordinators selections are given in details in [AQA+13]. VSUs send and receive control information over the CCH of WAVE/DSRC, where each coordinator of the three is responsible for a fixed number of segments. RSUs preserve channel usage history, where a day is split into a number of time slots for its corresponding road segment that may encompass more than one cluster. Member VSUs periodically sense all licensed channels using ED to identify the presence or absence of PUs. VSUs, then report, periodically, their hard sensing results for the channels they sensed along with their coordinates to the appropriate coordinator. On receipt of sensing reports from VSUs, coordinators compile results based on majority decision if more than one result is obtained for a given segment over the same channel. Hence, results for the space, time, and frequency are then sent to the main coordinator to be submitted to the RSU. RSUs exchange their database information with other RSUs, where each RSU stores the database for the segments covered by its Basic Service Set (BSS) as well as the segments covered by the BSS of the next RSU. Therefore, VSUs can utilize the spectrum proactively on their future path to their corresponding destinations. RSUs sort the database in order of high probability for the next time slots and share this information with the main coordinators, which in turn share it with their front and back coordinators. The main coordinator is responsible for compiling the results based on current availability and availability probability received from the RSU for the segments in its coverage range. Upon receiving a CR spectrum utilization request from a VSU moving in segment S_i and time slot T_k, the main coordinator sends back the channel numbers in order of higher probability of availability to the lower one for the next distance segments and time slot T_k.

Machine learning is adopted in [HWL+16] and [AS18] to exploit the spatiotemporal correlations in historical spectrum sensing data and predict, or have a prior knowledge of, the channel's availability probability. The objective is that when transmission load over DSRC channels is heavy, and vehicles decide to use TV White Space (TVWS), they have a list of channels ordered by their probability of availability to speed up the search for vacant licensed channels. Cooperation, or fusion, is based upon the Dirichlet Process (DP) that produces, for each channel, a probability of availability for the coming road segment, (i.e., a prior distribution), and then use a threshold probability to determine if a channel is idle or busy. The prior distribution produced by DP uses a posterior distribution or channel state transition probabilities calculated using a non-parametric HMM that exploits the historical sensing data collected from previous vehicles. In terms of implementation, wire-connected Access Points (APs) are installed at the beginning and at the end of every road segment. The AP at the beginning of a road segment broadcasts the derived channel availability rules, (i.e., posterior probabilities), to all vehicles entering the road segment, while the AP at the end of the road segment collects historical spectrum sensing data from all vehicles leaving the road segment. The data mining algorithm that produces the posterior distribution runs over a server at the end AP. The posterior distribution is passed to the beginning AP to be distributed over newly entering vehicles.

2.2.3 Database Assisted Techniques

An extension of the Cog-V2V distributed CSS technique is presented in [DFGAB13], where the authors investigate the optimal ratio between using CSS and querying a national spectrum database assuming a scenario of multi-interfaces, (e.g. DSRC, 2G/3G/4G, ... etc.), VSUs dynamically try to decide the detection mode to use. Furthermore, in [AACDFP14] and [AASDF+15], the authors aim to identify spatial regions and/or duration periods, where local sensing would be satisfactory and spectrum database queries are unnecessary. The objective is to reduce spectrum database queries in a dense network scenario to avoid congesting the spectrum database and the control channel with spectrum queries. The authors resort to a concept established through experimental studies, whereby at certain locations cellular Received Signal Strength Indicator (RSSI) is used as a good indicator of the accuracy of spectrum sensing for some TV channels owing to the common set of reflection, absorption-causing objects, and the large-scale path-loss. A vehicle collects RSSI values off cellular towers and determines the amount of correlation relative to saved TVWS saved data. A high degree of correlation implies local sensing results would be sufficiently accurate and a database query is not needed. In [AASDF+15], this concept is further enhanced by employing interference alignment techniques to increase the utilization of the control channel used to disseminate database queries.

2.3 Security Issues

CR vehicles learn from and adapt to their environment. Therefore, an adversary can manipulate the belief and behaviour of CR vehicles through false sensory input. This manipulation could have a significant impact on the network performance and can lead to a complete denial of service. In fact, CR-VANETs are more prone to security threats than traditional CRNs due to their dynamic nature resulting in greater difficulty in detecting and defending against attacks. In the literature, two major physical layer attacks are strongly related to CSS. These are PU Emulation (PUE) attacks and Spectrum Sensing Data Falsification (SSDF) attacks, also known as the Byzantine attack, [CPHR08]. Database assisted CSS techniques also face security threats such as location privacy and jamming. In the following we outline some proposed CSS with security threat mitigation techniques. Most of these techniques are proposed for the general CRNs, however some are specific to CR-VANETs.

2.3.1 CSS with Primary User Emulation (PUE) Mitigation Techniques

In a PUE attack, an adversary masquerades as a PU by changing its transmission characteristics (e.g., modulation, frequency, and power) to resemble that of a PU. Such an attack is either to maliciously deny service to the CR-VANET or to selfishly obtain higher access priority. A selfish attack would require the coordination of more than one node, while a denial of service attack in a given location can be administered by a single node. In all cases, both types of attacks can drastically limit available SOPs for legitimate CR vehicles. Mitigation techniques proposed for PUE attacks in traditional CRNs mainly rely on a combination of knowledge of true PU locations and RSSI. PUs are considered to be mainly TV towers, and hence while an attacker in the vicinity of a TV tower will pass the localization test, its received signal strength will be much weaker than a legitimate PU [SQC13].

The authors in [FFEGAEMEB19] propose a localization technique relying on trilateration and a Bayesian model for PUE position detection assuming uncertainty conditions. More specifically, anchor nodes use trilateration based on RSSI measurements of the signal coming from either a PU or a malicious PU emulator in order to detect location. At the same time a Bayesian decision model uses a cost function to check the legitimacy of the PU. Furthermore, a two-stage PUE attack prevention scheme is proposed in [SSM19], where learning and classification are performed at edge nodes and then core cloud nodes are responsible for deeper machine learning that takes into consideration historical data. The proposed method is compared to two other machine learning-based PUE attack prevention protocols and is found to reduce false alarm probability to the secondary network, and improve overall detection accuracy of the primary network. Due to mobility, localization, as well as signal strength estimation is more involved and needs to be updated more frequently in a CR-VANET. The impact of the vehicular environment on these mitigation techniques is yet to be fully understood.

2.3.2 CSS with Spectrum Sensing Data Falsification (SSDF) Mitigation Techniques

Spectrum Sensing Data Falsification (SSDF), also known as a Byzantine attack, is the second major physical layer attack. SSDF occurs when an attacker reports incorrect local spectrum sensing results to the FC in order to alter its spectrum decision. There are four SSDF attacking strategies. These are "Always Yes", where a Malicious SU (MSU) always sends "1" to the FC regardless of the sensing result, "Always No", where the MSU sends "0" to the FC regardless of the sensing result, "Opposite Attack", where the MSU sends an opposite result to what it or other SUs sense, and "Completely Random Attack", where the MSU sends random sensing information with some given probabilities. Mitigation approaches for the SSDF attack takes two directions. First, the FC needs to authenticate submitted sensing reports to prevent injection of false information. Second, developing more robust data fusion techniques that are less vulnerable to SSDF attacks by employing the concept of trust or reputation of a CR vehicle. For example, the trust or reputation of a SU would depend upon the accuracy of its sensing reports relative to the final sensing decision. Furthermore, SSDF attacks cause a reduction in a CRN's detection accuracy, which consequently degrades throughput and causes harmful interference to the operation of PUs due to more misdetection events. Therefore, trust and reputation management are needed to calculate and update a Reputation Value (RV) [LYP14] for SUs. In the following we shed some light over some centralized and distributed CSS techniques with SSDF attack mitigation.

Centralized Techniques

The authors in [NVD18] and [BZY17] propose the most basic reputation-based CSS to counter SSDF attacks, where the FC determines the trustworthiness of SUs by assessing their past behaviour. SUs with reputation values above a selected threshold, of 0.6, were discarded from the decision making. The threshold is preset and constant throughout the operation of CSS. Multiple other trust (or reputation) mechanisms have been proposed to combat SSDF attacks in [PYLL13, ZPT14, FLC15, CZX$^+$16, KSS17]. These efforts estimate the honesty of a SU by its historical behaviour and assign lower weights to sensing data from less honest SUs during the fusion process. In [FLL+18], the authors envision a centralized CSS mechanism where a SU requesting the status of a given PU is called an initiator while SUs that aid CSS are called collaborators. After receiving the sensing result of CSS about the PU status from the FC, initiators send a feedback to the FC about the validity of the sensing decision they received. These feedbacks are trusted by the FC. The authors then envision a Collusive False Feedback (CFF) attack, where attackers conspire with each other to form a collusive clique and exploit feedback data intentionally. More precisely, a CFF attacker is assigned to be disguised as an initiating SU that will send feedback to the FC in accordance with his conspirators' sensing data. This would increase their sensed trust value of the SU, and hence seen to be as honest with a high trust after several rounds of attack giving the attackers the opportunity to start injecting false sensing data and manipulate the FC sensing decision. The authors then propose a two-level defence mechanism called FeedGuard to detect CFF attackers. At the request-level, FeedGuard introduces the concept of feedback trust to reject CFF initiating SUs, and at the feedback-level FeedGuard checks the collusion frequency or feature between initiating and collaborating SUs.

Another centralized ED-HDF CSS mechanism that counters collusive SSDF attacks is considered in [SJRB18] based on a Collision Penalty (CP) [DMHS12] parameter. The PU penalizes the FC with a CP if it suffers collision, and the FC consequently penalizes the SUs by dividing the CP equally among all of them, irrespective of whether they are malicious or not. It is assumed that the FC knows the idle PU signal probability, and that smart malicious SUs can overhear the decisions of the other SUs. The authors then identify possible malicious strategies and adjust CP bounds accordingly. The impact of an imperfect CCC on the identification of MSUs is analyzed in [MXP+18]. The authors then propose a centralized ED-HDF reputation-based CSS scheme to differentiate malicious from Honest SUs (HSUs) under independent, cooperative, and mixed SSDF attacks. The FC maintains a threshold for each SU. If the reputation value of an SU is greater than that threshold it is classified as honest, otherwise it is classified as malicious. Obviously, the choice of a good reputation value threshold is crucial. The authors do not assume that the ratio of malicious

SUs to honest SUs is known to the FC as in [RACV10], or that the threshold is fixed and set to 0.5 as in [HGXE14], or that the CCC is ideal as in both [HGXE14] and [RACV10]. Centralized SDF-ED CSS mechanisms that use reputation to counter SSDF or Byzantine attack are proposed in [CPB08, CCCL12, CPB12, LW15, DFC15, SN16, WSW+17, WSY+18, WSWH18]. These are reputation-based versions of the sequential probability ratio test.

Machine-learning techniques also are useful in countering SSDF attacks. For example, the authors in [YLC19] propose a centralized ED-SDF CSS technique which uses Maximum Mean Discrepancy (MMD) [GBR+12] as a distance metric between sensing reports to distinguish between MSUs and HSUs. MMD maps the distributions of different sensing reports into a high-dimensional, nonlinear feature reproducing kernel Hilbert space associated with a kernel function suitable to achieve a good classification. With MMD, two different sensing reports generated by different SUs can be differentiated even when they have equal mean and variance. The FC then gives each SU's sensing report a weight which represent its distance from a genuine sensing report. The sensing decision is then calculated by comparing the summation of all weighted sensing reports to a threshold.

Clustering techniques also can be used to counter SSDF attacks. The basic idea is that HSUs will find themselves in the same cluster, while MSUs will be in a separate cluster. The authors in [RNMT18], propose using clustering techniques on SUs' sensing reports to detect and isolate SSDF attackers in a centralized ED-HDF CSS that assumes an ideal CCC and the majority decision fusion rule. An advantage of clustering techniques over reputation-based methods is that they do not require pre-defined thresholds for the system to operate.

As for CSS techniques proposed specifically for CR-VANETs, the authors in [LZG18] and [LZG17], address a challenge where a VSU could sporadically and randomly contribute with abnormal data, due to either accidental equipment failures or random malicious behaviours. This makes the CSS output decision inaccurate. Given the fact that the real occupancy state diagonal matrix is low-rank due to under-utilization of the licensed bands, and that abnormal events due to accidental equipment failures or random malicious behaviours are random and sporadic, then the corrupted data matrix is sparse. Therefore, the goal, at the FC, is to recover the real spectrum occupancy state matrix from the noisy and corrupted observations using the augmented Lagrangian multiplier approach. The authors propose the Low-Rank Matrix Recovery - Robust Cooperative Spectrum Sensing (LRMR-RCSS) algorithm for low traffic density environments. However, in a dense vehicular network the computational complexity of LRMR-RCSS, would be prohibitive due to large, highly-correlated matrices. Hence, the Weighted Low-Rank Matrix Recovery - Robust Cooperative Spectrum Sensing (WLRMR-RCSS) algorithm is introduced, which uses a distance-based correlation-aware VSU selection and weight assignment schemes to select a limited number of uncorrelated SUs having higher sensing reliability out of the total VSUs. WLRMR-RCSS takes advantage of spatial diversity while reducing cooperation and computation overhead. Another CSS scheme based on low-rank Matrix-Completion (MC) [CR09] is proposed in [QGP18] for MSUs detection, where channels sensed but corrupted by MSUs are removed before making the final decision using the Adaptive Outlier Pursuit (AOP) algorithm [YYO13, YYO12]. An estimation strategy for the rank of the sensing information matrix and the number of malicious users also is proposed to avoid requiring any prior information about the CSS network such as the ratio of MSUs to total SUs.

Distributed Techniques

A number of distributed CSS techniques with SSDF defence have been introduced in the literature. For example, the authors in [MV18b] test and compare the performance of two CSS schemes in countering the effects of SSDF attacks in a mobile CRN using the network simulator 2.31 (NS 2.31), namely the Cooperative Neighbouring Cognitive Radio Nodes (COOPON) [JHKI13] and Pinokio [TZWM12, TJPM13] schemes. Pinokio utilizes a Misbehaviour Detection System (MDS), which uses training data to profile the normal behaviour of network nodes and then detects MSUs by checking the bit rate behaviour of nodes. SUs that do not exhibit the normal expected behaviour are classified as malicious. The COOPON scheme tries to detect selfish MSUs through cooperation among legitimate neighbouring SUs. Neighbouring SUs exchange channel allocation information among each other to detect an overusing or selfish SU. Results show a performance degradation when increasing the number of MSUs in the network so they propose a new scheme which employs the Extreme Studentized Deviation Test to mitigate the SSDF attack in [MV18a]. The new scheme is more resilient to the increasing number of MSUs in the network.

A hybrid ED-HDF reputation-based CSS is proposed in [BWD19]. SUs are arranged in clusters and the leader of each cluster has the task of fusing reports from other SUs in the cluster. Cluster leaders then exchange fusion results to reach a final decision. Within a cluster, the cluster leader uses a weighted majority voting where weights are determined based on reputation. The reputation of SUs is calculated using an online learning-based algorithm, (i.e., an adaptive multiplicative weight update function). The rate of change of SUs' reputation is based upon the difference between the population of the majority and minority, in a term called confidence. The higher the confidence level the higher the rate the reputation increases or decreases. The use of an adaptive learning rate increases the speed of detecting MSUs. Insistent Spectrum Sensing Data Falsification (ISSDF) is a form of SSDF attack specifically aimed at distributed CSS schemes that are based on iterative average consensus where a MSU repeatedly broadcasts falsified sensing information in all consensus iterations to maximize their effect [VCM15, BK18]. The authors in [BK18] propose a distributed trust-based mitigation technique for ISSDF, where SUs analyze the trustworthiness of received sensing reports by considering the mobility and energy values of other SUs.

Finally, a special form of the SSDF attacks specific to CR-VANETs and coined Speed Adjustment Attack is introduced in [LGCP19]. In such an attack, multiple colluding attackers, selfish or malicious, aim to evade data accumulation detection schemes of a Distributed Cooperative Spectrum Sensing Algorithm (DCSSA), adopted from [LZL+12a, EUHK13, ZGL+15], by rapidly changing neighbour-sets through vehicles' speed adjustments algorithm. The attackers seek to maximize the number of neighbour-sets affected and minimize the number of attackers joining a single neighbour-set to maximize the efficiency of error diffusion. This can speed-up the spread of wrong sensing-data efficiently in a mobile highway scenario and hence increase the difficulty of detection.

2.3.3 Attacks against Spectrum Databases and Mitigation Techniques

Database aided CSS also face a multitude of security threats that can affect the accuracy of spectrum information it acquires or the privacy of PUs as well as SUs if their information are leaked in database query responses. In the following we briefly discuss some of these database related security threats and their mitigation. The first threat is false data injection into Spectrum Sensing Providers (SSPs) or databases. SSPs are crucial for crowdsourcing, a promising approach to offer effective sensing information over a large geographic region. SSPs out-source sensing duties to distributed mobile users, thus benefiting from the ubiquitous penetration of mobile devices into everyday life. SSPs then respond to sensing information requests from SUs as in database aided CSS. Therefore, SSPs are vulnerable to malicious sensing data injection attacks, where a MSU may opt to submit false ED reports to inflate or deflate the final average. Secure crowdsourcing-based CSS is discussed in [ZZZZ13, BZGW19, Alm19].

Location privacy for both PUs and SUs is another major concern for database aided CSS. A PU might hesitate to share its spectrum if its location's privacy is leaked by sensing reports or spectrum queries to the database. Furthermore, an attacker can infer a SU's location from its spectrum query or even its channel usage. Location privacy is investigated in a number of publications as in [GZL+13, CNDM19, DZL+19, GYH19, ZXZY19, CLG+19]. In [GZL+13] a Private Spectrum Availability Information Retrieval scheme utilizing a blind factor to hide the SU location is proposed to thwart location privacy leaking from SU queries. Another scheme leveraging encryption, interference calculation, and obfuscation methods is proposed in [CNDM19]. In [GYH19], multi-servers are used for private information retrieval that proves to be more efficient in terms of location privacy, while in [ZXZY19] the authors propose a witness selection mechanism to generate distributed location proofs that allow SUs to not provide location information to a database in the presence of MSUs. Finally, an efficient privacy-preserving spectrum allocation scheme for a crowdsourcing-based CSS architecture is proposed in [CLG+19].

The third database assisted CSS related security threat is radio jamming. Jamming is a Denial of Service (DoS) attack that disrupts communications at both the physical and link layers of a wireless network [ZXYY19]. In a database aided CSS scheme, a jammer could obtain spectrum information through database queries instead of stand-alone sensing where a database cannot, in general, distinguish a jammer from a normal SU. Query-based Jamming Attacks in database driven CRNs and a proposed Bayesian Jammer Inference method are investigated in [ZFL+16] and [FKB+19]. Anomaly-based jammer detection, a form of machine learning, is studied in [FNKF13].

2.4 Open Research Issues

The CSS techniques proposed in the literature for CR-VANETs make simplifying assumptions that motivate further research needed for practical implementation. In the following we discuss open research issue related to CSS in CR-VANETs. The work done on CSS for CR-VANETs mostly assume that an ideal control channel is available for the exchange of sensing reports and spectrum decisions. Even techniques designed for integration with the WAVE protocol, assume flawless exchange of all CR vehicles' coordination and sensing reports traffic during the CCH period. However, access to the CCH is random through carrier sense multiple access, and hence can experience collisions and loss of sensing reports from some CR vehicles. Furthermore, the CCH of WAVE is mainly intended for safety applications, some having strict delay and packet delivery rate requirements, and can be already congested during peak hours of traffic [FGOA10].

Secure CSS for traditional CRNs is not a new topic, however the efficacy of many secure CSS techniques in a CR-VANET is yet to be investigated. As discussed above, CR-VANETs have unique characteristics and face additional challenges that must be considered when mitigating security threats. For example, the maintenance of a trust or a reputation metric for each vehicle in a CR-VANET is a more challenging endeavour. The assessment of a CR vehicle reputation takes place at the FC, which is either a RSU for centralized techniques or an individual vehicle for distributed techniques. A FC, RSU or vehicle, needs to collect a large number of sensing reports from other CR vehicles to build corresponding reputation metrics. However, this may not be possible in a CR-VANET due to mobility. A CR vehicle will spend less time in the coverage of a single RSU, or has a changing neighbourhood as other CR vehicles dynamically join or leave its neighbourhood. Furthermore, making a reputation decision based on a limited number of sensing reports can be misleading, where a legitimate CR vehicle submitting inaccurate reports due to environmental conditions such as shadowing can be considered malicious. Finally, as pointed out in [CG08], security attacks can have a long-term impact on CSS techniques that employ learning methods. An example for that is a prediction CSS technique that utilized sensing statistics to calculate channels' availability probabilities would be more affected by PUE and SSDF attacks as they can span more than one spectrum decision round.

Extending security measures to span the entire network stack also is advocated in [CG08], which requires developing a sense of identity for CR vehicles and developing a mechanism for earning and using trust. The notion of identity allows building up learned statistics specific to individual neighbours rather than to all neighbours combined. For example, a CR vehicle does not only understand detected energy over a channel as another wireless device, or even differentiate between a PU and a CR vehicle; but also can distinguish two CR vehicles. This sense of identity enables a CR vehicle to learn trust metrics about its neighbouring CR vehicles. Trust should be quantified at different levels. At the medium access layer, trust would indicate if a vehicle is using more than its fair share of bandwidth, or is not willing to participate in forwarding packets, or trying to prevent other vehicles from communication. At the network layer, CR vehicles learn trust information about the broader network from each transmitted and received packet to develop policies about the routing and forwarding of received packets. One advantage of upper layer processing, is that the trust information exchanged is usually cryptographically protected. The propagation of the cognition capability up the communication stack of CR vehicles will motivate a multitude of cross-layer techniques that integrate security, spectrum sensing, spectrum access, and routing.

2.5 Summary

This chapter provides an overview of state of the art in CSS techniques proposed for CR-VANETs. We classified CSS techniques into detection techniques, prediction techniques, and database-assisted techniques. Prediction techniques use sensing statistics to determine the order of channels to sense in search for a SOP. We reviewed centralized, distributed, and hybrid CSS techniques in the aforementioned classes. We then reviewed two major physical layer attacks that face CSS. Namely, PUE and SSDF. We discussed the challenges of CR-VANETs that need to be considered when developing techniques to mitigate the effect of these attacks. Some open research issues are then discussed including the allocation of sensing responsibility to a selected number of vehicles to maximize detection accuracy while maintaining an acceptable control communication overhead, and extending the cognition capabilities up the communication stack to better address the security challenges of CR-VANETs.

Chapter 3

Decision-Based Cooperative Spectrum Sensing Using Random Medium Access

3.1 Introduction

Cooperative spectrum sensing is a powerful means of enhancing the spectrum awareness of cognitive radios in a fading environment by virtue of spatial diversity as opposed to stand-alone spectrum sensing. The duration of this collaborative endeavor is proportional to the sensing accuracy. However, an increase in sensing time causes a proportional loss in network throughput. Therefore, it is important to reduce spectrum sensing time given a spectrum sensing performance requirement, such as the probability of detection and/or false alarm, is satisfied. The tradeoff between sensing accuracy and throughput loss is referred to as sensing-throughput tradeoff [LZPH08].

The spectrum sensing time is a function of the local sensing time as well as the manner spectrum sensing data are collected from participating SUs. Reporting or collection of sensing data also are critical to any practical implementation of CSS. The details of sensing data reporting have been somehow overlooked in the literature, in spite of the thorough investigation of several CSS techniques in terms of performance analysis. Two sensing data collection methods have been identified in the literature: round-robin and random medium access. The first is to assign each participating SU an exclusive time slot to transmit its sensing data. This, however, requires continuous synchronization and management of allocated slots among SUs, especially when used in an ad-hoc setup where SUs continuously change their location like in a VANET. The other method is to use random medium access reporting, which is much simpler to implement. SUs are not allocated exclusive slots to report their sensing data, but use dialects of the celebrated Distributed Coordination Function (DCF) to coordinate access to a common control channel in a distributed manner. More specifically, when the reporting channel is detected idle, each terminal takes a random back off counter and transmits its report whenever this counter elapses. While it is waiting, a terminal will pause its counter whenever it detects another transmission. Random medium access reporting, intuitively, has two major effects on the CSS process: the number of received reports is now a random variable due to the non negligible probability of collision, and the reporting times need to be carefully balanced to achieve successful reporting while not sacrificing throughput. Also, it is usually assumed that SUs use a dedicated channel to report their sensing results separate from the primary channel. However, a dedicated reporting channel is not always available and SUs may have to report their sensing results to the FC over the primary channel they are detecting.

Multiple efforts have been directed at balancing the sensing-throughput tradeoff. Some works focused on optimizing the local sensing time to achieve a minimum sensing accuracy. These, however, usually rely on the statistical characteristics of the PUs' signals, which might not be available to the SUs. Different SUs might also need different sensing times as perceived PUs' signals characteristics, even when available, vary across distant SUs in an ad-hoc network. This limits the usefulness of local sensing time optimization, as terminals will not report to the FC until they all finish sensing.

Reporting time reduction also has been investigated in the literature. A number of researchers have investigated sequential detection with round-robin reporting, where instead of using fixed sample size at each SU, SUs can terminate the sensing process early once enough evidence is received about the PU activity. The FC in a centralized CSS scheme also can apply sequential testing. More specifically, in a two-tier sequential sensing scheme, SUs gather samples for a given spectrum band then compare the accumulated decision metric to a pair of decision thresholds, and then reports to the FC once the decision metric passes either threshold. SUs reports can be soft as in [NTK13] and [HSND11] or a hard local decision as in [KT07], [KT10], and [AM15]. The FC, itself, accumulates its own decision metric comparing it to a pair of thresholds as well, and then broadcasting its decision when either thresholds is passed and the CSS reporting process is terminated [SS08, KT10, XZR09, KG10, LZL12b, STZ13]. Determining the optimal sequential spectrum sensing time has been the focus of most of these studies. These works, however, assume terminals transmit their reports to the FC at particular time slots specified by and coordinated with the FC. Such a coordination is not always attainable. Furthermore, the agility of sequential sensing requires simultaneous sensing and reporting, and hence requires a dedicated Common Control Channel (CCC) [AM15]. While CR-VANETs, built over IEEE 802.11p PHY/MAC layers, have that, it still constitutes a burden over the WAVE/DSRC CCH that is originally intended for safety-related traffic. Moreover, using a CCC implies reporting can only start after all terminals have successfully made a decision or a maximum sensing time is reached, which would sacrifice the benefits of sequential detection.

Cognitive Radio MAC (CR-MAC) using random access based on the Request To Send (RTS)/Clear to Send (CTS) exchange of the IEEE 802.11 have been investigated in many studies as in [ZTSC07,JZS08,SZ08,LW11]. The RTS/CTS guarantees no interference to the PU before transmitting SUs' data, in addition to avoiding collisions among SUs [ZTSC07]. Three-phase RTS/CTS exchange is proposed in [JZS08] to exchange SOP information. The first phase is for contention and reservation where source and destination SUs exchange C-RTS/C-CTS messages while overhearing SUs refrain from accessing the shared medium. SOP information exchange occurs in the second phase using S-RTS/S-CTS messages. Finally, T-RTS/T-CTS messages are used to indicate the completion of data transmission. To accommodate CSS, the RTS packet function is extended in [LJ10a] to Sensing data and Request To Send (SRTS). Sensing data carried over SRTS packets are collected during a fixed collection period, where the average number of collected SRTS packets is a function of the length of the collection period. Therefore, the collection, (or reporting), period duration is predetermined according to the required sensing performance in what is known as the fixed collection period method [Lee15a]. This fixed collection period is improved by having an adaptive collection period in [Lee13a] and [Lee15a], where the optimal stopping time is determined based on the collected SRTS packets. As each time slot passes, the revenue vs. cost of ending the collection period is assessed. Backward induction is used to derive the expected revenue or cost of ending vs. extending the collection period.

In this chapter, we study the performance of decision-based cooperative spectrum sensing using random medium access. We derive closed form expressions for the detection and false alarm probabilities as explicit functions of the size of the contention window. We assume the absence of a dedicated reporting channel. Therefore, reports are transmitted over a shared channel, with the PU. The reporting channel, similar to the sensing channels, experience multi-path Rayleigh fading on top of the possible interference from PUs, so the possibility of decoding errors at the FC are accounted for. We also derive closed form expression for the average reporting time. Derived results can play a pivotal role in choosing the size of the contention window, and in choosing the number of reporting terminals. Computer simulations are used to verify the accuracy of the derived results. The remainder of this chapter is organized as follows. Section 3.2 describes the system model while Section 3.3 describes the etiquettes of cooperative spectrum sensing using random medium access. Performance analysis is conducted in Section 3.4. Numerical and simulations results are given in Section 3.5 while conclusions are drawn in Section 3.6.

3.2 System Model

We consider a network consisting of K CR terminals, $\mathrm{R}_1, \mathrm{R}_2, \ldots, \mathrm{R}_K$, distributed randomly within a circle of radius r, and a FC R_0 at the centre as shown in Figure 3.1. CR terminals share a frequency channel with a primary user, P, randomly located within the same circle. Cooperative spectrum sensing is employed by the CR terminals to examine the status, idle vs. busy, of P before using the channel.

Sensing and reporting channels follow a flat Rayleigh fading model. Hence, the average gain of the $\mathrm{P}-\mathrm{R}_0$, $\mathrm{P}-\mathrm{R}_k$, $k=1,2,\ldots,K$, and $\mathrm{R}_k-\mathrm{R}_0$, $k=1,2,\ldots,K$, channels are written as $\Omega_{p,0}=(d_{p,0})^{-\nu}$, $\Omega_{p,k}=(d_{p,k})^{-\nu}$, and $\Omega_{k,0}=(d_{k,0})^{-\nu}$, respectively, where $d_{p,0}$, $d_{p,k}$, and $d_{k,0}$ are the distances between P and R_0, between P and R_k, and between R_k and R_0, respectively, while $\nu=4$ is the path loss exponent. The transmission Signal to Noise Ratio (SNR) of P is $\rho_p \triangleq \frac{E_p}{\sigma^2}$, where E_p is the transmission energy and σ^2 is the variance of the additive white Gaussian noise. Similarly, the transmission SNR of R_k, $k=1,2,\ldots,K$, is denoted by ρ_k, and is written as $\rho_k=\frac{E_k}{\sigma^2}$, where E_k is the transmission energy. In this article, all CR terminals are assumed to have the same transmission energy, hence $\rho_1=\rho_2=\cdots=\rho_K=\rho$.

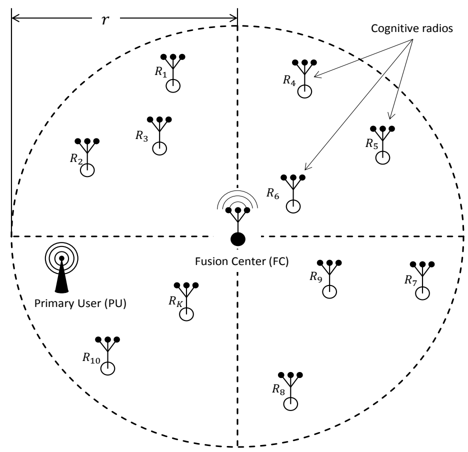

Figure 3.1: System model.

3.2.1 Energy Detection

CR terminals use Energy Detection (ED) to examine the status of the PU P. ED is employed locally at the CR terminals due to its simplicity, speed, ease of implementation and analysis. CR terminal R_k calculates an estimate ϕ_k of the present energy after sensing the channel for a sensing period t_s seconds by summing $2u=2t_sW$ sensing samples, where WHz is the channel bandwidth. CR terminal R_k, then compares ϕ_k to a decision threshold λ to get a local binary decision $d_k \in \{0,1\}$. More specifically, R_k sets $d_k=1$ if $\phi_k \geq \lambda$, otherwise it decides that $d_k = 0$. These local decisions correspond to the hypotheses P is active, denoted by $\mathcal{H}_1$, when $d_k = 1$, vs. P is idle, denoted by $\mathcal{H}_0$, when $d_k = 0$. The decision threshold λ is chosen such that all terminals operate at a given probability of false alarm, P_{fa}, which represents the probability of mistakenly assuming that P is active while it is idle and given by [DAS03]

$$P_{fa} \triangleq \Pr[\phi_k \geq \lambda | \mathcal{H}_0] = \frac{\Gamma(u, \frac{\lambda}{2})}{\Gamma(u)}, \tag{3.1}$$

where $\Gamma(\cdot)$ and $\Gamma(\cdot, \cdot)$ are the Gamma and upper incomplete Gamma functions, respectively [GR07]. Note that, the decision threshold λ varies from one SU to another, and from one time frame to another for the same SU. ED performance is also measured in terms of the probability of detection, $P_{d,k}$. This probability is defined as the probability of detecting that P is active, (i.e., $P_{d,k} \triangleq \Pr[\phi_k \geq \lambda | \mathcal{H}_1]$). Using the flat Rayleigh fading assumption, [DAS03] has shown that this probability can be written as

$$\begin{aligned} P_{d,k} &= e^{-\frac{\lambda}{2}} \sum_{i=0}^{u-2} \frac{\lambda^i}{2^i i!} + \left[\frac{1+\overline{\gamma}_{p,k}}{\overline{\gamma}_{p,k}}\right]^{u-1} \\ &\times \left\{ e^{\frac{-\lambda}{2(1+\overline{\gamma}_{p,k})}} - e^{-\frac{\lambda}{2}} \sum_{i=0}^{u-2} \frac{1}{i!} \left[\frac{\lambda \overline{\gamma}_{p,k}}{2(1+\overline{\gamma}_{p,k})}\right]^i \right\}, \end{aligned} \tag{3.2}$$

where $\overline{\gamma}_{p,k} = \rho_p \Omega_{p,k}$ is the average received SNR. Unlike P_{fa}, CR terminals generally experience different detection probabilities due to differences in sensing channel gains, hence, $P_{d,1} \neq P_{d,2} \neq \cdots \neq P_{d,K}$.

3.2.2 Decoding Errors

Local decisions are reported to the FC R_0 over imperfect wireless channels. We use Binary Phase Shift Keying (BPSK) modulation to marginalize potential decoding errors. We also require all reports received in outage to be discarded by the FC.
Let $\hat{d}_k$, $k = 1, 2, \ldots, K$ denote the decoded version of d_k received at R_0 from R_k. Furthermore, let ψ_k denote the received SNR, given the hypothesis $\mathcal{H}_0$ is true, and Signal to Interference plus Noise Ratio (SINR), given the hypothesis $\mathcal{H}_1$ is true. Accordingly, the proba-

bility that $\hat{d}_k$ is considered in the final decision by R_0 can be written as $\Pr[\psi_k \geq \gamma_{\mathrm{th}} | \mathcal{H}_j]$, $j = 0, 1$, where $\gamma_{\mathrm{th}} \triangleq 2^Q - 1$ is the outage threshold and Q is the spectral efficiency. Furthermore, the probability that $\hat{d}_k$ is decoded successfully by the FC R_0 is written as $\Pr[\hat{d}_k = d_k | \mathcal{H}_j] = 1 - P_{e,k|\mathcal{H}_j}$, where $P_{e,k|\mathcal{H}_j}$ is the corresponding decoding error probability.

In order to calculate the decoding error probability, $P_{e,k|\mathcal{H}_j}$, $j = 0, 1$, we average the conditional error probability of BSPK, (i.e., $Q(\sqrt{2\psi})$, where $Q(x)$ is the Gaussian Q-function), over the conditional Probability Density Function (PDF) $f_{\psi|\psi \geq \gamma_{\mathrm{th}}; \mathcal{H}_j}(\psi)$ as follows

$$P_{e,k|\mathcal{H}_j} = \int_{\gamma_{\mathrm{th}}}^{\infty} Q(\sqrt{2\psi}) f_{\psi_k|\psi \geq \gamma_{\mathrm{th}}; \mathcal{H}_j}(\psi) d\psi, \quad j = 0, 1. \tag{3.3}$$

To solve this integral, we need to find the conditional PDF $f_{\psi|\psi \geq \gamma_{\mathrm{th}}; \mathcal{H}_j}(\psi)$. Given the definition of a conditional distribution along with the Cumulative Distribution Function (CDF) of ψ_k under $\mathcal{H}_j$, $j = 0, 1$, given by [AAM15] as

$$F_{\psi_k|\mathcal{H}_j}(\psi) = \begin{cases} 1 - e^{-\psi/\overline{\gamma}_{k,0}}, & j = 0; \\ 1 - \frac{\overline{\gamma}_{k,0}}{\overline{\gamma}_{k,0} + \overline{\gamma}_{p,k}\psi} e^{-\psi/\overline{\gamma}_{k,0}}, & j = 1, \end{cases} \tag{3.4}$$

It can be readily shown that $f_{\psi_k|\psi \geq \gamma_{\mathrm{th}}; \mathcal{H}_j}(\psi)$ can be written as

$$f_{\psi_k|\psi_k \geq \gamma_{\mathrm{th}}; \mathcal{H}_j}(\psi) = \begin{cases} \frac{1}{\overline{\gamma}_{k,0}} e^{\gamma_{\mathrm{th}}/\overline{\gamma}_{k,0}} e^{-\psi/\overline{\gamma}_{k,0}}, & j = 0; \\ (\overline{\gamma}_{k,0} + \overline{\gamma}_{p,0}\gamma_{\mathrm{th}}) e^{\gamma_{\mathrm{th}}/\overline{\gamma}_{k,0}} e^{-\psi/\overline{\gamma}_{k,0}} & \\ \left[\frac{1}{\overline{\gamma}_{k,0}(\overline{\gamma}_{k,0} + \overline{\gamma}_{p,k}\psi)} + \frac{\overline{\gamma}_{p,0}}{(\overline{\gamma}_{k,0} + \overline{\gamma}_{p,0}\psi)^2} \right], & j = 1. \end{cases} \tag{3.5}$$

$$P_{e,k|\mathcal{H}_0} = Q\big(\sqrt{2\gamma_{\mathrm{th}}}\big) - e^{\gamma_{\mathrm{th}}/\overline{\gamma}_{k,0}}\sqrt{\frac{\overline{\gamma}_{k,0}}{\overline{\gamma}_{k,0}+1}}Q\left(\sqrt{2\gamma_{\mathrm{th}}\left(1+\frac{1}{\overline{\gamma}_{k,0}}\right)}\right), \tag{3.6a}$$

$$\begin{aligned} P_{e,k|\mathcal{H}_1} \approx \frac{a_L}{\overline{\gamma}_{p,0}}(\overline{\gamma}_{k,0}+\overline{\gamma}_{p,0}\gamma_{\mathrm{th}})e^{\gamma_{\mathrm{th}}/\overline{\gamma}_{k,0}}\Bigg\{\sum_{l=1}^{L+1}\frac{e^{(2b_l\overline{\gamma}_{k,0}+1)/\overline{\gamma}_{p,0}}}{\overline{\gamma}_{k,0}}\mathsf{E}_i\left[\left(\frac{1}{\overline{\gamma}_{k,0}}+2b_l\right)\left(\frac{\overline{\gamma}_{k,0}}{\overline{\gamma}_{p,0}}+\gamma_{\mathrm{th}}\right)\right] \\ +\sum_{l=1}^{L+1}\left(\frac{e^{-\gamma_{\mathrm{th}}(2b_l+1/\overline{\gamma}_{k,0})}}{\gamma_{\mathrm{th}}+\frac{\overline{\gamma}_{k,0}}{\overline{\gamma}_{p,0}}} - \left(2b_l+\frac{1}{\overline{\gamma}_{k,0}}\right)e^{(2b_l\overline{\gamma}_{k,0}+1)/\overline{\gamma}_{p,0}}\mathsf{E}_i\left[\left(\frac{1}{\overline{\gamma}_{k,0}}+2b_l\right)\left(\frac{\overline{\gamma}_{k,0}}{\overline{\gamma}_{p,0}}+\gamma_{\mathrm{th}}\right)\right]\right)\Bigg\}. \end{aligned} \tag{3.6b}$$

Using these expressions, along with the approximation of $Q(\sqrt{2\psi})$ proposed in [WLK11, Eqn.5], $P_{e,k|\mathcal{H}_j}$, $j = 0, 1$, can be obtained in closed forms as written in (3.6a) and (3.6b). In these expressions, $\mathsf{E}_i[x] = \int_x^\infty \frac{e^{-t}}{t}dt$ is the exponential integral function [GR07], $a_L = \frac{1}{2(L+1)}$, and $b_l = \frac{L+1}{\pi}\left[\cot\left(\frac{l-1}{2(L+1)}\pi\right) - \cot\left(\frac{l}{2(L+1)}\pi\right)\right]$ [WLK11].

3.3 Cooperative Spectrum Sensing

3.3.1 Random Medium Access

CR terminals contend to send their local decisions to the FC R_0 at the end of the local sensing period using random medium access as shown in Figure 3.2. To avoid collision, each CR terminal chooses a random counter, ϑ_k, from the window $[1, c_{\max}]$ according to the uniform distribution. Therefore, the probability that R_k chooses any counter value, say c_*, where $1 \le c_* \le c_{\max}$, is $\Pr[\vartheta_k = c_*] = \frac{1}{c_{\max}}$. CR terminal R_k waits $\vartheta_k t_{ts}$ seconds before transmitting, where t_{ts} is the duration of a time slot, which is equivalent to the time needed to transmit a single local report. A CR terminal keeps listening to the channel while waiting for its timer to expire. If the CR terminal detects a transmission, it pauses its counter until the transmission ends[1]. Note that, transmissions are based on unacknowledged broadcasts. Hence, the transmissions of two or more terminals will collide if they accidently chose the

[1]Intuitively, this is based on the assumption that network terminals are within the transmission range of each other.

same counter. Since, terminals can not transmit and receive at the same time, collisions are not detected by transmitting CR terminals.

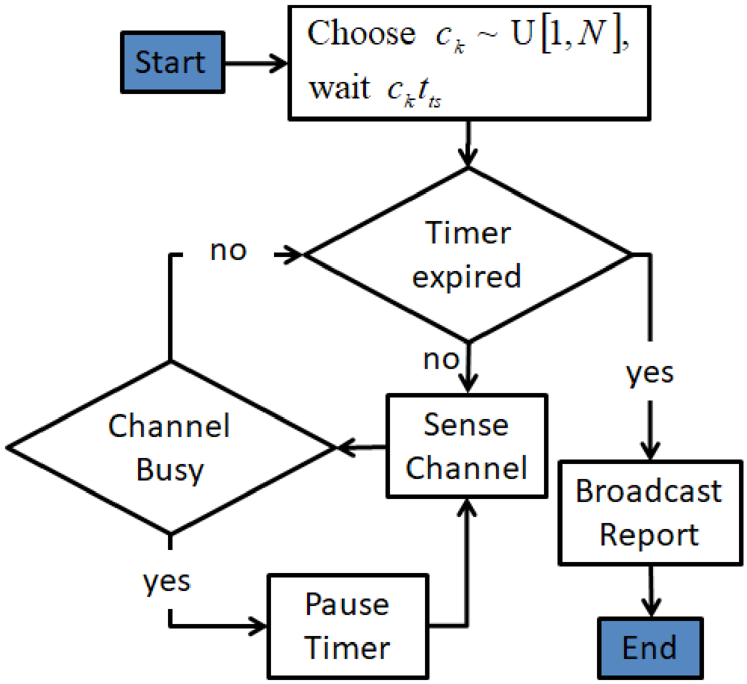

Figure 3.2: Block Diagram of the Random Medium Access Reporting Process.

3.3.2 Decision Combining

The FC R_0 calculates a decision metric, D, after the reporting by combining successfully received decisions from the terminals. Let $\mathcal{M}$ denote the set of successfully received decisions, where $0 \leq |\mathcal{M}| \leq K$, $|\cdot|$ is the cardinality of the set $\mathcal{M}$, then D can be written as $D = \hat{d}_1 + \hat{d}_2 + \cdots + \hat{d}_{|\mathcal{M}|}$. The FC decision is made by comparing D with a decision threshold D_{th}. In this chapter, we use the logical OR fusion rule, and hence $D_{\text{th}} = 1$. If $D \geq D_{\text{th}}$, then R_0 decides that P is active, otherwise, it decides that P is idle. If no local sensing decisions are received, (i.e., $|\mathcal{M}| = 0$), then the FC R_0 makes no decision and the cooperative spectrum sensing process is repeated in what is referred to as a "fail to sense" event.

3.4 Performance Analysis

3.4.1 Probability of Detection and Probability of False Alarm

According to the aforementioned decision rule, R_0 decides that P is active only when it successfully receives at least a single report with a value of "1". Hence, the overall probabilities of detection and false alarm, denoted by Q_d and Q_{fa}, respectively, can be written

$$Q_d \triangleq \Pr[D \geq 1|\mathcal{H}_1] = 1 - \Pr[D = 0|\mathcal{H}_1], \tag{3.7a}$$

$$Q_{fa} \triangleq \Pr[D \geq 1|\mathcal{H}_0] = 1 - \Pr[D = 0|\mathcal{H}_0]. \tag{3.7b}$$

For a decision to be made, the number of elements in $\mathcal{M}$ has to be nonzero. Hence, it can take any value between '1' and 'K'. In either case, there has to be an equal number of counters that are taken by a single terminal, and that each of these terminals has to have a decoded decision of "0". Mathematically speaking, Q_d and Q_{fa} can be rewritten using the total probability theorem as

$$Q_d = 1 - \sum_{\zeta=1}^{K} \Pr[|\mathcal{M}| = \zeta|\mathcal{H}_1] \Pr[D = 0|\mathcal{H}_1; \zeta], \tag{3.8a}$$

$$Q_{fa} = 1 - \sum_{\zeta=1}^{K} \Pr[|\mathcal{M}| = \zeta|\mathcal{H}_0] \Pr[D = 0|\mathcal{H}_0; \zeta]. \tag{3.8b}$$

A transmitted decision d_k is considered an element of $\mathcal{M}$ if it did not collide with any other transmission, and if it was received without an outage. The independence between these two events allows us to expand $\Pr[|\mathcal{M}| = \zeta|\mathcal{H}_j]$, $j = 0, 1$ as $\Pr[|\mathcal{M}| = \zeta|\mathcal{H}_j] = \Pr[K_{\text{alone}} = \zeta, N_{\text{success}} = \zeta|\mathcal{H}_j] = \Pr[K_{\text{alone}} = \zeta] \Pr[N_{\text{success}} = \zeta|\mathcal{H}_j]$, where K_{alone} is the number of counters chosen by a single terminal, while N_{success} is the number of reports that have not experienced outage. To proceed, we first need to calculate the probabilities $\Pr[K_{\text{alone}} = \zeta]$ and $\Pr[N_{\text{success}} = \zeta|\mathcal{H}_j]$, $j = 0, 1$.

The random variable K_{alone} corresponds to a special case of combinatorics where a number of terminals, K, will be distributed over a number of counters, $c_{\max}$, such that only ζ terminals will have unique counters, while the remaining $K-\zeta$ terminals will be sharing counters. More specifically, there will be at least two terminals per counter, and hence, the maximum number of chosen counters will be $\zeta+\hat{\zeta}$, where $\hat{\zeta} \triangleq \left\lfloor \frac{1}{2}(K-\zeta) \right\rfloor$. Using the r-associated Stirling numbers of the second kind [Com74, Sec.6.2], the probability $\Pr[K_{\text{alone}}=\zeta]$ can be written as

$$\begin{aligned}\Pr[K_{\text{alone}}=\zeta] &= \frac{1}{c_{\max}^{K}}\binom{K}{\zeta}\binom{c_{\max}}{\zeta} \\ &\times \sum_{i=1}^{\hat{\zeta}} S_r(K-\zeta,i,2)\binom{c_{\max}-\zeta}{i} i!,\end{aligned} \tag{3.9}$$

where the $\frac{1}{c_{\max}^{K}}$ factor if the probability of choosing K counters, $\binom{K}{\zeta}\binom{c_{\max}}{\zeta}$ is the number of different ways of assigning ζ counters to ζ terminals, while the summation term is the number of ways of allocating the remaining $K-\zeta$ terminals to a maximum of $\hat{\zeta}$ counters such that each counter is chosen by at least two terminals. Finally, $S_r(n,k)$ is the r-associated Stirling number of the second kind defined using the recursion

$$S_r(n+1,k) = kS_r(n,k) + \binom{n}{r-1} S_r(n-r+1,k-1), \tag{3.10}$$

where $S_r(n,k)=0$ for $n<rk$.

Next, the probability $\Pr[N_{\text{success}}=\zeta|\mathcal{H}_j]$, $j=0,1$, can be written as

$$\Pr[N_{\text{success}}=\zeta|\mathcal{H}_j] = \sum_{n=1}^{N(\zeta)} \mathbf{A}_{n|\mathcal{H}_j}\overline{\mathbf{A}}_{n|\mathcal{H}_j}, \tag{3.11}$$

where $N(\zeta) \triangleq \binom{K}{\zeta} = \frac{(K)!}{(K-\zeta)!\zeta!}$ is the number of permutations of K elements taken ζ at a time, $\mathbf{A}_{n|\mathcal{H}_j}$ is the product of the probabilities $\Pr[\psi_k \geq \gamma_{\text{th}}|\mathcal{H}_j]$, $j=0,1$, of the ζ terminals chosen in the n^{th} permutation, while $\overline{\mathbf{A}}_{n|\mathcal{H}_j}$ is the product of the probabilities $1-\Pr[\psi_k \geq \gamma_{\text{th}}|\mathcal{H}_j]$, $j=0,1$, of the remaining $k-\zeta$ terminals in the n^{th} permutation. The probability $\Pr[\psi_k \geq \gamma_{\text{th}}|\mathcal{H}_j]$, $j=0,1$, can be calculated using (3.4) since $\Pr[\psi_k \geq \gamma_{\text{th}}|\mathcal{H}_j] = 1-F_{\psi_k|\mathcal{H}_j}(\gamma_{\text{th}})$, $j=0,1$.

Finally, the probability $\Pr[D = 0|\mathcal{H}_j; \zeta]$ in (3.8a) and (3.8b) can be calculated similar to (3.11) but using different probabilities. More specifically, we can write

$$\Pr[D = 0|\mathcal{H}_j; \zeta] = \sum_{n=1}^{N(\zeta)} \mathbf{B}_{n|\mathcal{H}_j} \overline{\mathbf{B}}_{n|\mathcal{H}_j}, \tag{3.12}$$

where $\mathbf{B}_{n|\mathcal{H}_j}$ and $\overline{\mathbf{B}}_{n|\mathcal{H}_j}$ are defined similar to $\mathbf{A}_{n|\mathcal{H}_j}$ and $\overline{\mathbf{A}}_{n|\mathcal{H}_j}$, but using different probabilities. Instead of using $\Pr[\psi_k \geq \gamma_{\text{th}}|\mathcal{H}_j]$ and its complement, $\mathbf{B}_{n|\mathcal{H}_j}$ and $\overline{\mathbf{B}}_{n|\mathcal{H}_j}$ are defined using the probability $\Pr[\hat{d}_k = 0|\mathcal{H}_j]$, $j = 0, 1$, $k = 1, 2, \ldots, K$, and its complement. Using (3.1), (3.2), (3.6a), and (3.6b), this probability can be written as

$$\begin{aligned} \Pr[\hat{d}_k = 0|\mathcal{H}_0] &= \Pr[\phi_k < \lambda|\mathcal{H}_0](1 - P_{e,k|\mathcal{H}_0}) \\ &+ \Pr[\phi_k \geq \lambda|\mathcal{H}_0] P_{e,k|\mathcal{H}_0} \\ &= 1 - P_{fa} - P_{e,k|\mathcal{H}_0} + 2P_{fa} P_{e,k|\mathcal{H}_0}, \end{aligned} \tag{3.13}$$

when $j = 0$, and

$$\begin{aligned} \Pr[\hat{d}_k = 0|\mathcal{H}_1] &= \Pr[\phi_k < \lambda|\mathcal{H}_1](1 - P_{e,k|\mathcal{H}_1}) \\ &+ \Pr[\phi_k \geq \lambda|\mathcal{H}_1] P_{e,k|\mathcal{H}_1} \\ &= 1 - P_{d,k} - P_{e,k|\mathcal{H}_1} + 2P_{d,k} P_{e,k|\mathcal{H}_1}, \end{aligned} \tag{3.14}$$

when $j = 1$.

By substituting (3.9), (3.11), and (3.12) in (3.8a) and (3.8b), the desired detection and false alarm probabilities can be rewritten in (3.15a) and (3.15b) respectively.

$$
\begin{aligned}
Q_d = 1 - \sum_{\zeta=1}^{K} \Bigg\{ & \Bigg[\frac{1}{c_{\max}^{K}} \binom{K}{\zeta} \binom{c_{\max}}{\zeta} \sum_{i=1}^{\hat{\zeta}} S_r(K-\zeta, i, 2) \binom{c_{\max}-\zeta}{i} i! \Bigg] \\
& \Bigg[\sum_{n=1}^{N(\zeta)} \mathbf{A}_{n|\mathcal{H}_1} \overline{\mathbf{A}}_{n|\mathcal{H}_1} \Bigg] \Bigg[\sum_{n=1}^{N(\zeta)} \mathbf{B}_{n|\mathcal{H}_1} \overline{\mathbf{B}}_{n|\mathcal{H}_1} \Bigg] \Bigg\}, \qquad (3.15a) \\
Q_{fa} = 1 - \sum_{\zeta=1}^{K} \Bigg\{ & \Bigg[\frac{1}{c_{\max}^{K}} \binom{K}{\zeta} \binom{c_{\max}}{\zeta} \sum_{i=1}^{\hat{\zeta}} S_r(K-\zeta, i, 2) \binom{c_{\max}-\zeta}{i} i! \Bigg] \\
& \Bigg[\sum_{n=1}^{N(\zeta)} \mathbf{A}_{n|\mathcal{H}_0} \overline{\mathbf{A}}_{n|\mathcal{H}_0} \Bigg] \Bigg[\sum_{n=1}^{N(\zeta)} \mathbf{B}_{n|\mathcal{H}_0} \overline{\mathbf{B}}_{n|\mathcal{H}_0} \Bigg] \Bigg\}. \qquad (3.15b)
\end{aligned}
$$

3.4.2 Reporting Time

Another important performance metric is the reporting time. Following the etiquettes of the random medium access described in Section 3.3, reporting time can be written as the summation of two components as follows

$$t_{\text{rep}} = (\hat{\vartheta} + K_{\text{dist}}) t_{ts}, \qquad (3.16)$$

where $\hat{\vartheta} \triangleq \max\{\vartheta_1, \vartheta_2, \ldots, \vartheta_K\}$ is the maximum chosen counter while K_{dist} is the number of distinct counters[2]. Based on this formulation, it can be readily deduced that $2t_{ts} \leq t_{\text{rep}} \leq (c_{\max} + K)t_{ts}$. The average value of this time, denoted by $\bar{t}_{\text{rep}}$, can be obtained by taking the expectation of (3.16) as follows

$$\bar{t}_{\text{rep}} = \mathbb{E}\big[\hat{\vartheta}\big] t_{ts} + \mathbb{E}\big[K_{\text{dist}}\big] t_{ts}, \qquad (3.17)$$

where $\mathbb{E}[\cdot]$ is the expectation operator. The mean value of $\hat{\vartheta}$ can be obtained as follows. First, the probability $\Pr[\hat{\vartheta} \leq \theta]$ can be written as

$$\Pr[\hat{\vartheta} \leq \zeta] \triangleq F_{\hat{\vartheta}}(\zeta) = \left(\frac{\zeta}{c_{\max}} \right)^{K}. \qquad (3.18)$$

[2]It should be emphasized that K_{dist} and K_{alone} are two different random variables.

Next, by taking the difference between $F_{\hat{\vartheta}}(\zeta)$ and $F_{\hat{\vartheta}}(\zeta-1)$, the corresponding PDF can be written as

$$f_{\hat{\vartheta}}(\zeta) \triangleq \Pr[\hat{\vartheta}=\zeta] = \left(\frac{\zeta}{c_{\max}}\right)^K - \left(\frac{\zeta-1}{c_{\max}}\right)^K. \tag{3.19}$$

Hence, the desired mean value, $\mathbb{E}[\hat{\vartheta}]$, can be written as

$$\mathbb{E}[\hat{\vartheta}] = \frac{1}{c_{\max}} \sum_{\zeta=1}^{c_{\max}} \left\{\zeta^{K+1} - \zeta(\zeta-1)^K\right\}. \tag{3.20}$$

On the other hand, the PDF of K_{dist} can be obtained using the Stirling number of the second kind [GR07, 9.744]. More specifically, we can write

$$\Pr[K_{\text{dist}}=\zeta] = \binom{c_{\max}}{\zeta} \frac{1}{c_{\max}^K} \sum_{j=0}^{\zeta} (-1)^{\zeta-j} \binom{\zeta}{j} j^K, \tag{3.21}$$

where $\binom{c_{\max}}{\zeta}$ is the number of unique ways of choosing ζ counters from a set of $c_{\max}$ counters, while the summation term is the number of ways of distributing K terminals over these ζ counters. Using this PDF, the mean value, $\mathbb{E}[K_{\text{dist}}]$, can be obtained as

$$\mathbb{E}\left[K_{\text{dist}}\right] = \frac{1}{c_{\max}^K} \sum_{\zeta=1}^{K} \zeta \binom{c_{\max}}{\zeta} \sum_{j=0}^{\zeta} (-1)^{\zeta-j} \binom{\zeta}{j} j^K. \tag{3.22}$$

3.5 Numerical and Simulation Results

In this section we evaluate the accuracy of the derived results by comparing them to simulation results. We also will compare the results to the round-robin case, where reports are transmitted in a pre-scheduled manner. Fig. 3.3 shows the detection probability as a function of $c_{\max}$ for different values of K. Intuitively, the smaller the value of $c_{\max}$ the more collisions the terminals will endure. Hence, the number of successfully received decisions will be small which will decrease the detection probability. Observe that even when $c_{\max} = K$, the random nature of counter selection forces a non-negligible number of collisions. Fig. 3.4 shows the relative average reporting time, (i.e., $\frac{\bar{t}_{\text{rep}}}{t_{ts}}$), as a function of K. Interestingly, this figure shows that random medium access requires more reporting time than round-robin reporting only when the number of terminals is small. When the number of terminals grow, this behaviour is reversed. In all of our results we verified that the upper and lower limits of the 95% confidence interval are so close that they practically coincide with the simulation points, (i.e., the sample distribution mean). For more on the calculation of the 95% confidence interval see Appendix A.

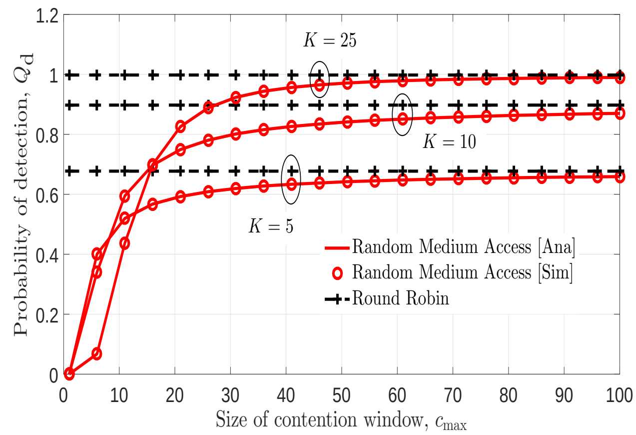

Figure 3.3: Detection probability as a function of $c_{\max}$ for different values of K. The following parameters are used: $r = 1$, $Q = 0.2$, $\rho_p = -10$dB and $\rho = 5$dB.

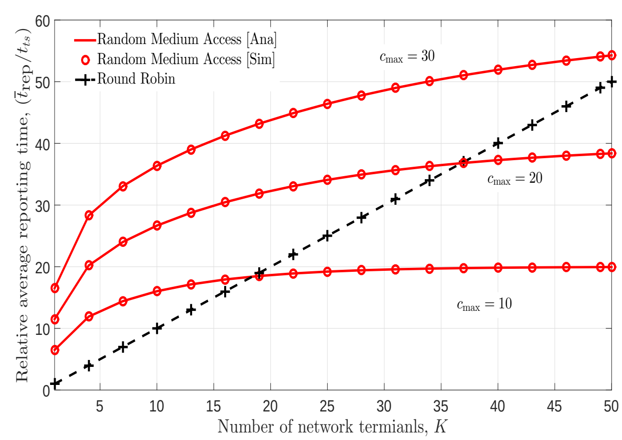

Figure 3.4: Relative average reporting time, $\bar{t}_{\text{rep}}/t_{ts}$ as a function of K for different values of $c_{\max}$.

3.6 Summary

The problem of decision-based cooperative spectrum sensing using random medium access is presented. We have derived closed form expressions for the detection and false alarm probabilities, in addition to the average reporting time. The derived results showed direct dependence of these metrics on the number of network terminals as well as the size of the contention window.

Chapter 4

Cooperative Spectrum Sensing Using Random Medium Access Sequential Reporting

4.1 Introduction

In the previous chapter we studied the performance of decision-based CSS using random medium access, the OR-decision rule at the FC, and a fixed reporting phase duration. In this chapter, we study decision-based CSS using random medium access sequential reporting and a K-out-of-M decision rule at the FC. Early termination sequential reporting allows the FC to terminate the reporting phase once it receives sufficient evidence about the status of the primary user, and hence has the potential of reducing the duration of the CSS reporting phase and increasing the overall system throughput.

The majority of works on CSS assumes scheduled reporting in a round-robin manner, which requires the presence of a central terminal to coordinate it in a Time Division Medium Access (TDMA) manner. On the other hand, terminals in a vehicular network for example access the common control channel using random medium access based on certain access categories. Hence, the average reporting time and the final decision varies based on the number of vehicles that successfully transmit their local decisions, or sensing information in general, to the entire network. Therefore, we are interested in random medium access-based reporting using unacknowledged transmissions, (e.g., the case of vehicular networks using IEEE802.11p, where terminals use random back-offs to avoid colliding with each other). Each terminal chooses a random back-off counter before accessing the channel. Once this counter expires, the terminal performs a clear channel assessment. If the channel is found empty, the terminal transmits its decision, otherwise, it choose another back-off counter and repeats the same process.

The current principal works in the field of random medium access reporting are [LJ10b, Lee13b, Lee15b]. In these works, the authors considered a centralized network where the duration of the random medium access period is designed to strike a balance between spectrum sensing accuracy and throughput. In our work, the reporting period is not predetermined, but rather depends upon reaching enough evidence to terminate the reporting phase. More specifically, In this chapter, our objective is to derive the detection and false alarm probabilities as well as the average reporting time, in number of time slots, as functions of the medium access process. This will indicate to us the possible reduction in the reporting phase duration of decision-based CSS using sequential reporting and the K-out-of-M decision rule at the FC. The remainder of this chapter is organized as follows. Section 4.2 describes the system model while performance analysis is conducted in Section 4.3. Numerical and simulations results are given in Section 4.4 while conclusions are drawn in Section 4.5.

4.2 System Model

We consider the network shown in Fig. 4.1 consisting of K CR terminals, $\mathrm{R}_1, \mathrm{R}_2, \ldots, \mathrm{R}_K$, randomly distributed within a circle of radius r centred around a FC R_0. The objective is to examine the status of a PU transmitter, P, that is located within the same circle. In doing so, terminals $\{\mathrm{R}_k\}_{k=1}^{K}$ use hard decision fusion centralized CSS according to the K-out-of-M decision rule. The channels between all terminals are assumed to follow a flat Rayleigh fading model. The transmission SNR of P is $\rho_p \triangleq \frac{E_p}{\sigma^2}$, where E_p is the transmission energy

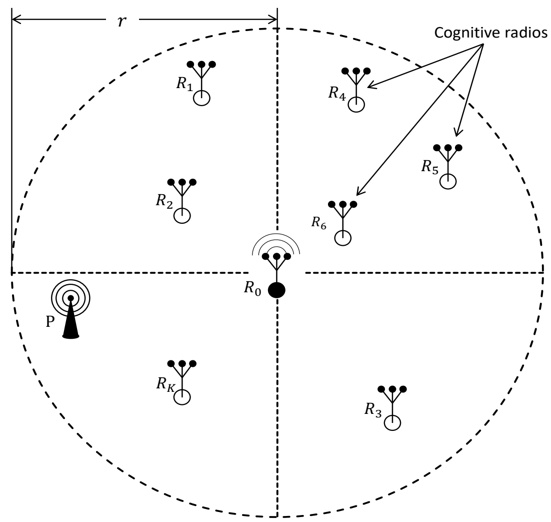

Figure 4.1: System model.

of P and σ^2 is the additive white Gaussian noise variance. Similarly, the transmission SNR of CR terminals $\{\mathrm{R}_k\}_{k=1}^{K}$ are denoted by $\rho_1 = \rho_2 = \cdots = \rho_K = \rho = \frac{E}{\sigma^2}$, where the transmission energy E is the same for all CR terminals.

4.2.1 Energy Detection

Energy detection is used to examine the status of PU P. After listening to the channel for T_s seconds, terminal $\{\mathrm{R}_k\}_{k=1}^{K}$ calculates an estimate of the present energy by summing $2u = 2T_sW$ samples of the channel, where WHz is the channel bandwidth. This estimate, denoted by $\{\phi_k\}_{k=1}^{K}$, is then compared to a decision threshold, λ, to make a local decision $\{d_k\}_{k=1}^{K} \in \{0, 1\}$. More specifically, if $\{\phi_k\}_{k=1}^{K}$ meets or exceeds λ, then $\{\mathrm{R}_k\}_{k=1}^{K}$ sets $\{d_k\}_{k=1}^{K} = 1$, otherwise, it decides that $\{d_k\}_{k=1}^{K} = 0$. These local decisions correspond to choosing that P is active (denoted by $\mathcal{H}_1$), when $d_k = 1$, and that P is inactive (denoted by $\mathcal{H}_0$), when $d_k = 0$ respectively. The decision threshold λ is chosen such that all terminals operate at a preset probability of a false alarm, denoted by P_{fa}, given by [DAS03]

$$P_{fa} \triangleq \Pr[\phi_k \geq \lambda | \mathcal{H}_0] = \frac{\Gamma(u, \frac{\lambda}{2})}{\Gamma(u)}, \tag{4.1}$$

where $\Gamma(\cdot)$ and $\Gamma(\cdot,\cdot)$ are the Gamma and upper incomplete Gamma functions, respectively [GR07]. In addition to this probability, the performance of energy detection is measured using the probability of detection. Recalling the Rayleigh fading assumption for the $\mathrm{P}-\{\mathrm{R}_k\}_{k=1}^{K}$ sensing channel, the detection probability of $\{\mathrm{R}_k\}_{k=1}^{K}$ can be written as [DAS03]

$$\begin{aligned} P_{d,k} &= e^{-\frac{\lambda}{2}}\sum_{i=0}^{u-2}\frac{\lambda^i}{2^i i!} + \left[\frac{1+\overline{\gamma}_{p,k}}{\overline{\gamma}_{p,k}}\right]^{u-1} \\ &\times \left\{e^{\frac{-\lambda}{2(1+\overline{\gamma}_{p,k})}} - e^{-\frac{\lambda}{2}}\sum_{i=0}^{u-2}\frac{1}{i!}\left[\frac{\lambda\overline{\gamma}_{p,k}}{2(1+\overline{\gamma}_{p,k})}\right]^i\right\}, \end{aligned} \tag{4.2}$$

where $\overline{\gamma}_{p,k}=\rho_p\Omega_{p,k}$ is the average SNR, $\Omega_{p,k}=(d_{p,k})^{-\nu}$ is the average channel gain, $d_{p,k}$ is the distance between P and $\{\mathrm{R}_k\}_{k=1}^{K}$, and $\nu=4$ is the path-loss exponent. It should be remarked that unlike the case of probability of a false alarm, different terminals have different probabilities of detection, (i.e., $P_{d,1}\neq P_{d,2}\neq\cdots\neq P_{d,K}$), because $\Omega_{p,1}\neq\Omega_{p,2}\neq\cdots\neq\Omega_{p,K}$.

4.2.2 Decoding Errors

Case of $\mathcal{H}_0$

After making local decisions, CR terminals transmit their local decisions to the FC R_0 using BPSK modulation. The received signals at R_0 can accordingly be written as $y_{k,0}=\sqrt{E}h_{k,0}(2d_k-1)+n_0$, $k=1,2,\ldots,K$, where $h_{k,0}$ is the channel coefficient while n_0 is a zero-mean additive white Gaussian noise with variance σ^2. We assume the FC R_0 has perfect knowledge of the channel coefficients, $h_{k,0}$, hence it uses coherent detection to obtain a decoded version of d_k, denoted by $\hat{d}_k$. The received SNR at the FC can then be written as $\gamma_{k,0}\triangleq\frac{E}{\sigma^2}|h_{k,0}|^2=\rho|h_{k,0}|^2$. Due to the Rayleigh fading assumption, the received SNR $\gamma_{k,0}$ is an exponentially distributed random variable with mean value $\overline{\gamma}_{k,0}=\rho\Omega_{k,0}$, where $\Omega_{k,0}\triangleq\left(d_{k,0}\right)^{-\nu}$, and $d_{k,0}$ is the distance between $\{\mathrm{R}_k\}_{k=1}^{K}$ and the FC R_0.

The FC R_0 excludes reports that experience a capacity outage to reduce the impact of decoding errors. More specifically, R_0 excludes $\mathrm{R}_{k,0}$'s report if the channel spectral efficiency $C_{k,0}=\frac{1}{2}\log(1+\gamma_{k,0})$ fell below R_k's transmit spectral efficiency, q. This is equivalent to the condition $\gamma_{k,0} < \gamma_{\text{th}}$, where $\gamma_{\text{th}} \triangleq 2^{2q} - 1$. Therefore, the decoded local decision, $\hat{d}_k$, experiences a decoding error with probability $P_{e,k|\mathcal{H}_0}$ that can be written as

$$P_{e,k|\mathcal{H}_0} \triangleq \Pr[\hat{d}_k \neq d_k|\mathcal{H}_0] = \int_{\gamma_{\text{th}}}^{\infty} Q(\sqrt{2\gamma}) f_{\gamma|\gamma\geq\gamma_{\text{th}};\mathcal{H}_0}(\gamma) d\gamma, \tag{4.3}$$

where $Q(\cdot)$ is the Gaussian Q-function, $Q(\sqrt{2\gamma})$ is the conditional bit error probability of BPSK, while $f_{\gamma_{k,0}|\gamma_{k,0}\geq\gamma_{\text{th}};\mathcal{H}_0}(\gamma)$ is the conditional Probability Density Function (PDF) of $\gamma_{k,0}$ given that $\gamma_{k,0} \geq \gamma_{\text{th}}$. Using the exponential PDF of $\gamma_{k,0}$, given by $f_{\gamma_{k,0}}(\gamma) = \frac{1}{\overline{\gamma}_{k,0}} e^{-\gamma/\overline{\gamma}_{k,0}}$, it can be readily shown that

$$f_{\gamma_{k,0}|\gamma_{k,0}\geq\gamma_{\text{th}};\mathcal{H}_0}(\gamma) = \begin{cases} 0, & \gamma < \gamma_{\text{th}}; \\ \frac{1}{\overline{\gamma}_{k,0}} e^{\gamma_{\text{th}}/\overline{\gamma}_{k,0}} e^{-\gamma/\overline{\gamma}_{k,0}}, & \gamma \geq \gamma_{\text{th}}. \end{cases} \tag{4.4}$$

Hence, solving (4.3) using (4.4) we can write a closed-form expression for $P_{e,k|\mathcal{H}_0}$ as

$$\begin{aligned} P_{e,k|\mathcal{H}_0} &= Q\big(\sqrt{2\gamma_{\text{th}}}\big) - e^{\gamma_{\text{th}}/\overline{\gamma}_{k,0}} \sqrt{\frac{\overline{\gamma}_{k,0}}{\overline{\gamma}_{k,0}+1}} \\ &\times Q\left(\sqrt{2\gamma_{\text{th}}\left(1+\frac{1}{\overline{\gamma}_{k,0}}\right)}\right). \end{aligned} \tag{4.5}$$

Case of $\mathcal{H}_1$

When the PU P is active, the received signal at the FC R_0 becomes $y_{k,0} = \sqrt{E} h_{k,0}(2d_k - 1) + \sqrt{E_p} h_{p,0} s + n_0$, $k = 1, 2, \ldots, K$, where $h_{p,0}$ is the coefficient of the P-R_0 channel, while s is the constant-amplitude modulated transmitted signal of the PU P. Due to our coherent detection assumption, the Signal to Interference plus Noise Ratio (SINR) at the FC R_0 given by $\psi_{k,0} \triangleq \frac{E|h_{k,0}|^2}{E_p|h_{p,0}|^2+\sigma^2} = \frac{\gamma_{k,0}}{\gamma_{p,0}+1}$, where $\gamma_{p,0} \triangleq \frac{E_p}{\sigma^2}|h_{p,0}|^2$. After comparing $\psi_{k,0}$ to γ_{th} and discarding capacity outage instances, the probability of decoding error experienced by the decoded local decision, $\hat{d}_k$, can be written as

$$\begin{aligned} P_{e,k|\mathcal{H}_1} &\triangleq \Pr[\hat{d}_k \neq d_k|\mathcal{H}_1] \\ &= \int_{\gamma_{\mathrm{th}}}^{\infty} Q(\sqrt{2\psi}) f_{\psi_{k,0}|\psi_{k,0}\geq\gamma_{\mathrm{th}};\mathcal{H}_1}(\psi) d\psi, \end{aligned} \tag{4.6}$$

where $\Pr[\cdot]$ is the probability operator while $f_{\psi_{k,0}|\psi_{k,0}\geq\gamma_{\mathrm{th}};\mathcal{H}_1}(\psi)$ is the conditional PDF of $\psi_{k,0}$ given that $\psi_{k,0} \geq \gamma_{\mathrm{th}}$. To obtain this PDF, we start by finding the Cumulative Distribution Function (CDF) $F_{\psi_{k,0}}(\psi)$ using the definition of $\psi_{k,0}$. Because $\gamma_{k,0}$ and $\gamma_{p,0}$ are exponential random variables, it can be shown that $F_{\psi_{k,0}}(\psi)$ is written as [SS10,AAI13]

$$F_{\psi_{k,0}}(\psi) = 1 - \frac{\overline{\gamma}_{k,0}}{\overline{\gamma}_{k,0} + \overline{\gamma}_{p,0}\psi} e^{-\psi/\overline{\gamma}_{k,0}}. \tag{4.7}$$

Next, $f_{\psi_{k,0}|\psi_{k,0}\geq\gamma_{\mathrm{th}};\mathcal{H}_1}(\psi)$ is calculated using the definition of a conditional distribution [PP02], giving us

$$f_{\psi_{k,0}|\psi_{k,0}\geq\gamma_{\mathrm{th}};\mathcal{H}_1}(\psi) \triangleq \frac{\partial}{\partial\psi} \begin{cases} 0, & \psi < \gamma_{\mathrm{th}}; \\ \frac{F_{\psi_{k,0}}(\psi) - F_{\psi_{k,0}}(\gamma_{\mathrm{th}})}{1 - F_{\psi_{k,0}}(\gamma_{\mathrm{th}})}, & \psi \geq \gamma_{\mathrm{th}}, \end{cases} \tag{4.8}$$

which, after using (4.7) and some mathematical manipulations, gives us

$$\begin{aligned} &f_{\psi_{k,0}|\psi_{k,0}\geq\gamma_{\mathrm{th}};\mathcal{H}_1}(\psi) = \\ &\begin{cases} 0, & \psi < \gamma_{\mathrm{th}}; \\ \begin{aligned} &\frac{(\overline{\gamma}_{k,0} + \overline{\gamma}_{p,0}\gamma_{\mathrm{th}})}{\overline{\gamma}_{k,0}(\overline{\gamma}_{k,0} + \overline{\gamma}_{p,0}\psi)} e^{(\gamma_{\mathrm{th}}-\psi)/\overline{\gamma}_{k,0}} \\ &+ \frac{\overline{\gamma}_{p,0}(\overline{\gamma}_{k,0} + \overline{\gamma}_{p,0}\gamma_{\mathrm{th}})}{(\overline{\gamma}_{k,0} + \overline{\gamma}_{p,0}\psi)^2} e^{(\gamma_{\mathrm{th}}-\psi)/\overline{\gamma}_{k,0}} \end{aligned}, & \psi \geq \gamma_{\mathrm{th}}. \end{cases} \end{aligned} \tag{4.9}$$

Finally, by solving (4.6) using (4.9) and [WLK11, Eqn.5], $P_{e,k|\mathcal{H}_1}$ can be written in the closed-form given in (4.10). In this expression, $\mathsf{E}_i[x] = \int_x^\infty \frac{e^{-t}}{t} dt$ is the exponential integral function [AAI13] while the coefficients $\{b_{\{}l\}\}_{l=1}^{L+1}$ are given in [WLK11] as $b_l =$

$\frac{L+1}{\pi}\left[\cot\left(\frac{l-1}{2(L+1)}\pi\right)-\cot\left(\frac{l}{2(L+1)}\pi\right)\right]$.

$$P_{e,k|\mathcal{H}_1} \approx \frac{1}{2(L+1)\overline{\gamma}_{p,0}}(\overline{\gamma}_{k,0}+\overline{\gamma}_{p,0}\gamma_{\text{th}})e^{\gamma_{\text{th}}/\overline{\gamma}_{k,0}} \times\Bigg\{\sum_{l=1}^{L+1}\frac{e^{(2b_l\overline{\gamma}_{k,0}+1)/\overline{\gamma}_{p,0}}}{\overline{\gamma}_{k,0}}\mathsf{E}_i\left[\left(\frac{1}{\overline{\gamma}_{k,0}}+2b_l\right)\left(\frac{\overline{\gamma}_{k,0}}{\overline{\gamma}_{p,0}}+\gamma_{\text{th}}\right)\right]+\sum_{l=1}^{L+1}\Bigg(\frac{e^{-\gamma_{\text{th}}(2b_l+1/\overline{\gamma}_{k,0})}}{\gamma_{\text{th}}+\frac{\overline{\gamma}_{k,0}}{\overline{\gamma}_{p,0}}} -\left(2b_l+\frac{1}{\overline{\gamma}_{k,0}}\right)e^{(2b_l\overline{\gamma}_{k,0}+1)/\overline{\gamma}_{p,0}}\mathsf{E}_i\left[\left(\frac{1}{\overline{\gamma}_{k,0}}+2b_l\right)\left(\frac{\overline{\gamma}_{k,0}}{\overline{\gamma}_{p,0}}+\gamma_{\text{th}}\right)\right]\Bigg)\Bigg\}. \quad (4.10)$$

4.2.3 Random Medium Access

CR terminals $\{\mathrm{R}_k\}_{k=1}^{K}$ contend to transmit their reports to the FC R_0 using random medium access. In particular, each CR terminal, independently, chooses a random back-off counter, $\{c_k\}_{k=1}^{K}$ from the range $[1, N]$, where N is the number of time slots in the reporting window. Once c_k expires, R_k transmits its local decision. This work examines the case where counters are assumed to follow a discrete uniform distribution with a Probability Mass Function (PMF) of $\Pr[c_k = n] = \frac{1}{N}$, $n \in \{1, 2, \ldots, N\}$.

4.2.4 Sequential Reporting

Random medium access reporting consumes, on average, more time slots than round robin reporting [AASM16]. This is undesirable for an agile CSS scheme. Sequential reporting is used to mitigate this by terminating the reporting process once the FC R_0 receives sufficient evidence about the PU status. The FC R_0 maintains a decision metric, Θ_n, and updates it at the end of every time slot using the recursion $\Theta_n = \Theta_{n-1} + \theta_n$, where $\theta_n \in [0, 1]$ is the newly received evidence about the status of P. By default, $\theta_n = 0$ unless R_0 receives a single report at the n^{th} time slot that is not in outage and has a decoded value of 1. The FC, R_0, terminates the reporting process and makes a final decision that P is active, (i.e., chooses $\mathcal{H}_1$), once Θ_n meets the decision threshold, $\Theta_{\text{th}} \in [1, K]$. Two early termination schemes are defined according to the way a $\mathcal{H}_0$ decision is announced as noted below:

Early Termination 1

In the first early termination rule, ET_1, the FC R_0 chooses $\mathcal{H}_0$ only when the number of remaining time slots, $N - n$, cannot bridge the gap between Θ_n and Θ_{th}. That is when

$$\Theta_n + (N - n) < \Theta_{\mathrm{th}} \Rightarrow \Theta_n = \Theta_{\mathrm{th}} + n - N - 1. \tag{4.11}$$

The 1 in the last expression comes from the fact that R_0 terminates the reporting process immediately once the condition $\Theta_n + (N - n) < \Theta_{\mathrm{th}}$ is met.

Early Termination 2 (Faster $\mathcal{H}_0$ Decision)

The aim of the second early termination rule, ET_2, is to reduce the time needed to make a $\mathcal{H}_0$ decision, (i.e., P is idle), and hence R_0 will choose $\mathcal{H}_0$ once it receives Θ_{th} "0" reports, where a "i" report is a report received by R_0 with $\hat{d}_k = i, i \in \{0, 1\}$, or if the number of remaining time slots, $N - n$, cannot bridge the gab between Θ_n and Θ_{th}. If the FC R_0 receives Θ_{th} "0" reports then

$$\Theta_n = \Delta_n - \Theta_{\mathrm{th}}; \Delta_n < 2\Theta_{\mathrm{th}} \tag{4.12}$$

where Δ_n is the number of reports received by R_0 after n time slots.

4.3 Performance Analysis

We investigate the system performance in terms of the probability of detection (Q_d), the probability of a false alarm (Q_{fa}), and the average number of time slots needed to make a decision under each hypothesis, (i.e., $\overline{N}_{\mathcal{H}_j}, j \in \{0, 1\}$). The probability of detection is the probability of making a $\mathcal{H}_1$ decision when the PU is active, (i.e., $\Pr[\mathcal{H}_1|\mathcal{H}_1]$), while the probability of a false alarm is the probability of making an $\mathcal{H}_1$ decision when the PU is idle, (i.e., $\Pr[\mathcal{H}_1|\mathcal{H}_0]$).

4.3.1 Probability of Detection, Q_d, and False Alarm, Q_{fa}.

An event of detection occurs once Θ_n reaches Θ_{th}, which can happen at $n = \Theta_{\text{th}}, \Theta_{\text{th}} + 1, \ldots, N$. Hence, Q_d can be written as

$$\begin{aligned} Q_d \;=\; & \Pr\Big[(\Theta_{\Theta_{\text{th}}} = \Theta_{\text{th}}) \bigcup (\Theta_{\Theta_{\text{th}}+1} = \Theta_{\text{th}}) \bigcup \ldots \\ & \bigcup (\Theta_N = \Theta_{\text{th}})\Big]. \end{aligned} \tag{4.13}$$

To turn this into a sum of probabilities, we can replace the individual events with the mutually exclusive sequence of conditional events $\Theta_{\Theta_{\text{th}}} = \Theta_{\text{th}}|\Theta_{\Theta_{\text{th}}-1} = \Theta_{\text{th}} - 1, \Theta_{\Theta_{\text{th}}+1} = \Theta_{\text{th}}|\Theta_{\Theta_{\text{th}}} = \Theta_{\text{th}} - 1, \ldots, \Theta_N = \Theta_{\text{th}}|\Theta_N - 1 = \Theta_{\text{th}} - 1$. Accordingly, for ET_1, (4.13) can be rewritten as

$$\begin{aligned} Q_{d,ET_1} &= \sum_{n=\Theta_{\text{th}}}^{N} \Pr[\Theta_n = \Theta_{\text{th}}|\Theta_{n-1} = \Theta_{\text{th}} - 1; \mathcal{H}_1] \\ &= \sum_{n=\Theta_{\text{th}}}^{N} \Pr[\Theta_n = \Theta_{\text{th}}|\theta_n = 1; \mathcal{H}_1]. \end{aligned} \tag{4.14}$$

The condition $(\theta_n = 1)$ in (4.14) ensures the events $\Theta_{\Theta_{\text{th}}} = \Theta_{\text{th}}|\Theta_{\Theta_{\text{th}}-1} = \Theta_{\text{th}} - 1, \Theta_{\Theta_{\text{th}}+1} = \Theta_{\text{th}}|\Theta_{\Theta_{\text{th}}} = \Theta_{\text{th}} - 1, \ldots, \Theta_N = \Theta_{\text{th}}|\Theta_N - 1 = \Theta_{\text{th}} - 1$ are mutually exclusive.

The overall probability of detection for the second early termination rule, given by Q_{d,ET_2}, differs slightly from Q_{d,ET_1} to account for the fact that an event of detection, $\Theta_n = \Theta_{\text{th}}$, has to occur before Θ_{th} "0" reports are received by R_0. Therefore, Q_{d,ET_2} can be written as

$$\begin{aligned} Q_{d,ET_2} &= \sum_{n=\Theta_{\text{th}}}^{N} \Pr[\Theta_n = \Theta_{\text{th}}|\Theta_{n-1} = \Theta_{\text{th}} - 1; \Delta_n < 2\Theta_{\text{th}}; \mathcal{H}_1] \\ &= \sum_{n=\Theta_{\text{th}}}^{N} \Pr[\Theta_n = \Theta_{\text{th}}|\theta_n = 1; \Delta_n < 2\Theta_{\text{th}}; \mathcal{H}_1]. \end{aligned} \tag{4.15}$$

Therefore, the conditional Probability Mass Functions (PMF) $\Pr[\Theta_n = \Theta_{\text{th}}|\theta_n = 1; \mathcal{H}_1]$ and $\Pr[\Theta_n = \Theta_{\text{th}}|\theta_n = 1; \Delta_n < 2\Theta_{\text{th}}; \mathcal{H}_1]$ are needed to calculate Equations (4.14) and (4.15). To do that we note that the decision metric Θ_n follows the Binomial distribution, where successive time-slots represent a sequence of symmetrical Bernoulli trials, whether R_0 successfully receives a report or not. Not receiving a report means that the time-slot is idle or experiencing a collision and/or outage. The trials are symmetric across time-slots as terminals select their counter value following the uniform distribution. Also, the local detection and decoding error probabilities of R_0 are independent of the reporting time-slot. Note that this is not true for the heuristic energy-based priority reporting scheme.

Let the probability of successfully receiving a report be $\varrho_{\mathcal{H}_j}, j \in \{0,1\}$, then due to the mutual independence between collision and outage events we can write

$$\begin{aligned}\varrho_{\mathcal{H}_0} =& \sum_{k=1}^{K}(\frac{1}{N}) \times (\frac{N-1}{N})^{K-1} \times \Pr[\gamma_{k,0} \geq \gamma_{\text{th}}|\mathcal{H}_0],\\ \varrho_{\mathcal{H}_1} =& \sum_{k=1}^{K}(\frac{1}{N}) \times (\frac{N-1}{N})^{K-1} \times \Pr[\psi_{k,0} \geq \gamma_{\text{th}}|\mathcal{H}_1],\end{aligned} \tag{4.16}$$

This probability, $\varrho_{\mathcal{H}_j}$, is averaged by simulation to remove its dependence on the fading and the terminals' choice of counters. A successful reception can be further split into a "1" report, and "0" report. Using $P_{d,k}$, P_{fa}, and $P_{e,k}$, we can write the probability of successfully receiving a "1", $\rho_{\mathcal{H}_j}$, and that of receiving a "0", $\varsigma_{\mathcal{H}_j}$, as

$$\begin{aligned}\rho_{\mathcal{H}_0} =& \varrho_{\mathcal{H}_0} \times [P_{fa}(1-P_{e,k|\mathcal{H}_0}) + (1-P_{fa})P_{e,k|\mathcal{H}_0}],\\ \rho_{\mathcal{H}_1} =& \varrho_{\mathcal{H}_1} \times [P_{d,k}(1-P_{e,k|\mathcal{H}_1}) + (1-P_{d,k})P_{e,k|\mathcal{H}_1}],\\ \varsigma_{\mathcal{H}_0} =& \varrho_{\mathcal{H}_0} \times [P_{fa} \cdot P_{e,k|\mathcal{H}_0} + (1-P_{fa})(1-P_{e,k|\mathcal{H}_0})],\\ \varsigma_{\mathcal{H}_1} =& \varrho_{\mathcal{H}_1} \times [P_{d,k} \cdot P_{e,k|\mathcal{H}_1} + (1-P_{d,k})(1-P_{e,k|\mathcal{H}_1})].\end{aligned} \tag{4.17}$$

The conditional PMFs in (4.14) and (4.15) can then be calculated by dividing the N time-slots before and after time-slot n. The value of θ_n is fixed to $i \in \{0,1\}$, while the before part has $(n-1)$ time-slots which can host any combination of $(\zeta - i)$ "1" reports and $(\delta - 1 + i)$ "0" reports, where δ represents the number of zeros before n and is varied from $(1-i)$ to $(n-\zeta)$. The number of time-slots where there are no successful receptions will then be $(n-\zeta-\delta)$. The after part of the sequence of time-slots is not constrained to a given number of "1" or "0" reports and hence we need to cover all possible combinations.

The conditional PMF $\Pr[\Theta_n = \zeta | \theta_n = i; \mathcal{H}_j]$ is then given by

$$\begin{aligned}\Pr[\Theta_n = \zeta | \theta_n = i; \mathcal{H}_j] = &\binom{n-1}{\zeta - i} \cdot \rho_{\mathcal{H}_j}^{\zeta} \\ &\times \left[\sum_{\delta=1-i}^{n-\zeta} \binom{n-1-\zeta+i}{\delta-1+i} \cdot \varsigma_{\mathcal{H}_j}^{\delta} \cdot (1-\varrho_{\mathcal{H}_j})^{n-\zeta-\delta} \right] \\ &\times \left[\sum_{q=0}^{N-n} \binom{N-n}{q} \cdot \varrho_{\mathcal{H}_j}^{q} \cdot (1-\varrho_{\mathcal{H}_j})^{N-n-q} \right], i,j \in \{0,1\}. \end{aligned} \tag{4.18}$$

The probability of detection at the FC for ET_1, Q_{d,ET_1}, can then be obtained by substituting (4.18) into (4.14). Furthermore, the conditional PMF $\Pr[\Theta_n = \Theta_{\text{th}} | \theta_n = 1; \Delta_n < 2\Theta_{\text{th}}; \mathcal{H}_1]$ can be written as

$$\begin{aligned}\Pr[\Theta_n = \zeta | \theta_n = i; \Delta_n < 2\zeta; \mathcal{H}_j] = &\binom{n-1}{\zeta - i} \cdot \rho_{\mathcal{H}_j}^{\zeta} \\ &\times \left[\sum_{\delta=1-i}^{\min(n-\zeta,\zeta-1)} \binom{n-1-\zeta+i}{\delta-1+i} \cdot \varsigma_{\mathcal{H}_j}^{\delta} \cdot (1-\varrho_{\mathcal{H}_j})^{n-\zeta-\delta} \right] \\ &\times \left[\sum_{q=0}^{N-n} \binom{N-n}{q} \cdot \varrho_{\mathcal{H}_j}^{q} \cdot (1-\varrho_{\mathcal{H}_j})^{N-n-q} \right], i,j \in \{0,1\}. \end{aligned} \tag{4.19}$$

Also, $Q_{d,ET_{2,3}}$ can then be obtained by substituting (4.19) into (4.15). Finally, we note that the probability of a false alarm at the FC, Q_{fa}, for all early termination schemes can be obtained in a similar fashion simply replacing $\mathcal{H}_1$ with $\mathcal{H}_0$ in (4.14) and (4.15) and accordingly in (4.18) and (4.19) respectively.

4.3.2 Average Number of Time Slots

In this section we look at the average number of time-slots needed before making a decision under each hypothesis, $\overline{N}_{\mathcal{H}_j}$. Early Termination (ET) occurs after time-slot n if Θ_n reaches Θ_{th}, where an $\mathcal{H}_1$ decision is made. Declaring a $\mathcal{H}_0$ decision differs from ET_1 to ET_2. Declaring these two decisions, (i.e., $\mathcal{H}_0$ and $\mathcal{H}_1$), cannot occur at the same time. Hence, total probability theorem can be used as in [AAM15] to calculate the probability of making a decision after time-slot n, denoted $P_{n|\mathcal{H}_j}$, as the sum of probabilities of making these two decisions after time slot n. Therefore, the average number of time-slots needed before making a decision under hypothesis $\mathcal{H}_j, j \in \{0,1\}$, can be written as

$$\overline{N}_{\mathcal{H}_j} = \sum_{n=\Theta_{\text{th}}}^{N} n \times P_{n|\mathcal{H}_j}, j \in \{0,1\}, \tag{4.20}$$

In the following we outline the closed-form expressions of $P_{n|\mathcal{H}_j}, j \in \{0,1\}$, for ET_1, and, ET_2.

Early Termination 1

The FC, R_0, declares a $\mathcal{H}_0$ decision when Θ_n reaches $(\Theta_{\text{th}} + n - N - 1)$, and declares a $\mathcal{H}_1$ decision when Θ_n reaches Θ_{th}. The term $P_{n|\mathcal{H}_j}, j \in \{0,1\}$, is then given by

$$\begin{aligned} P_{n|\mathcal{H}_j} &= \Pr[(\Theta_n = \Theta_{\text{th}}) \bigcup (\Theta_n = \Theta_{\text{th}} + n - N - 1)], \\ &= \Pr[\Theta_n = \Theta_{\text{th}} | \theta_n = 1; \mathcal{H}_j] + \\ &\quad \Pr[\Theta_n = \Theta_{\text{th}} + n - N - 1 | \theta_n \neq 1; \mathcal{H}_j]. \end{aligned} \tag{4.21}$$

The term, $\Pr[\Theta_n = \Theta_{\text{th}} | \theta_n = 1; \mathcal{H}_j]$, is given by (4.18), while the term $\Pr[\Theta_n = \Theta_{\text{th}} + n - N - 1 | \theta_n \neq 1; \mathcal{H}_j]$ is given by

$$\begin{aligned} &\Pr[\Theta_n = \Theta_{\text{th}} + n - N - 1 | \theta_n \neq 1; \mathcal{H}_j] = \\ &\qquad \binom{n-1}{\Theta_{\text{th}} + n - N - 1} \cdot \rho_{\mathcal{H}_j}^{\Theta_{\text{th}}+n-N-1} \\ &\qquad \times \Bigg[\sum_{\delta=0}^{N-\Theta_{\text{th}}} \binom{N-\Theta_{\text{th}}}{\delta} \cdot \big[\varsigma_{\mathcal{H}_j}^{\delta} \cdot (1-\varrho_{\mathcal{H}_j})^{N-\Theta_{\text{th}}-\delta} \\ &\qquad\qquad \cdot (1-\rho_{\mathcal{H}_j}) \cdot (1-\varrho_{\mathcal{H}_j})^{N-\Theta_{\text{th}}-\delta} \big] \Bigg] \\ &\qquad\qquad \times \Bigg[\sum_{q=0}^{N-n} \binom{N-n}{q} \cdot \varrho_{\mathcal{H}_j}^{q} \cdot (1-\varrho_{\mathcal{H}_j})^{N-n-q} \Bigg], j \in \{0,1\}. \end{aligned} \tag{4.22}$$

Early Termination 2

The FC, R_0, declares a $\mathcal{H}_0$ decision when Θ_n reaches $(\Delta_n - \Theta_{\text{th}})$ or $(\Theta_{\text{th}} + n - N - 1)$, and declares a $\mathcal{H}_1$ decision when Θ_n reaches Θ_{th}. The term $P_{n|\mathcal{H}_j}, j \in \{0, 1\}$, is then given by

$$\begin{aligned}
P_{n|\mathcal{H}_j} = \Pr[(\Theta_n = \Theta_{\text{th}}) \bigcup (\Theta_n = \Delta_n - \Theta_{\text{th}}) \\
\bigcup (\Theta_n = \Theta_{\text{th}} + n - N - 1)], \\
= \Pr[\Theta_n = \Theta_{\text{th}} | \theta_n = 1; \Delta_n < 2\Theta_{\text{th}}; \mathcal{H}_j] + \\
\Pr[\Theta_n = \Delta_n - \Theta_{\text{th}} | \theta_n = \text{“0”}; \\
\max(0, \Theta_{\text{th}} + n - N) \leq \Theta_n \leq \min(\Theta_{\text{th}} - 1, n - \Theta_{\text{th}}); \mathcal{H}_j] + \\
\Pr[\Theta_n = \Theta_{\text{th}} + n - N - 1 | \theta_n \neq \text{“1”}; \mathcal{H}_j]. \quad (4.23)
\end{aligned}$$

The term, $\Pr[\Theta_n = \Theta_{\text{th}} | \theta_n = 1; \Delta_n < 2\Theta_{\text{th}}; \mathcal{H}_j]$, is given by (4.19), while the terms $\Pr[\Theta_n = \Delta_n - \Theta_{\text{th}} | \theta_n = \text{“0”}; \max(0, \Theta_{\text{th}} + n - N) \leq \Theta_n \leq \min(\Theta_{\text{th}} - 1, n - \Theta_{\text{th}}); \mathcal{H}_j]$ and $\Pr[\Theta_n = \Theta_{\text{th}} + n - N - 1 | \theta_n \neq \text{“1”}; \mathcal{H}_j]$ are given by

$$\begin{aligned}
&\Pr[\Theta_n = \Delta_n - \Theta_{\text{th}} | \theta_n = \text{“0”}; \\
&\max(0, \Theta_{\text{th}} + n - N) \leq \Theta_n \leq \min(\Theta_{\text{th}} - 1, n - \Theta_{\text{th}}); \mathcal{H}_j] = \\
&\Bigg[\sum_{\Theta_n = \max(0, \Theta_{\text{th}} + n - N)}^{\min(\Theta_{\text{th}} - 1, n - \Theta_{\text{th}})} \binom{n-1}{\Theta_n} \cdot \rho_{\mathcal{H}_j}^{\Theta_n} \cdot \binom{n - 1 - \Theta_n}{\Theta_{\text{th}} - 1} \\
&\cdot \varsigma_{\mathcal{H}_j}^{\Theta_{\text{th}}} \cdot (1 - \varrho_{\mathcal{H}_j})^{n - \Theta_{\text{th}} - \Theta_n} \Bigg] \\
&\times \left[\sum_{q=0}^{N-n} \binom{N-n}{q} \cdot \varrho_{\mathcal{H}_j}^{q} \cdot (1 - \varrho_{\mathcal{H}_j})^{N-n-q} \right], j \in \{0, 1\}. \quad (4.24)
\end{aligned}$$

$$
\begin{aligned}
&\Pr[\Theta_n = \Theta_{\mathrm{th}} + n - N - 1 | \theta_n \neq \text{“1”}; \mathcal{H}_j] = \\
&\qquad\qquad \binom{n-1}{\Theta_{\mathrm{th}} + n - N - 1} \cdot \rho_{\mathcal{H}_j}^{\Theta_{\mathrm{th}} + n - N - 1} \\
&\qquad \times \Bigg[\sum_{\delta=0}^{\Theta_{\mathrm{th}}-1} \binom{N - \Theta_{\mathrm{th}}}{\delta} \cdot \Big[\varsigma_{\mathcal{H}_j}^{\delta} \cdot (1 - \varrho_{\mathcal{H}_j})^{N - \Theta_{\mathrm{th}} - \delta} \\
&\qquad\qquad \cdot (1 - \rho_{\mathcal{H}_j}) \cdot (1 - \varrho_{\mathcal{H}_j})^{N - \Theta_{\mathrm{th}} - \delta} \Big] \Bigg] \\
&\qquad\qquad \times \Bigg[\sum_{q=0}^{N-n} \binom{N-n}{q} \cdot \varrho_{\mathcal{H}_j}^{q} \cdot (1 - \varrho_{\mathcal{H}_j})^{N-n-q} \Bigg], j \in \{0, 1\}. \quad (4.25)
\end{aligned}
$$

Note the similarity between equations (4.22) and (4.25), where the main difference is in the boundary conditions of some of the summation functions.

4.4 Numerical and Simulation Results

4.4.1 Accuracy of Derived Results

We now look at the accuracy of the derived results by comparing our analysis to simulation results for different parameter values. The following parameter values are common in all results: CR terminals transmit SNR $\rho = 6$ dB, PU transmit SNR $\rho_p = 0$ dB, radius $r = 1$, spectral efficiency $q = 0.1$ bits/sec/Hz, and the sampling parameter $u = 20$. The number of CR terminals K, the maximum contention window size N, and the decision threshold Θ_{th} are all specified on the figures. Initially, we test the first early termination rule, ET_1, varying the contention window, N, the pre-determined probability of a false alarm at each terminal, P_{fa}, and for $\Theta_{\mathrm{th}} = 2$. Fig. 4.2 shows the detection performance by plotting the probability of misdetection, $Q_m = 1 - Q_d$, vs. the probability of a false alarm, Q_{fa}, at the FC. The average number of time slots needed to make a decision, (i.e., the speed of the sequential reporting paradigm), for ET_1 is shown in Fig. 4.3. We can see that ET_1 can reduce the reporting time by 25-50%. Next we look at the detection performance of ET_2 in Fig. 4.4, this time using $\Theta_{th} = 6$ and different N values. The reporting speed is shown in Fig. 4.5. Again we can see significant reporting duration reduction using ET_2. However,

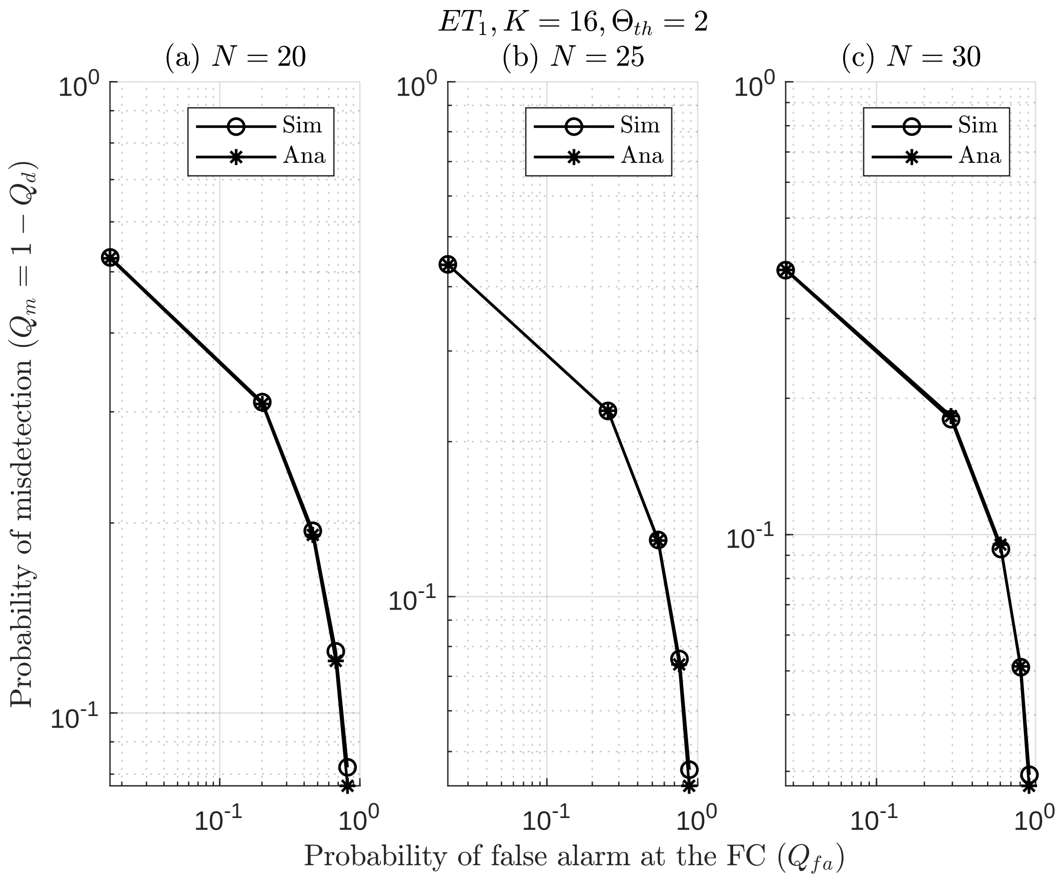

Figure 4.2: Probability of misdetection vs. Probability of a false alarm at the FC for first early termination rule, ET_1, with different contention window sizes, (a) $N = 20$, (b) $N = 25$, (c) $N = 30$.

unlike ET_1, ET_2 performance is better with lower P_{fa}, as ET_2 benefits from more "0" reports reaching the FC. Generally, analytical results closely predict, though not identical to, simulation results. We believe the reason for that is a very slight difference between the derived probabilities, $\rho, \varrho, \& \varsigma$, and their simulation values. Also, we do assume that all time slots have the exact same $\rho, \varrho, \& \varsigma$, however investigating simulation results we find very slight differences that can lead to bigger deviations when raised to high power values.

4.4.2 Comparing the Different Early Termination Rules

In this part, we compare ET_1 and ET_2 in Fig. 4.6 and Fig. 4.7. It is clear that at lower Θ_{th} values, ET_1 has higher detection performance as opposed to ET_2. The reporting time

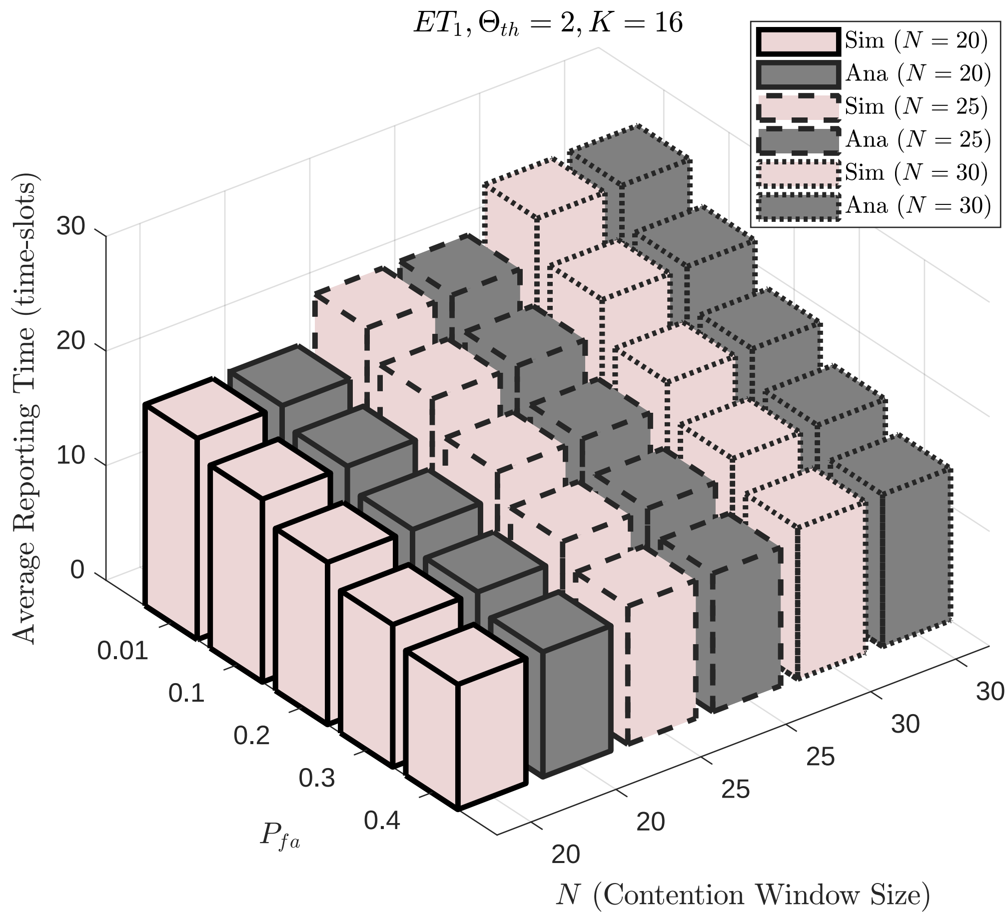

Figure 4.3: Average reporting time for the first early termination rule, ET_1.

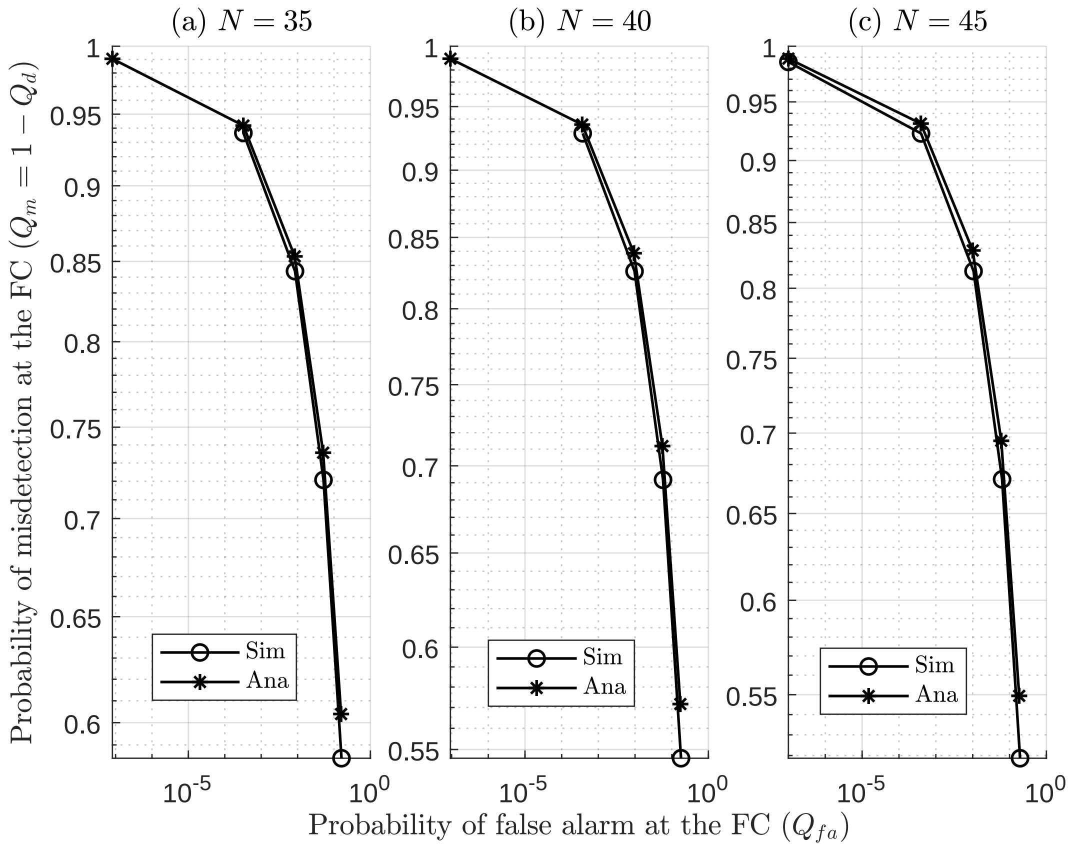

Figure 4.4: Probability of misdetection vs. Probability of a false alarm at the FC for ET_2 (Faster $\mathcal{H}_0$ Decision), with different N values.

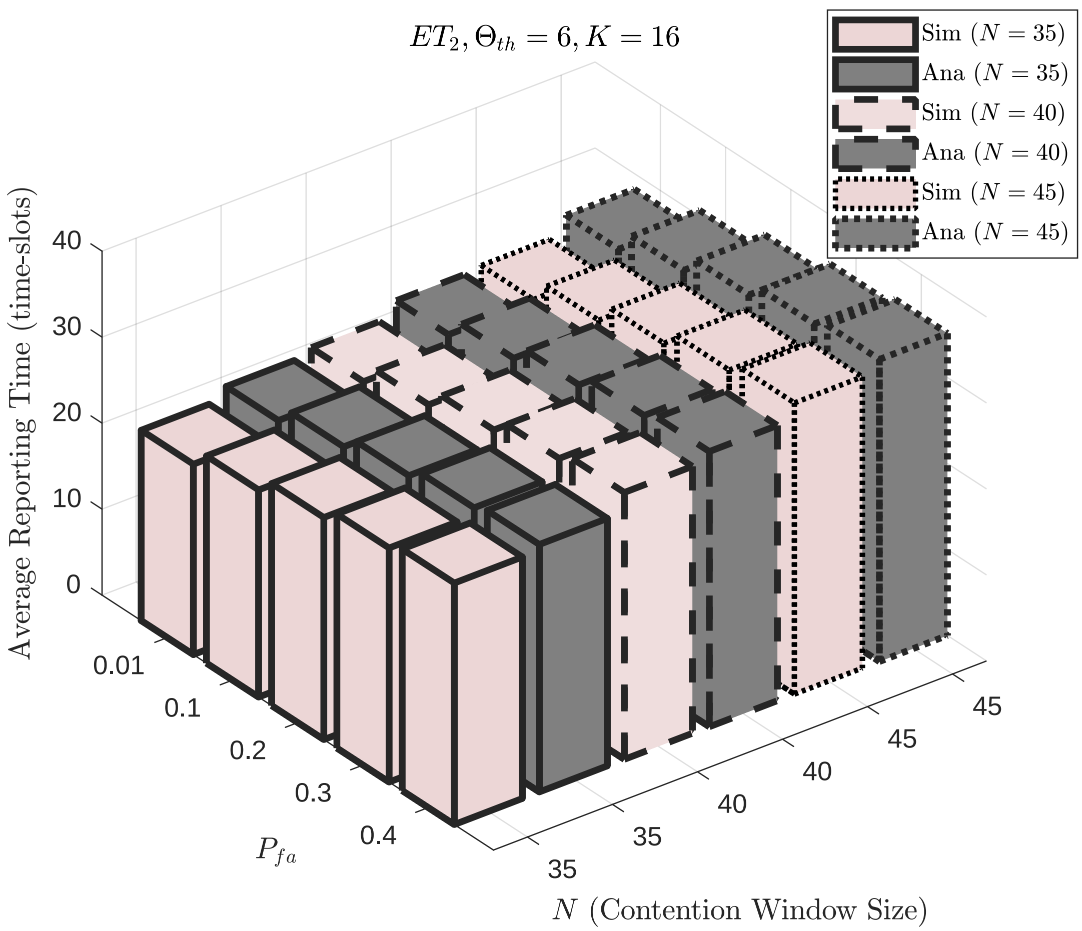

Figure 4.5: Average reporting time for ET_2 (Faster $\mathcal{H}_0$ Decision).

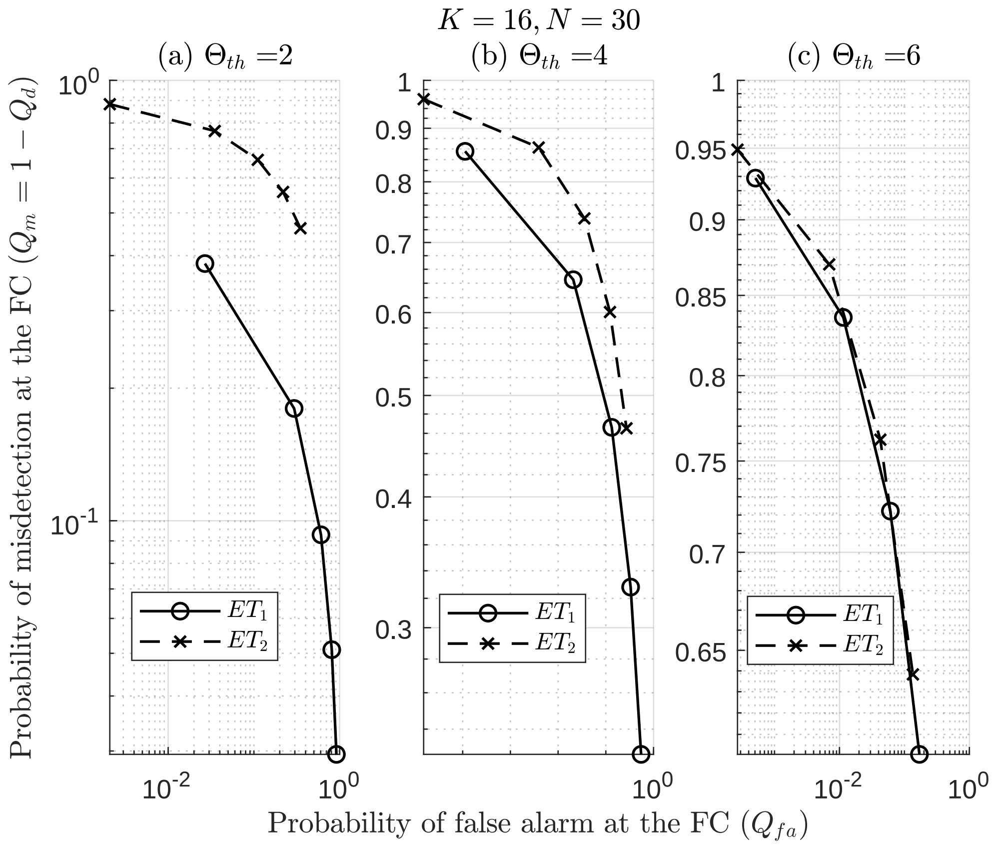

Figure 4.6: Probability of misdetection vs. Probability of a false alarm at the FC, ET_1 vs. ET_2, (a) $\Theta_{\text{th}} = 2$, (b) $\Theta_{\text{th}} = 4$, (c) $\Theta_{\text{th}} = 6$.

reduction ET_2 offers might not justify significant loss of detection performance. However, for higher Θ_{th} values, the detection performance of ET_1 and ET_2 start to converge, while ET_2 still offers good reporting duration reduction.

4.5 Summary

In this chapter we studied decision-based CSS using random medium access sequential reporting and using the K-out-of-M decision rule. Two early termination rules have been investigated with the objective of reducing the decision reporting duration, and hence increase network throughput. Closed-form expressions have been derived for the average reporting time, as well as the probabilities of detection and false alarm for both early termination rules. Computer simulations were then used to validate the accuracy of derived

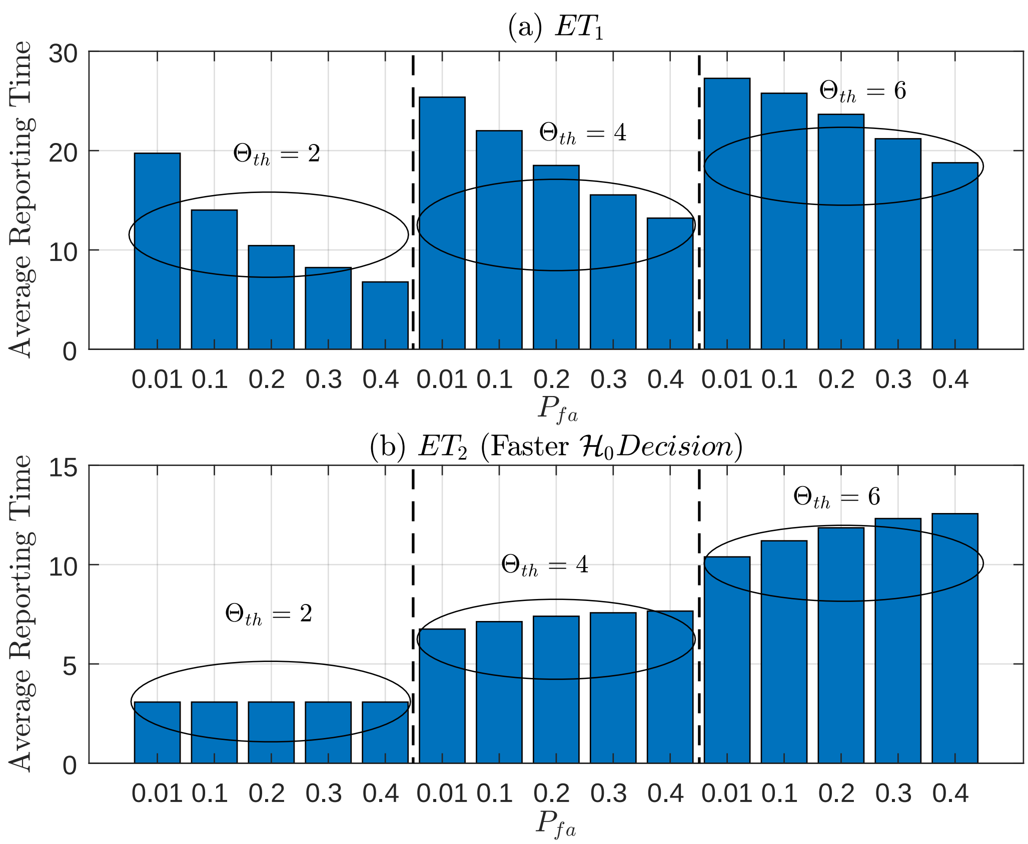

Figure 4.7: Average reporting time, ET_1 vs. ET_2, $\Theta_{\text{th}} \in \{2, 4, 6\}$.

expressions. Simulation results show derived expressions are quite accurate.

Chapter 5

Energy-Based Random Medium Access Reporting

5.1 Introduction

This chapter builds upon chapter 4 by introducing an energy-based priority-driven random medium access reporting process. This process prioritizes CR terminals based on the quality of their local sensing in order to enhance PU detection accuracy while minimizing the reporting time. This heuristic reporting scheme focuses only on the sensing channel information that is local to each CR terminal with no need for feedback from the FC. A priority-driven scheme that also exploits information about the reporting channel towards the FC will require feedback from the FC which can be a topic for future research. The remainder of this chapter is organized as follows. Section 5.2 describes the system model. Numerical and simulations results are given in Section 5.3 and finally conclusions and future work are presented in Section 5.4.

5.2 System Model

We consider the same system model given in Chapter 4 where K CR terminals, $\mathrm{R}_1, \mathrm{R}_2, \ldots, \mathrm{R}_K$, are randomly distributed within a circle of radius r centered around a FC R_0. The objective is to examine the status of a PU transmitter, P, that is located within the same circle. In doing so, terminals $\{\mathrm{R}_k\}_{k=1}^{K}$ use hard decision fusion centralized CSS according to the K-out-of-M decision rule. The channels between all terminals are assumed to follow a flat Rayleigh fading model. All CR terminals use the same transmit energy E that is different from the PU P transmit energy given by E_p.

5.2.1 Random Medium Access

CR terminals $\{\mathrm{R}_k\}_{k=1}^{K}$ contend to transmit their reports to the FC R_0 using random medium access. CR terminals independently choose random back-off counters, $\{c_k\}_{k=1}^{K}$ and once c_k expires, R_k transmits its local decision. We use the work done in Chapter 4 as a base scenario where counters $\{c_k\}_{k=1}^{K}$ are independent identically distributed uniform random variables with a range $[1, N]$, where N is the number of time slots in the reporting window with a Probability Mass Function (PMF) of $\Pr[c_k = n] = \frac{1}{N}$, $n = 1, 2, \ldots, N$. Next, we describe how the counters $\{c_k\}_{k=1}^{K}$ are chosen for the proposed heuristic energy-based priority reporting scheme.

Heuristic Energy-based Priority Reporting Scheme

A CR terminal k is given a higher access priority to the reporting channel by decreasing its contention window. That is $c_k \sim U[1, N_{k,new}]$, where $N_{k,new} < N$ is the new contention window length for CR terminal k. To ensure a lower priority for a CR terminal k with a high $N_{k,new}$, a sliding window can be defined by changing the left limit from 1 to $(N_{k,new} - SW_{size})$, where SW_{size} is the length of the sliding window. Also, to avoid collisions among multiple CR terminals with very small $N_{k,new}$, we can define a minimum contention window length MW_{size}. In the following, we go over the details of the heuristic energy-based priority reporting scheme.

Define an array of thresholds related to the decision threshold λ as follows

$$\lambda^{\mathbf{th}} = [\frac{\alpha\lambda(N-1)}{N}, \frac{\alpha\lambda(N-2)}{N}, \cdots, \frac{2\alpha\lambda}{N}, \frac{\alpha\lambda}{N}, 0], \tag{5.1}$$

where α is a design factor to be pre-determined through extensive simulation. Each terminal, $\{\mathrm{R}_k\}_{k=1}^{K}$, then uses its local energy detection result, ϕ_k, to select a variable $\Im_k$ where $\lambda^{\mathbf{th}}(\Im_k - 1) > \phi_k \geq \lambda^{th}(\Im_k)$ and $\lambda^{\mathbf{th}}(0) \triangleq \infty$. The counters $\{c_k\}_{k=1}^{K}$ are then chosen according to

$$c_k \sim U[1, \mathbf{Ctr_{Asc}}(\Im_k)], \tag{5.2}$$

where $\mathbf{Ctr_{Asc}} = \{1, 2, 3, \ldots, N-2, N-1, N\}$. Therefore, the variables $\{\Im_k\}_{k=1}^{K}$ reflect reporting priority, where a smaller $\Im_k$ value corresponds to a higher priority due to higher local energy detection results ϕ_k. In order to limit collisions among competing terminals, we introduce a sliding window with length SW_{size} time-slots, where the counters are chosen as follows

$$\begin{aligned} c_k \quad \sim \quad & U[\max(1, \mathbf{Ctr_{Asc}}(\Im_k) - SW_{size} + 1), \\ & \mathbf{Ctr_{Asc}}(\Im_k)]. \end{aligned} \tag{5.3}$$

Furthermore, we introduce a minimum window size, MW_{size}, to reduce collisions among terminals with very small counters, (i.e., with very high priority), as follows

$$\begin{aligned} c_k \quad \sim \quad & U[\max(1, \mathbf{Ctr_{Asc}}(\Im_k) - SW_{size} + 1), \\ & \max(MW_{size}, \mathbf{Ctr_{Asc}}(\Im_k))]. \end{aligned} \tag{5.4}$$

Finding the optimum $(\alpha, SW_{size}, MW_{size})$ combination for this heuristic requires extensive simulation campaigns.

5.2.2 Sequential Reporting

We test the proposed heuristic energy-based priority reporting scheme with both early termination rules introduced in Chapter 4, where the FC R_0 maintains a decision metric, Θ_n, and updates it at the end of every time slot using the recursion $\Theta_n = \Theta_{n-1} + \theta_n$, where $\theta_n \in [0, 1]$ is the newly received evidence about the status of P. By default, $\theta_n = 0$ unless R_0 receives a single report at the n^{th} time slot that is not in outage and has a decoded value of 1. The FC, R_0, terminates the reporting process and makes a final decision that P is active, (i.e., chooses $\mathcal{H}_1$), once Θ_n meets the decision threshold, $\Theta_{\text{th}} \in [1, K]$. Recall the two early termination schemes were defined according to the way an $\mathcal{H}_0$ decision is announced as follows.

Early Termination 1 (ET_1)

Choose $\mathcal{H}_0$ when the number of remaining time slots, $N-n$, cannot bridge the gap between Θ_n and Θ_{th}. That is when

$$\Theta_n + (N - n) < \Theta_{\text{th}} \Rightarrow \Theta_n = \Theta_{\text{th}} + n - N - 1. \tag{5.5}$$

Early Termination 2 (Faster $\mathcal{H}_0$ Decision) (ET_2)

Choose $\mathcal{H}_0$ if the remaining $N - n$ time slots cannot bridge the gap between Θ_n and Θ_{th}, or once Θ_{th} "0" reports are received, that is when

$$\Theta_n = \Delta_n - \Theta_{\text{th}}; \Delta_n < 2\Theta_{\text{th}}, \tag{5.6}$$

where Δ_n is the number of reports received by R_0 after n time slots.

5.3 Numerical and Simulation Results

In this part, we investigate the performance of the Energy-based Heuristic Reporting Priority Scheme with both early termination rules, (i.e., ET_1 and ET_2). The energy-based heuristic is compared against the case when all local counters, $\{c_k\}_{k=1}^{K}$ are drawn from identical uniform distributions in the range $[1, N]$. We call this case "Base". In the following, unless mentioned otherwise, we use the same simulation parameters as in Chapter 4.

First, we tried different α values without using a sliding reporting window, (i.e., $SW_{size} = MW_{size} = 0$), in Figures 5.1 to 5.6 using different contention window sizes, (i.e., $N \in$

$\{20, 25, 30\}$). The energy-based heuristics achieves a very tiny improvement in detection speed for ET_1, but with an equivalent tiny degradation of detection performance. For ET_2, however, the energy-based heuristic provides a detection performance improvement for a slight increase in detection speed.

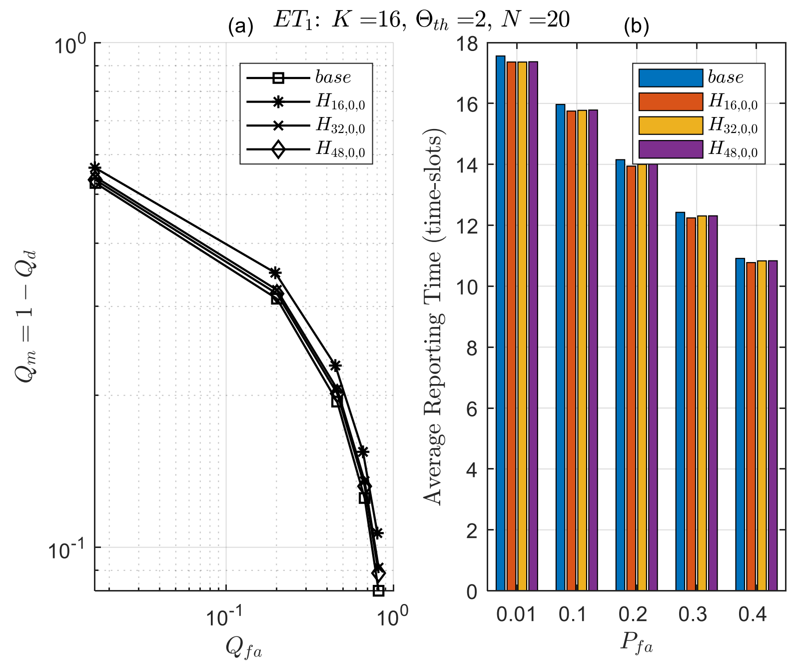

Figure 5.1: (a) Probability of misdetection vs. Probability of false alarm at the FC (Q_{fa}) (b) Average reporting time in time-slots vs. local Probability of false alarm (P_{fa}).

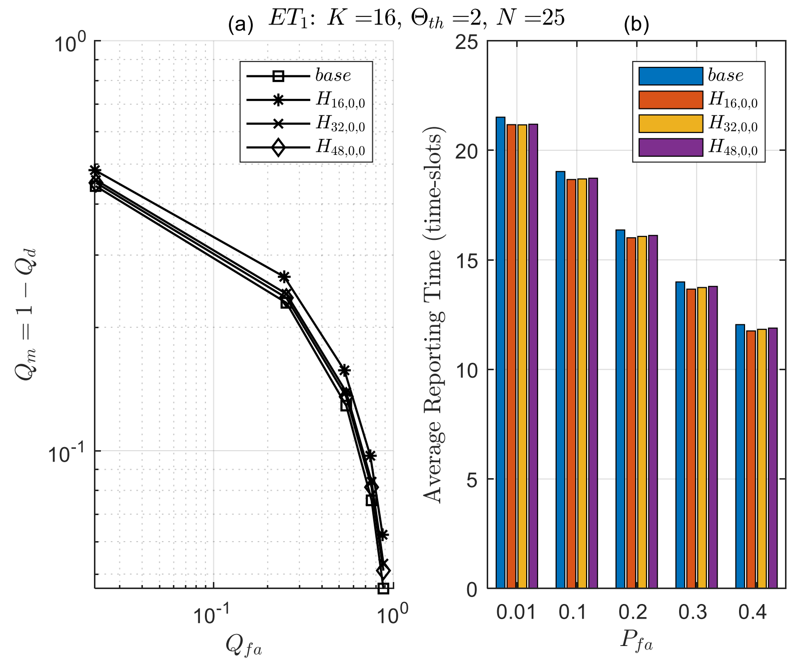

Figure 5.2: (a) Probability of misdetection vs. Probability of false alarm at the FC (Q_{fa}) (b) Average reporting time in time-slots vs. local Probability of false alarm (P_{fa}).

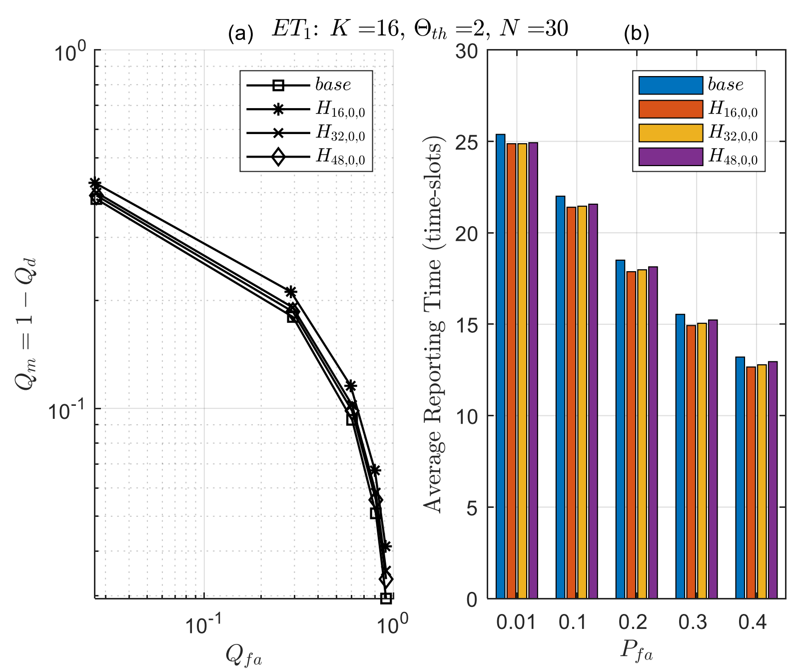

Figure 5.3: (a) Probability of misdetection vs. Probability of false alarm at the FC (Q_{fa}) (b) Average reporting time in time-slots vs. local Probability of false alarm (P_{fa}).

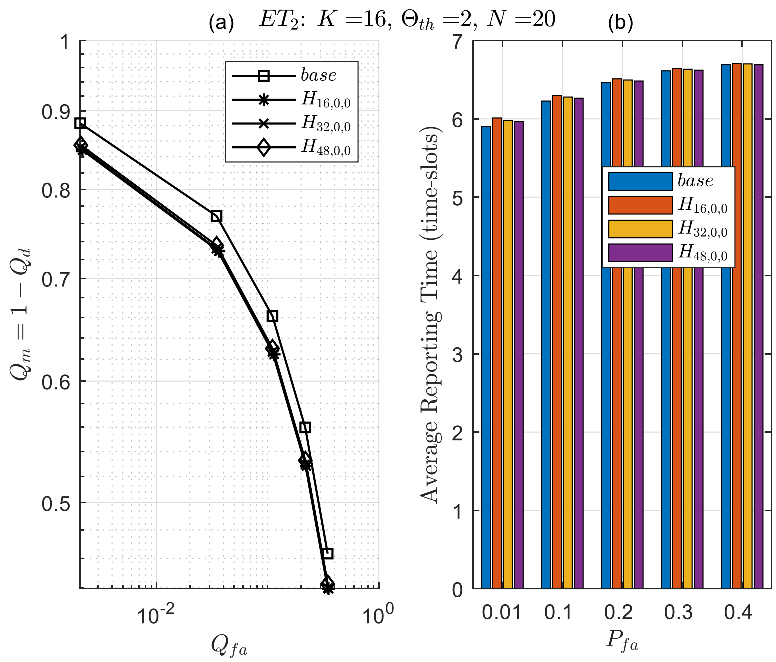

Figure 5.4: (a) Probability of misdetection vs. Probability of false alarm at the FC (Q_{fa}) (b) Average reporting time in time-slots vs. local Probability of false alarm (P_{fa}).

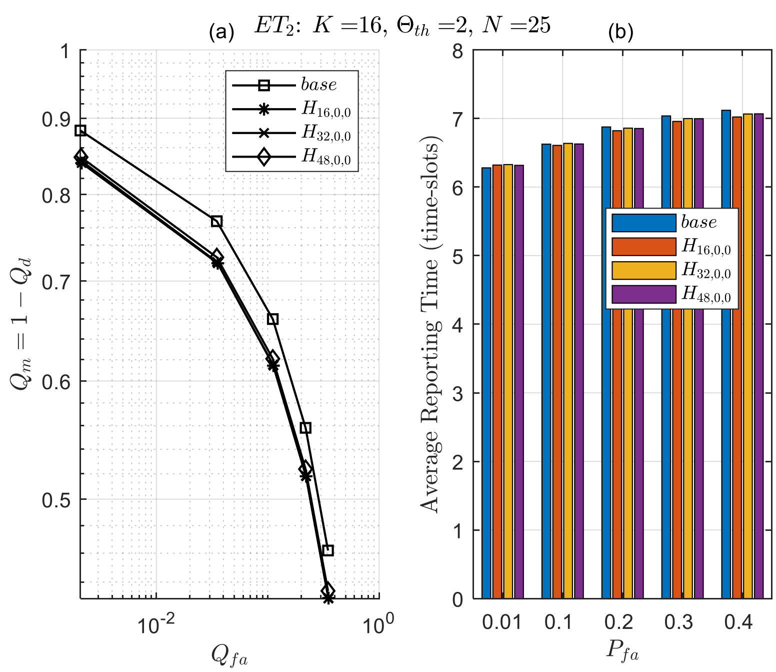

Figure 5.5: (a) Probability of misdetection vs. Probability of false alarm at the FC (Q_{fa}) (b) Average reporting time in time-slots vs. local Probability of false alarm (P_{fa}).

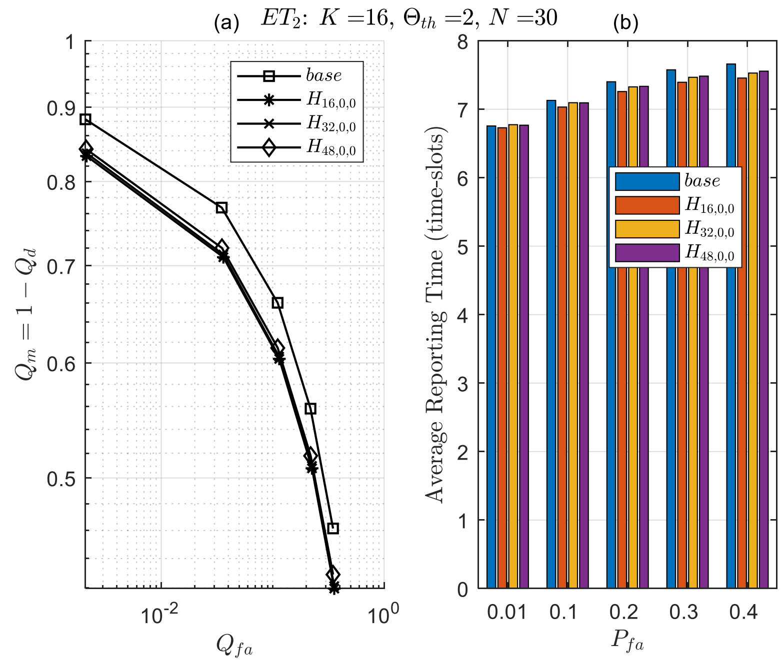

Figure 5.6: (a) Probability of misdetection vs. Probability of false alarm at the FC (Q_{fa}) (b) Average reporting time in time-slots vs. local Probability of false alarm (P_{fa}).

For the second step, we fix α to 32 and try different combinations of the sliding-window and minimum-window sizes in Figures 5.7 to 5.14, (i.e., $SW_{size}, MW_{size} \in \{0, 4, 8, 12, 16\}$). Figure 5.13 shows that for ET_1, a $SW_{size} = 16$, a $MW_{size} = 4$, and $\alpha = 32$ result in improved detection performance and speed as compared to the base scenario at lower P_{fa} values. As for the second early termination rule, ET_2, the gain in detection performance due to the sliding reporting window is accompanied with a significant detection speed loss. Clearly, a more thorough investigation trying all possible $(\alpha, SW_{size}, MW_{size})$ triplets is still needed to evaluate the efficacy of the sliding reporting window method.

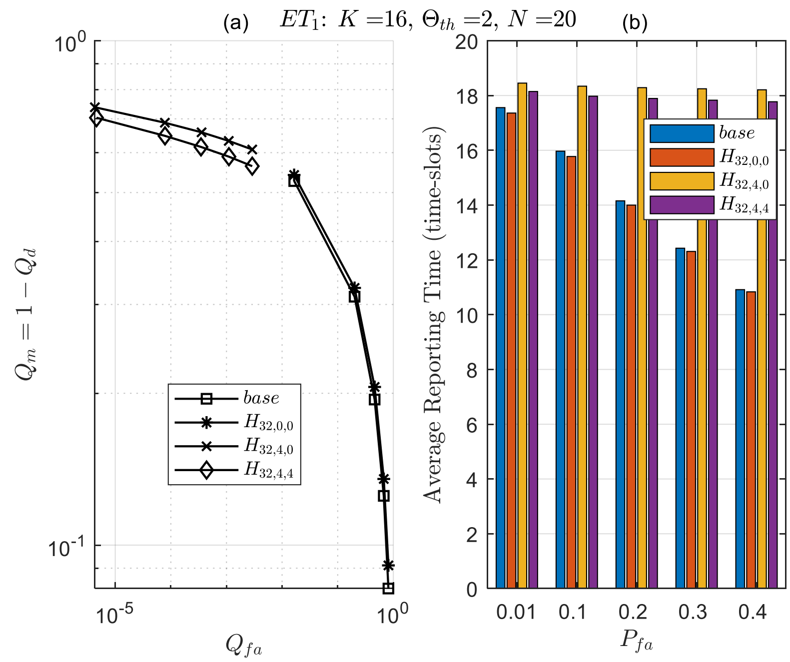

Figure 5.7: (a) Probability of misdetection vs. Probability of false alarm at the FC (Q_{fa}) (b) Average reporting time in time-slots vs. local Probability of false alarm (P_{fa}).

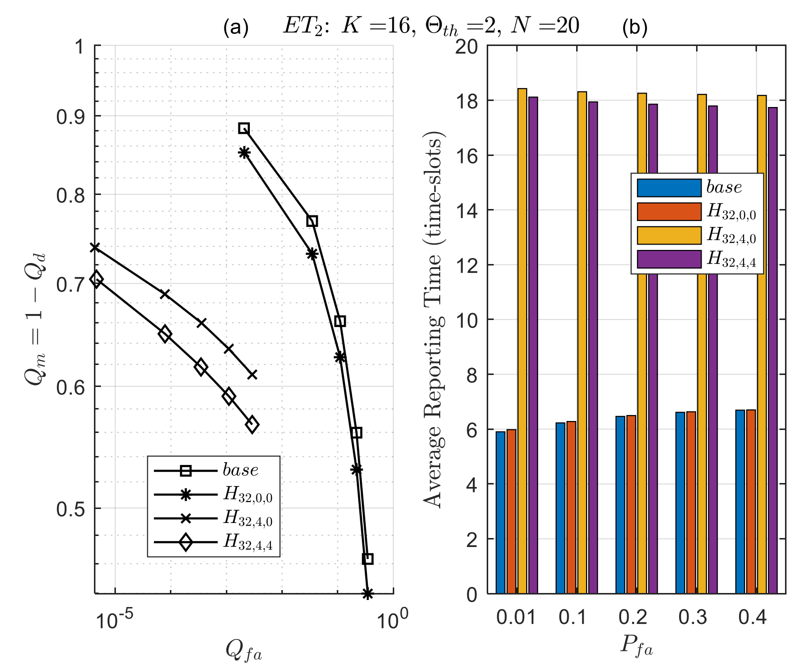

Figure 5.8: (a) Probability of misdetection vs. Probability of false alarm at the FC (Q_{fa}) (b) Average reporting time in time-slots vs. local Probability of false alarm (P_{fa}).

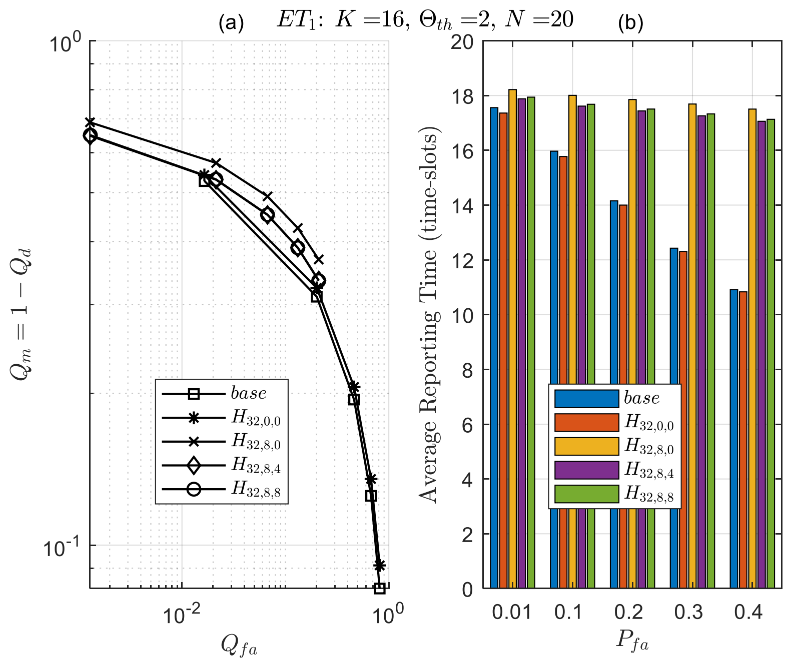

Figure 5.9: (a) Probability of misdetection vs. Probability of false alarm at the FC (Q_{fa}) (b) Average reporting time in time-slots vs. local Probability of false alarm (P_{fa}).

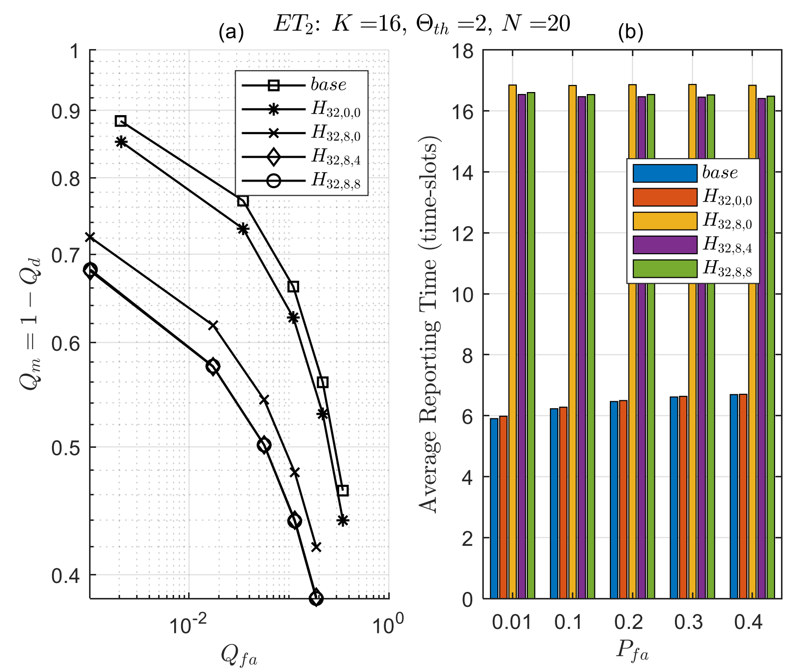

Figure 5.10: (a) Probability of misdetection vs. Probability of false alarm at the FC (Q_{fa}) (b) Average reporting time in time-slots vs. local Probability of false alarm (P_{fa}).

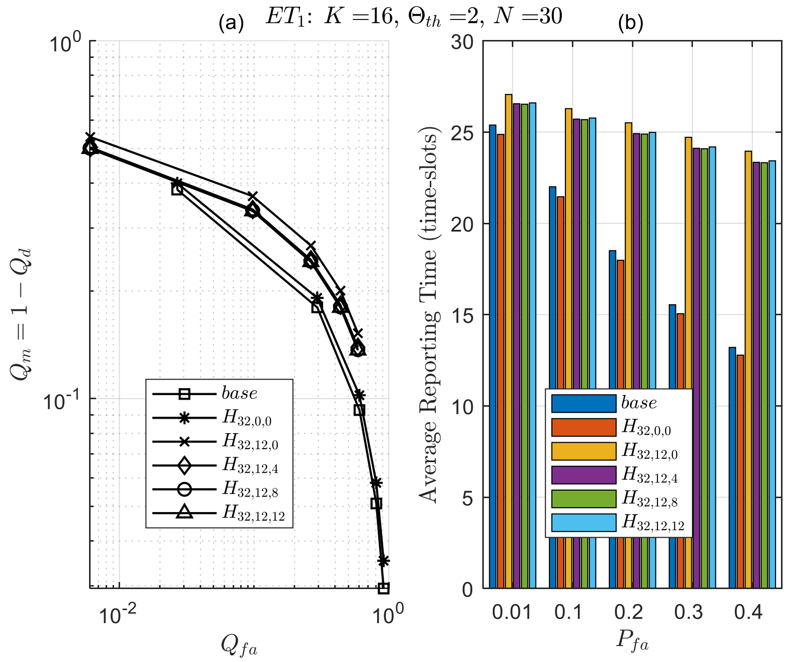

Figure 5.11: (a) Probability of misdetection vs. Probability of false alarm at the FC (Q_{fa}) (b) Average reporting time in time-slots vs. local Probability of false alarm (P_{fa}).

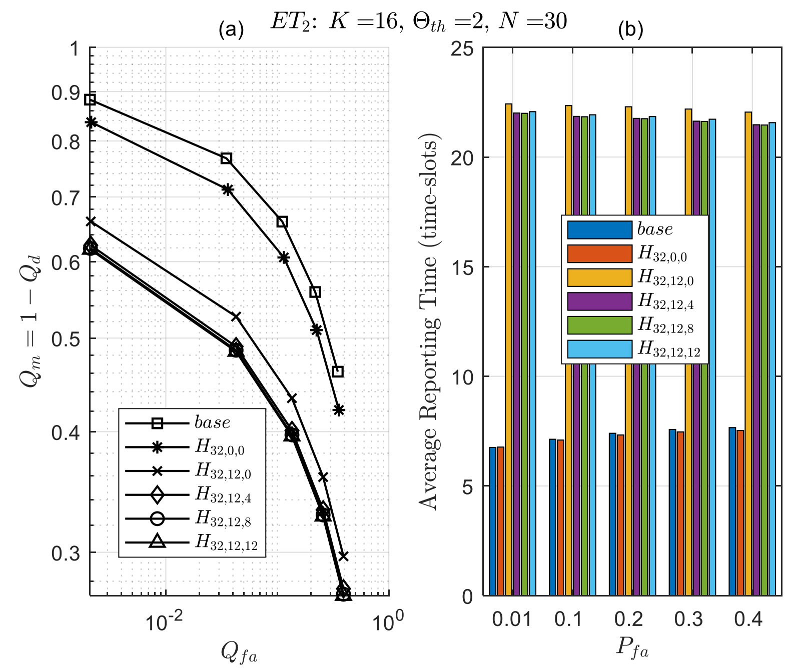

Figure 5.12: (a) Probability of misdetection vs. Probability of false alarm at the FC (Q_{fa}) (b) Average reporting time in time-slots vs. local Probability of false alarm (P_{fa}).

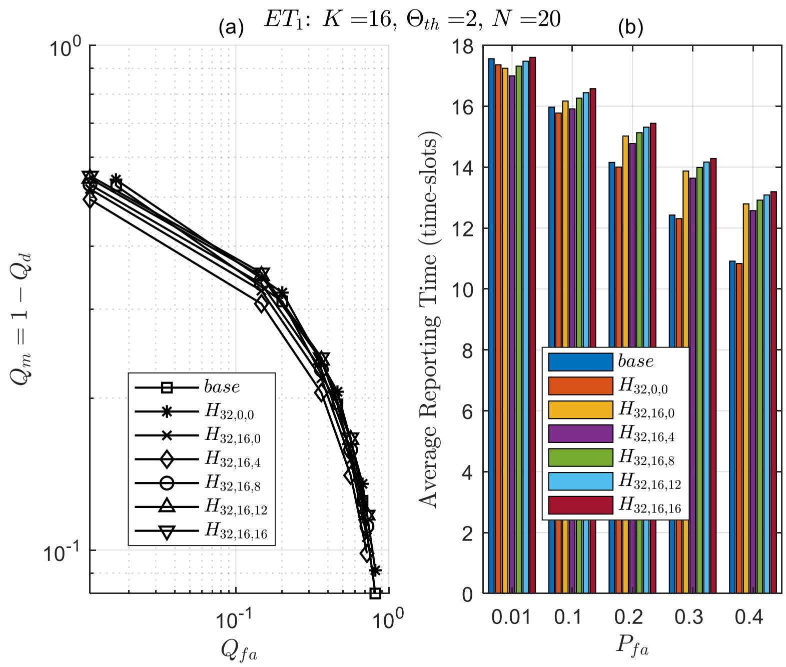

Figure 5.13: (a) Probability of misdetection vs. Probability of false alarm at the FC (Q_{fa}) (b) Average reporting time in time-slots vs. local Probability of false alarm (P_{fa}).

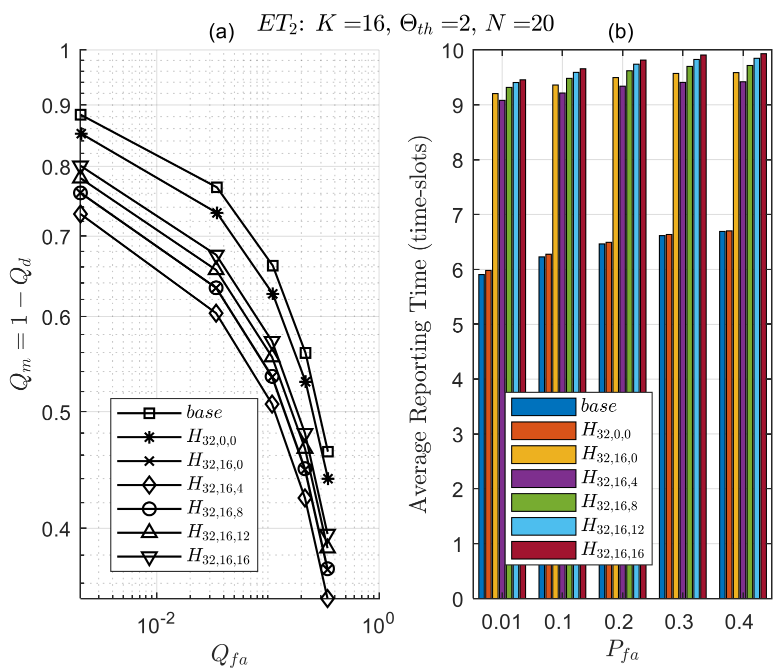

Figure 5.14: (a) Probability of misdetection vs. Probability of false alarm at the FC (Q_{fa}) (b) Average reporting time in time-slots vs. local Probability of false alarm (P_{fa}).

The third step is to increase the decision threshold Θ_{th} to 4 in Figures 5.15 and 5.16. We can see that the energy-based heuristic still slightly outperforms the base scenario in both detection performance and speed. In Figures 5.17 and 5.18, we increase the radius r from 1 to 2 in order to spread the CR terminals and make the PU more difficult to detect. Compared to Figure 5.3 for ET_1, the energy-based heuristic started to catch up with the base scenario in detection performance while still slightly outperforming the base in detection speed. For ET_2, the trend in Figure 5.18 is very close to that in Figure 5.6.

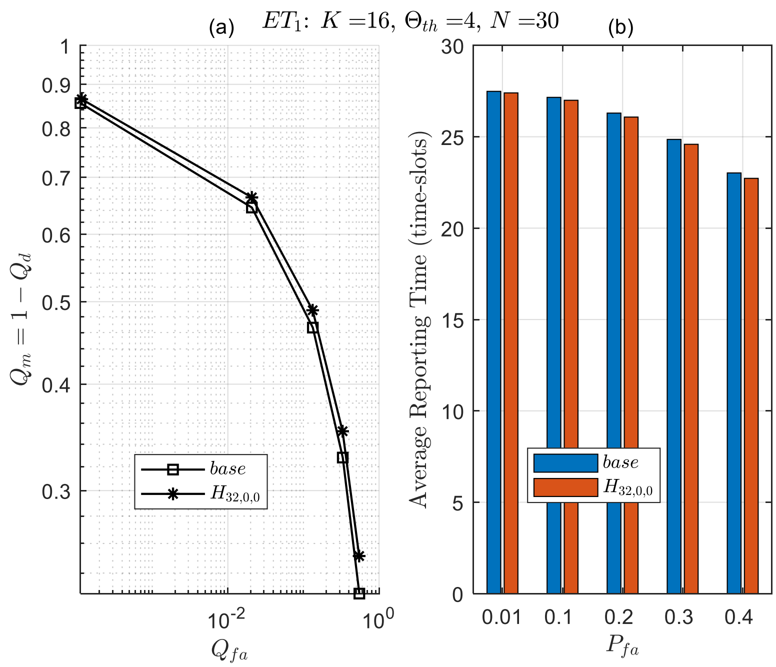

Figure 5.15: (a) Probability of misdetection vs. Probability of false alarm at the FC (Q_{fa}) (b) Average reporting time in time-slots vs. local Probability of false alarm (P_{fa}).

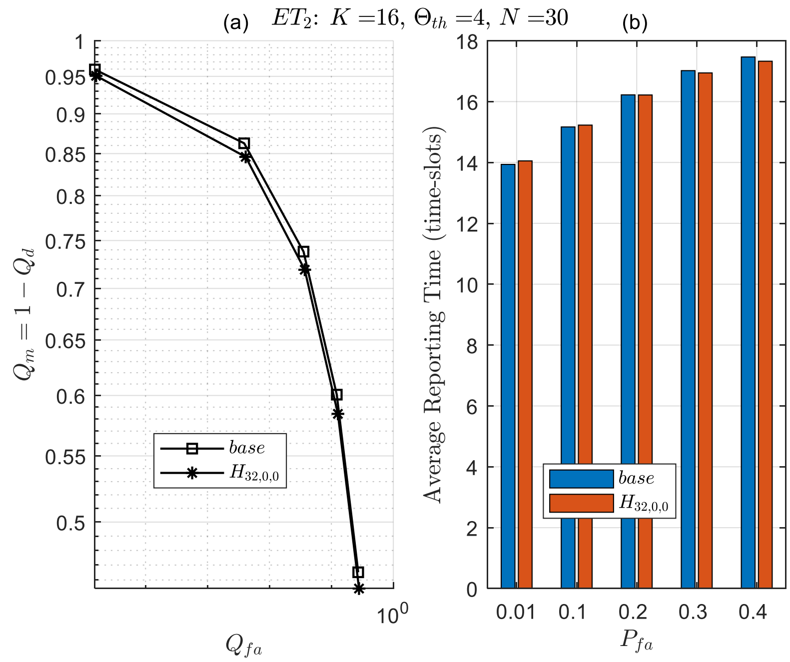

Figure 5.16: (a) Probability of misdetection vs. Probability of false alarm at the FC (Q_{fa}) (b) Average reporting time in time-slots vs. local Probability of false alarm (P_{fa}).

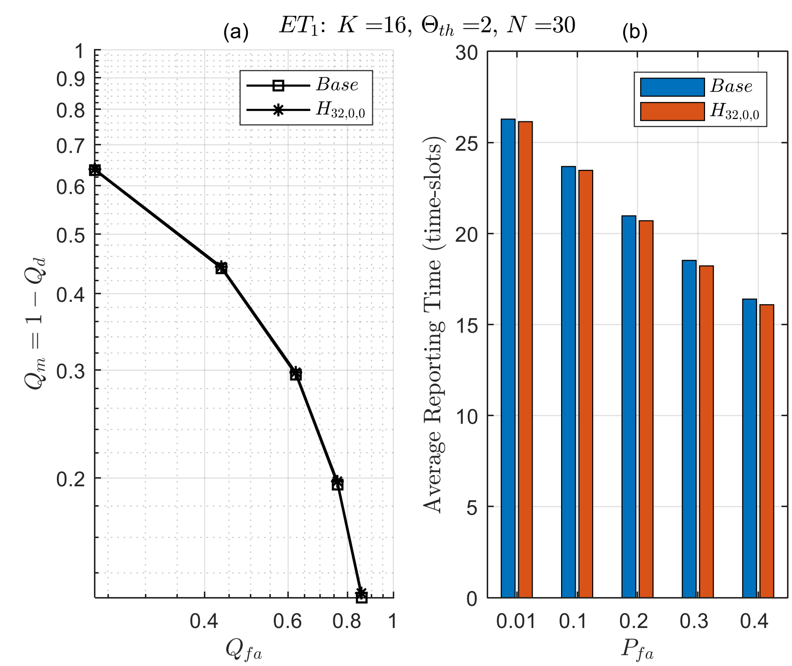

Figure 5.17: (a) Probability of misdetection vs. Probability of false alarm at the FC (Q_{fa}) (b) Average reporting time in time-slots vs. local Probability of false alarm (P_{fa}).

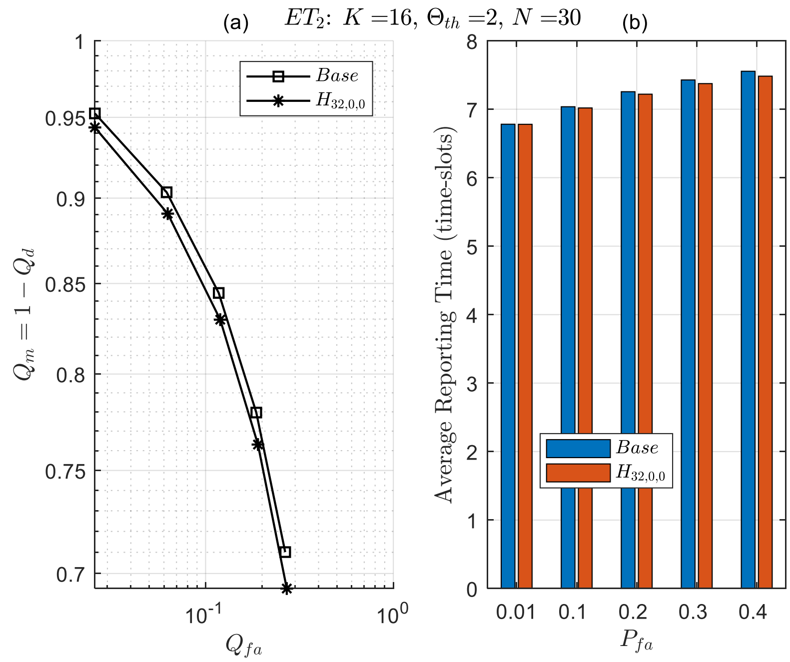

Figure 5.18: (a) Probability of misdetection vs. Probability of false alarm at the FC (Q_{fa}) (b) Average reporting time in time-slots vs. local Probability of false alarm (P_{fa}).

5.4 Summary

In this chapter we introduced an Energy-based Heuristic Reporting Priority Scheme using both random medium access early termination rules proposed in chapter 4. This heuristic reporting scheme favours CR terminals more capable of detecting the PU in reporting to the FC. We then used computer simulations to test our proposed energy-based sequential reporting scheme and compared it to the base scheme that uses independent identically and uniformly distributed counters as in Chapter 4. The proposed heuristic scheme shows slight improvements over the base uniform approach, however it calls for further investigation and a more involved simulation campaign to find its optimum configuration parameters. The energy-based heuristic scheme focus only on the sensing channel between the CR terminal and the PU. For future work, we would like to investigate sequential reporting priority schemes that also utilize information about the reporting channel through some form of feedback mechanism from the FC. Moreover, the proposed reporting scheme's parameters,

$\alpha, SW_{size}, MW_{size}$, are sensitive to the sensing environment and hence more work is needed on the training phase of the system to choose the optimal reporting parameters.

Chapter 6

Conclusion and Future Work

6.1 Concluding Remarks

In this thesis, we looked at the problem of agile cooperative spectrum sensing in CR-VANETs. More specifically, the reporting phase of the CSS process. We consider hard-decision reporting strategies based on random medium access using unacknowledged transmissions, (e.g., the case of vehicular networks using IEEE802.11p). Cognitive radio terminals employ random back-offs to avoid reports colliding with each other. This leads to additional delay and a random number of reports reaching the central FC. Our objective was then to derive closed form expressions for the overall probabilities of detection and false alarm at the FC as well as the average reporting time. These expressions are then verified with intensive computer simulations. The next step was to investigate sequential decision making schemes wherein the FC can terminate the reporting phase early once sufficient information about the status of the channel is received. We then looked into giving different reporting priorities to CR terminals based on their ability to detect the primary user. The contributions of this thesis are as follows:

- We studied decision-based cooperative spectrum sensing using random medium access, and derived closed form expressions for the detection and false alarm probabilities as explicit functions of the size of the contention window. We assumed the absence of a dedicated reporting channel and hence reports are transmitted over a channel shared with the PU. We accounted for the possibility of decoding errors at the FC due to the multi-path Rayleigh fading experienced over the reporting and the sensing channels. We then derived closed form expressions for the detection and false alarm probabilities and the average reporting time as explicit functions of the size of the contention window assuming the OR-decision rule is used by the FC. The objective of these results was to indicate the appropriate contention window size for a given number of reporting terminals.

- We then generalized the previous point to decision-based CSS using random medium access sequential reporting and the K-out-of-M decision rule. We devised two early termination rules with the objective of reducing the decision reporting duration and hence increasing the network throughput. Closed-form expressions have then been derived for the probabilities of detection and false alarm and the average reporting time for both early termination rules, and validated using computer simulations.

- We then introduced an Energy-based Heuristic Reporting Priority Scheme using both random medium access early termination rules proposed before. The Energy-based heuristic reporting priority scheme favours CR terminals more capable of detecting the PU in reporting to the FC. Computer simulations were then used to test the proposed energy-based sequential reporting scheme and compare it to the base or control scheme where all CR terminals have the same reporting priority.

6.2 Future Work

The results presented in this thesis raises some interesting topics for future research and the following is a list of some directions to pursue next:

- The work done in this thesis considers Hard Decision Fusion (HDF) at the FC. A straightforward extension is to investigate the impact of using multiple sensing thresholds at CR terminals locally to mimic a Soft Decision Fusion (SDF) system.

- The proposed energy-based heuristic reporting priority scheme shows only slight improvements over the base or control scheme. However; it calls for further investigation and a more involved simulation campaign to find its optimum configuration parameters.

- The energy-based heuristic scheme focus only on the sensing channel between the CR terminal and the PU. For future work, we would like to investigate sequential reporting priority schemes that also utilize information about the reporting channel and that may require feedback from the FC.

- There is a need to further investigate how feedback from the FC help reinforce confidence of a CR terminal in its ability to detect the PU and the quality of its reporting channel to the FC.

- The proposed reporting scheme's parameters, $\alpha, SW_{size}, MW_{size}$, are chosen a priori according to off-line simulations. However; these parameters depend upon the PU transmit power, the number of CR terminals, etc. In a dynamic system where many environmental parameters are continuously changing, more work is needed on the training phase of such a CSS reporting scheme.

- An important future step is to expand our work to a network of successive cells in a highway or urban vehicular scenario using different vehicular mobility models. Investigating the impact of mobility on the detection performance and speed of CSS using random medium access reporting vs. that of a stand-alone sensing scenario would be a significant contribution to CSS research.

- Investigating algorithms to select a dispersed subset of CR terminals to participate in the reporting process is an interesting research direction. The dispersion of reporting CR terminals increases spatial diversity needed for efficient CSS. Optimizing the size of the subset of reporting CR terminals is also of great importance to reduce the reporting phase duration.

- A very interesting extension of this thesis is to investigate the impact of malicious

CR terminals, wether independent or coordinated, engaged in PUE or SSDF attacks over the performance and speed of CSS using random medium access reporting.

References

[AAAT19] F. A. Awin, Y. M. Alginahi, E. Abdel-Raheem, and K. Tepe. Technical issues on cognitive radio-based internet of things systems: A survey. *IEEE Access*, 7:97887–97908, 2019.

[AACDFP14] Abdulla Al-Ali, Kaushik Chowdhury, Marco Di Felice, and Jarkko Paavola. Querying spectrum databases and improved sensing for vehicular cognitive radio networks. In *Communications (ICC), 2014 IEEE International Conference on*, pages 1379–1384. IEEE, 2014.

[AAdSAGAdA13] Rausley Adriano Amaral de Souza, Dayan Adionel Guimaraes, and Andre Antonio dos Anjos. Simulation platform for performance analysis of cooperative eigenvalue spectrum sensing with a realistic receiver model under impulsive noise. In Dr. Lorenzo Galati Giordano, editor, *Vehicular Technologies - Deployment and Applications*. InTech, Feb 2013.

[AAI13] A. Abu Alkheir and M. Ibnkahla. An accurate approximation of the exponential integral function using a sum of exponentials. *IEEE Communications Letters*, 17(7):1364–1367, Jul. 2013.

[AAM15] A. Abu Alkheir and H.T. Mouftah. Sequential hard-decision fusion for agile cooperative spectrum sensing. In *IEEE International Conference on Communication Workshop (ICCW)*, pages 1014–1019, June 2015.

[AASDF+15] Abdulla K Al-Ali, Yifan Sun, Marco Di Felice, Jarkko Paavola, and Kaushik R Chowdhury. Accessing spectrum databases using interference alignment in vehicular cognitive radio networks. *IEEE Transactions on Vehicular Technology*, 64(1):263–272, 2015.

[AASM16] A. A. Ahmed, A. A. Alkheir, D. Said, and H. T. Mouftah. Decision-based cooperative spectrum sensing using random medium access. In *IEEE Canadian Conference on Electrical and Computer Engineering (CCECE)*, pages 1–5, May 2016.

[ALB11] Ian F. Akyildiz, Brandon F. Lo, and Ravikumar Balakrishnan. Cooperative spectrum sensing in cognitive radio networks: A survey. *Phys. Commun.*, 4(1):40–62, Mar. 2011.

[Alm19] Hisham M Almasaeid. Maximizing achievable transmission time in cognitive radio networks under sensor-aided crowdsourced spectrum sensing. *The Computer Journal*, 2019.

[AM15] Ala Abu Alkheir and Hussein T Mouftah. Sequential hard-decision fusion for agile cooperative spectrum sensing. In *Communication Workshop (ICCW), 2015 IEEE International Conference on*, pages 1014–1019. IEEE, 2015.

[AQA+13] SH Abbassi, IM Qureshi, BR Alyaei, H Abbasi, and K Sultan. An efficient spectrum sensing mechanism for cr-vanets, j. *Basic Appl. Sci. Res*, 3:12, 2013.

[AQAA15] Shahid H Abbassi, Ijaz M Qureshi, Hameer Abbasi, and Bahman R Alyaie. History-based spectrum sensing in CR-VANETs. *EURASIP Journal on Wireless Communications and Networking*, 2015(1):1–12, 2015.

[AS18] P Anushiya and M Suganthi. Energy detection based spectrum sensing data mining for safety-message delivery in cr enabled vanet. In *2018 2nd International Conference on Inventive Systems and Control (ICISC)*, pages 1130–1133. IEEE, 2018.

[AW17] Bengi Aygun and Alexander M Wyglinski. A voting-based distributed cooperative spectrum sensing strategy for connected vehicles. *IEEE Transactions on Vehicular Technology*, 66(6):5109–5121, 2017.

[BD15] Richard E Bellman and Stuart E Dreyfus. *Applied dynamic programming*, volume 2050. Princeton university press, 2015.

[BDGD12] I.H. Brahmi, S. Djahel, and Y. Ghamri-Doudane. A Hidden Markov Model based scheme for efficient and fast dissemination of safety messages in VANETs. In *IEEE Global Communications Conference (GLOBECOM)*, pages 177–182, Dec 2012.

[BIV+11] D. Borota, G. Ivkovic, R. Vuyyuru, O. Altintas, I. Seskar, and P. Spasojevic. On the Delay to Reliably Detect Channel Availability in Cooperative Vehicular Environments. In *IEEE Vehicular Technology Conference (VTC-Spring)*, pages 1–5, May 2011.

[BK18] H. T. Batool and R. S. Kawitkar. Performance investigation of insistent spectrum sensing data falsification on cogntive radio networks. In *2018 Second International Conference on Intelligent Computing and Control Systems (ICICCS)*, pages 1907–1911, June 2018.

[BLZ09] K. Ben Letaief and Wei Zhang. Cooperative communications for cognitive radio networks. *Proceedings of the IEEE*, 97(5):878 –893, May 2009.

[BSA+15] Kim Baraka, Lise Safatly, Hassan Artail, Ali Ghandour, and Ali El-Hajj. An infrastructure-aided cooperative spectrum sensing scheme for vehicular ad hoc networks. *Ad Hoc Networks*, 25:197 – 212, 2015.

[BWD19] R. Biswas, J. Wu, and X. Du. Mitigation of the spectrum sensing data falsifying attack in cognitive radio networks. In *ICC 2019 - 2019 IEEE International Conference on Communications (ICC)*, pages 1–6, May 2019.

[BZGW19] S. Bayhan, A. Zubow, P. Gawłowicz, and A. Wolisz. Smart contracts for spectrum sensing as a service. *IEEE Transactions on Cognitive Communications and Networking*, 5(3):648–660, Sep. 2019.

[BZY17] Ping Bai, Xun Zhang, and Fang Ye. Reputation-based beta reputation system against ssdf attack in cognitive radio networks. In *2017 Progress in Electromagnetics Research Symposium-Fall (PIERS-FALL)*, pages 792–799. IEEE, 2017.

[CCCL12] Chi-Yuan Chen, Yao-Hsin Chou, Han-Chieh Chao, and Chi-Hsiang Lo. Secure centralized spectrum sensing for cognitive radio networks. *Wireless Networks*, 18(6):667–677, 2012.

[CG08] T.C. Clancy and N. Goergen. Security in Cognitive Radio Networks: Threats and Mitigation. In *International Conference on Cognitive Radio Oriented Wireless Networks and Communications (CrownCom)*, pages 1–8, May 2008.

[CHS+07] L. Cheng, B. E. Henty, D. D. Stancil, F. Bai, and P. Mudalige. Mobile vehicle-to-vehicle narrow-band channel measurement and characterization of the 5.9 ghz dedicated short range communication (dsrc) frequency band. *IEEE Journal on Selected Areas in Communications*, 25(8):1501–1516, Oct 2007.

[CLG+19] Max Curran, Xiao Liang, Himanshu Gupta, Omkant Pandey, and Samir R Das. Procsa: Protecting privacy in crowdsourced spectrum allocation. In *European Symposium on Research in Computer Security*, pages 556–576. Springer, 2019.

[CMB04] D. Cabric, S.M. Mishra, and R.W. Brodersen. Implementation issues in spectrum sensing for cognitive radios. In *Proc. Conference Record of the Thirty-Eighth Asilomar Conference on Signals, Systems and Computers*, pages 772–776, 7-10 Nov. 2004.

[CNDM19] Qingqing Cheng, Diep Nguyen, Eryk Dutkiewicz, and Markus Dominik Mueck. Preserving honest/dishonest users' operational privacy with blind interference calculation in spectrum sharing system. *IEEE Transactions on Mobile Computing*, 2019.

[Com74] Louis Comtet. *Advanced Combinatorics: The Art of Finite and Infinite Expansions*. Springer Science+Business Media B.V., May 1974.

[CPB08] Ruiliang Chen, J-M Park, and Kaigui Bian. Robust distributed spectrum sensing in cognitive radio networks. In *IEEE INFOCOM 2008-The 27th Conference on Computer Communications*, pages 1876–1884. IEEE, 2008.

[CPB12] Ruiliang Chen, Jung-Min Jerry Park, and Kaigui Bian. Robustness against byzantine failures in distributed spectrum sensing. *Computer Communications*, 35(17):2115–2124, 2012.

[CPHR08] Ruiliang Chen, Jung-Min Park, Y.T. Hou, and J.H. Reed. Toward secure distributed spectrum sensing in cognitive radio networks. *IEEE Communications Magazine*, 46(4):50–55, April 2008.

[CR09] Emmanuel J Candès and Benjamin Recht. Exact matrix completion via convex optimization. *Foundations of Computational mathematics*, 9(6):717, 2009.

[CWH11] Yilun Chen, Ami Wiesel, and Alfred O Hero. Robust shrinkage estimation of high-dimensional covariance matrices. *IEEE Transactions on Signal Processing*, 59(9):4097–4107, 2011.

[CZX+16] Huifang Chen, Ming Zhou, Lei Xie, Kuang Wang, and Jie Li. Joint spectrum sensing and resource allocation scheme in cognitive radio networks with spectrum sensing data falsification attack. *IEEE Transactions on Vehicular Technology*, 65(11):9181–9191, 2016.

[DAS03] F.F. Digham, M.-S. Alouini, and M.K. Simon. On the energy detection of unknown signals over fading channels. In *Proc. IEEE ICC*, pages 3575 – 3579 vol.5, May 2003.

[DAS07] F. F. Digham, M. Alouini, and M. K. Simon. On the energy detection of unknown signals over fading channels. *IEEE Transactions on Communications*, 55(1):21–24, Jan 2007.

[DD16] Deepa Das and Susmita Das. Adaptive resource allocation scheme for cognitive radio vehicular ad-hoc network in the presence of primary user emulation attack. *IET Networks*, 6(1):5–13, 2016.

[DFC15] Hong Du, Shuang Fu, and Hongna Chu. A credibility-based defense ssdf attacks scheme for the expulsion of malicious users in cognitive radio. *International Journal of Hybrid Information Technology*, 8(9):269–280, 2015.

[DFCB10a] M. Di Felice, K.R. Chowdhury, and L. Bononi. Analyzing the potential of cooperative cognitive radio technology on inter-vehicle communication. In *Wireless Days (WD), 2010 IFIP*, pages 1–6, Oct 2010.

[DFCB10b] M. Di Felice, K.R. Chowdhury, and L. Bononi. Analyzing the potential of cooperative Cognitive Radio technology on inter-vehicle communication. In *International Federation for Information Processing (IFIP) Wireless Days (WD)*, pages 1–6, Oct 2010.

[DFCB11a] M. Di Felice, K.R. Chowdhury, and L. Bononi. Cooperative spectrum management in cognitive Vehicular Ad Hoc Networks. In *IEEE Vehicular Networking Conference (VNC)*, pages 47–54, Nov 2011.

[DFCB11b] M. Di Felice, K.R. Chowdhury, and L. Bononi. Cooperative spectrum management in cognitive vehicular ad hoc networks. In *Vehicular Networking Conference (VNC), 2011 IEEE*, pages 47–54, Nov 2011.

[DFCB13] Marco Di Felice, Kaushik Roy Chowdhury, and Luciano Bononi. *Cognitive Radio Vehicular Ad Hoc Networks: Design, Implementation, and Future Challenges*, pages 619–644. John Wiley and Sons, Inc., 2013.

[DFDMCB12] M. Di Felice, R. Doost-Mohammady, K.R. Chowdhury, and L. Bononi. Smart radios for smart vehicles: Cognitive vehicular networks. *Vehicular Technology Magazine, IEEE*, 7(2):26–33, June 2012.

[DFGAB13] M. Di Felice, A.J. Ghandhour, H. Artail, and L. Bononi. Integrating Spectrum Database and Cooperative Sensing for Cognitive Vehicular Networks. In *IEEE Vehicular Technology Conference (VTC-Fall)*, pages 1–7, Sept 2013.

[DLC+18] H. Ding, X. Li, Y. Cai, B. Lorenzo, and Y. Fang. Intelligent data transportation in smart cities: A spectrum-aware approach. *IEEE/ACM Transactions on Networking*, 26(6):2598–2611, Dec 2018.

[DMA97] Geoff Davis, Stephane Mallat, and Marco Avellaneda. Adaptive greedy approximations. *Constructive approximation*, 13(1):57–98, 1997.

[DMHS12] Lingjie Duan, Alexander W Min, Jianwei Huang, and Kang G Shin. Attack prevention for collaborative spectrum sensing in cognitive radio networks. *IEEE Journal on Selected Areas in Communications*, 30(9):1658–1665, 2012.

[DZCF17] Haichuan Ding, Chi Zhang, Ying Cai, and Yuguang Fang. Smart cities on wheels: A newly emerging vehicular cognitive capability harvesting network for data transportation. *IEEE Wireless Communications*, 25(2):160–169, 2017.

[DZL+19] Xuewen Dong, Tao Zhang, Di Lu, Guangxia Li, Yulong Shen, and Jianfeng Ma. Preserving geo-indistinguishability of the primary user in dynamic spectrum sharing. *IEEE Transactions on Vehicular Technology*, 68(9):8881–8892, 2019.

[EKM18] Nada Elgaml, Ahmed Khattab, and Hebat-Allah Mourad. Slotted ieee 802.11 p contention for overhead-free spectrum sensing in cr-vanets. In *Consumer Communications & Networking Conference (CCNC), 2018 15th IEEE Annual*, pages 1–6. IEEE, 2018.

[EUHK13] Waleed Ejaz, Najam Ul Hasan, and Hyung Seok Kim. Distributed cooperative spectrum sensing in cognitive radio for ad hoc networks. *Computer Communications*, 36(12):1341–1349, 2013.

[Eze10] A. Ezell. Explaining international it application leadership: Intelligent transportation systems. Technical report, University of Zurich, Department of Informatics, Jan 2010.

[EZL+15] Joy Eze, Sijing Zhang, Enjie Liu, Elias E Chinedum, and Q Yu Hong. Cognitive radio aided internet of vehicles (iovs) for improved spectrum resource allocation. In *Computer and Information Technology; Ubiquitous Computing and Communications; Dependable, Autonomic and Secure Computing; Pervasive Intelligence and Computing (CIT/IUCC/DASC/PICOM), 2015 IEEE International Conference on*, pages 2346–2352. IEEE, 2015.

[EZLE18a] J. Eze, S. Zhang, E. Liu, and E. Eze. Cognitive radio-enabled internet of vehicles: a cooperative spectrum sensing and allocation for vehicular communication. *IET Networks*, 7(4):190–199, 2018.

[EZLE18b] Joy Eze, Sijing Zhang, Enjie Liu, and Elias Eze. Cognitive radio-enabled internet of vehicles: a cooperative spectrum sensing and allocation for vehicular communication. *IET Networks*, 2018.

[Fer04] JL Fernández. Modelling impulsive interference in dvb-t: Statistical analysis, test waveforms and receiver performance. *EBU Technical Review*, 2004.

[FFEGAEMEB19] Wassim Fassi Fihri, Hassan El Ghazi, Badr Abou El Majd, and Faissal El Bouanani. A decision-making approach for detecting the primary user emulation attack in cognitive radio networks. *International Journal of Communication Systems*, 32(15):e4026, 2019. e4026 dac.4026.

[FGOA10] K. Fawaz, A. Ghandour, M. Olleik, and H. Artail. Improving reliability of safety applications in vehicle ad hoc networks through the implementation of a cognitive network. In *IEEE International Conference on Telecommunications (ICT)*, pages 798–805, April 2010.

[FKB+19] M. Farrukh, A. Krayani, M. Baydoun, L. Marcenaro, Y. Gao, and C. S. Regazzoni. Learning a switching bayesian model for jammer detection in the cognitive-radio-based internet of things. In *2019 IEEE 5th World Forum on Internet of Things (WF-IoT)*, pages 380–385, April 2019.

[FLC15] Jingyu Feng, Guangyue Lu, and Hong Chang. Behave well: how to win a pop vacant band via cooperative spectrum sensing. *KSII Transactions on Internet and Information Systems (TIIS)*, 9(4):1321–1336, 2015.

[FLL+18] J. Feng, S. Li, S. Lv, H. Wang, and A. Fu. Securing cooperative spectrum sensing against collusive false feedback attack in cognitive radio networks. *IEEE Transactions on Vehicular Technology*, 67(9):8276–8287, Sep. 2018.

[FNKF13] Zubair Md Fadlullah, Hiroki Nishiyama, Nei Kato, and Mostafa M Fouda. Intrusion detection system (ids) for combating attacks against cognitive radio networks. *IEEE network*, 27(3):51–56, 2013.

[GBR+12] Arthur Gretton, Karsten M Borgwardt, Malte J Rasch, Bernhard Schölkopf, and Alexander Smola. A kernel two-sample test. *Journal of Machine Learning Research*, 13(Mar):723–773, 2012.

[GdSB13] Dayan A Guimaraes, Rausley AA de Souza, and André N Barreto. Performance of cooperative eigenvalue spectrum sensing with a realistic receiver model under impulsive noise. *Journal of Sensor and Actuator networks*, 2(1):46–69, 2013.

[GR07] I. S. Gradshteyn and I. M. Ryzhik. *Table of Integrals, Series, and Products*. Academic Press, San Diego, CA, seventh edition edition, 2007.

[Gre16] John Greenough. The connected car report: Forecasts, competing technologies, and leading manufacturers. *Business Insider*, 2016.

[GS08] Amir Ghasemi and Elvino S Sousa. Spectrum sensing in cognitive radio networks: requirements, challenges and design trade-offs. *IEEE Communications magazine*, 46(4), 2008.

[GSMJ18] K. K. Ghanshala, S. Sharma, S. Mohan, and R. C. Joshi. Cloud-based cognitive radio adhoc vehicular network architecture: A next-generation smart city. In *2018 IEEE 9th Annual Information Technology, Electronics and Mobile Communication Conference (IEMCON)*, pages 145–150, Nov 2018.

[GT90] Georgios B Giannakis and Michail K Tsatsanis. Signal detection and classification using matched filtering and higher order statistics. *IEEE Transactions on Acoustics, Speech, and Signal Processing*, 38(7):1284–1296, 1990.

[GYH19] Mohamed Grissa, Attila A Yavuz, and Bechir Hamdaoui. Location privacy in cognitive radios with multi-server private information retrieval. *IEEE Transactions on Cognitive Communications and Networking*, 2019.

[GZL+13] Zhaoyu Gao, Haojin Zhu, Yao Liu, Muyuan Li, and Zhenfu Cao. Location privacy in database-driven cognitive radio networks: Attacks and countermeasures. In *2013 Proceedings IEEE INFOCOM*, pages 2751–2759. IEEE, 2013.

[HCK11] Hsing-yi Hsieh, Han-Kui Chang, and Meng-Lin Ku. Higher-order statistics based sequential spectrum sensing for cognitive radio. In *ITS Telecommunications (ITST), 2011 11th International Conference on*, pages 696–701. IEEE, 2011.

[HGXE14] Chowdhury S Hyder, Brendan Grebur, Li Xiao, and Max Ellison. Arc: Adaptive reputation based clustering against spectrum sensing data falsification attacks. *IEEE Transactions on mobile computing*, 13(8):1707–1719, 2014.

[HSND11] Laila Hesham, Ahmed Sultan, Mohammed Nafie, and Fadel Digham. Cooperative sensing with sequential ordered transmissions to secondary fusion center. In *Acoustics, Speech and Signal Processing (ICASSP), 2011 IEEE International Conference on*, pages 2988–2991. IEEE, 2011.

[HWL+16] Xin-Lin Huang, Jun Wu, Wenfeng Li, Zhifeng Zhang, Fusheng Zhu, and Minghao Wu. Historical spectrum sensing data mining for cognitive radio enabled vehicular ad-hoc networks. *IEEE Transactions on Dependable and Secure Computing*, 13(1):59–70, 2016.

[JHKI13] Minho Jo, Longzhe Han, Dohoon Kim, and Hoh Peter In. Selfish attacks and detection in cognitive radio ad-hoc networks. *IEEE network*, 27(3):46–50, 2013.

[JZL+16] Eze C Joy, Sijing Zhang, Enjie Liu, Efor E Theresa, and Eze C Elias. Cognitive radio aided vehicular ad-hoc networks with efficient spectrum allocation and qos guarantee. In *Automation and Computing (ICAC), 2016 22nd International Conference on*, pages 156–161. IEEE, 2016.

[JZS08] Juncheng Jia, Qian Zhang, and Xuemin Sherman Shen. Hc-mac: A hardware-constrained cognitive mac for efficient spectrum management. *IEEE journal on selected areas in communications*, 26(1):106–117, 2008.

[KG10] Seung-Jun Kim and Georgios B Giannakis. Sequential and cooperative sensing for multi-channel cognitive radios. *IEEE Transactions on Signal Processing*, 58(8):4239–4253, 2010.

[KLC+17] SONG Kai, Fu-qiang LIU, WANG Chao, Nguyen Ngoc Van, and Li-jun ZU. Spectrum sensing with largest eigenvalue in cooperative cognitive vehicular networks. *DEStech Transactions on Computer Science and Engineering*, 2017.

[KNP12] Ziad Khalaf, Amor Nafkha, and Jacques Palicot. Blind spectrum detector for cognitive radio using compressed sensing and symmetry property of the second order cyclic autocorrelation. In *Cognitive Radio Oriented Wireless Networks and Communications (CROWNCOM), 2012 7th International ICST Conference on*, pages 291–296. IEEE, 2012.

[KSS17] Sumit Kar, Srinivas Sethi, and Ramesh Kumar Sahoo. A multi-factor trust management scheme for secure spectrum sensing in cognitive radio networks. *Wireless Personal Communications*, 97(2):2523–2540, 2017.

[KT07] Nikhil Kundargi and Ahmed Tewfik. Hierarchical sequential detection in the context of dynamic spectrum access for cognitive radios. In *Electronics, Circuits and Systems, 2007. ICECS 2007. 14th IEEE International Conference on*, pages 514–517. IEEE, 2007.

[KT10] N. Kundargi and A. Tewfik. Doubly sequential energy detection for distributed dynamic spectrum access. In *IEEE International Conference on Communications (ICC)*, pages 1–5, May 2010.

[Lee13a] Dong-Jun Lee. Adaptive cooperative spectrum sensing using random access in cognitive radio networks. In *Personal Indoor and Mobile Radio Communications (PIMRC), 2013 IEEE 24th International Symposium on*, pages 1835–1839. IEEE, 2013.

[Lee13b] Dong-Jun Lee. Adaptive cooperative spectrum sensing using random access in cognitive radio networks. In *IEEE International Symposium on Personal Indoor and Mobile Radio Communications (PIMRC)*, pages 1835–1839, Sep. 2013.

[Lee15a] D. Lee. Adaptive random access for cooperative spectrum sensing in cognitive radio networks. *IEEE Transactions on Wireless Communications*, 14(2):831–840, Feb 2015.

[Lee15b] Dong-Jun Lee. Adaptive random access for cooperative spectrum sensing in cognitive radio networks. *IEEE Transactions on Wireless Communications*, 14(2):831–840, Feb 2015.

[LGCP19] H. Li, Y. Gu, J. Chen, and Q. Pei. Speed adjustment attack on cooperative sensing in cognitive vehicular networks. *IEEE Access*, 7:75925–75934, 2019.

[LI10] Husheng Li and D.K. Irick. Collaborative Spectrum Sensing in Cognitive Radio Vehicular Ad Hoc Networks: Belief Propagation on Highway. In *IEEE Vehicular Technology Conference (VTC-Spring)*, pages 1–5, May 2010.

[LJ10a] Dong-Jun Lee and Myung-Sung Jang. Optimal access period for cooperative spectrum sensing in cognitive radio networks. In *Wireless Information Technology and Systems (ICWITS), 2010 IEEE International Conference on*, pages 1–4. IEEE, 2010.

[LJ10b] Dong-Jun Lee and Myung-Sung Jang. Optimal access period for cooperative spectrum sensing in cognitive radio networks. In *IEEE International Conference on Wireless Information Technology and Systems (ICWITS)*, pages 1–4, Aug 2010.

[LSZ$^+$18] Xi Li, Tiecheng Song, Yueyue Zhang, Guojun Chen, and Jing Hu. A hybrid cooperative spectrum sensing scheme based on spatial-temporal correlation for cr-vanet. In *2018 IEEE 87th Vehicular Technology Conference (VTC Spring)*, pages 1–6. IEEE, 2018.

[LW11] Dong-Jun Lee and Hyuk Wu. Spectrum sensing time minimizing access delay of ieee 802.11-like mac in cognitive radio networks. *IEEE Communications Letters*, 15(11):1249–1251, 2011.

[LW15] Jianqi Lu and Ping Wei. Improved cooperative spectrum sensing based on the reputation in cognitive radio networks. *International Journal of Electronics*, 102(5):855–863, 2015.

[LXY+14] Yi Liu, Shengli Xie, Rong Yu, Yan Zhang, Xi Zhang, and Chau Yuen. Exploiting temporal and spatial diversities for spectrum sensing and access in cognitive vehicular networks. *Wireless Communications and Mobile Computing*, 15(17):2079–2094, 2014.

[LYP14] Mee Hong Ling, Kok-Lim Alvin Yau, and Geong Sen Poh. Trust and reputation management in cognitive radio networks: a survey. *Security and Communication Networks*, 7(11):2160–2179, 2014.

[LZG17] Xia Liu, Zhimin Zeng, and Caili Guo. Robust cooperative spectrum sensing in dense cognitive vehicular networks. In *Proc. ICCC*, pages 1–6, 2017.

[LZG18] Xia Liu, Zhimin Zeng, and Caili Guo. Robust and low-complexity cooperative spectrum sensing via low-rank matrix recovery in cognitive vehicular networks. *Wireless Communications and Mobile Computing*, 2018, 2018.

[LZL+12a] Sheng Liu, Haojin Zhu, Shuai Li, Xu Li, Cailian Chen, and Xinping Guan. An adaptive deviation-tolerant secure scheme for distributed cooperative spectrum sensing. In *2012 IEEE Global Communications Conference (GLOBECOM)*, pages 603–608. IEEE, 2012.

[LZL12b] Lu Lu, Xiangwei Zhou, and Geoffrey Ye Li. Optimal sequential detection in cognitive radio networks. In *Wireless Communications and Networking Conference (WCNC), 2012 IEEE*, pages 289–293. IEEE, 2012.

[LZPH08] Ying-Chang Liang, Yonghong Zeng, E.C.Y. Peh, and Anh Tuan Hoang. Sensing-throughput tradeoff for cognitive radio networks. *Wireless Communications, IEEE Transactions on*, 7(4):1326 –1337, apr. 2008.

[MTC17] Daniela Mazza, Daniele Tarchi, and Giovanni E Corazza. A unified urban mobile cloud computing offloading mechanism for smart cities. *IEEE Communications Magazine*, 55(3):30–37, 2017.

[MV18a] S. Mapunya and M. Velempini. The design of byzantine attack mitigation scheme in cognitive radio ad-hoc networks. In *2018 International Conference on Intelligent and Innovative Computing Applications (ICONIC)*, pages 1–4, Dec 2018.

[MV18b] Sekgoari Mapunya and Mthulisi Velempini. Investigating spectrum sensing security threats in cognitive radio networks. In *Ad Hoc Networks*, pages 60–68. Springer, 2018.

[MXP+18] L. Ma, Y. Xiang, Q. Pei, Y. Xiang, and H. Zhu. Robust reputation-based cooperative spectrum sensing via imperfect common control channel. *IEEE Transactions on Vehicular Technology*, 67(5):3950–3963, May 2018.

[NS18] S Lakshmi Nandan and T Sudha. Cooperative spectrum sensing in cr-vanet with small-sized data sets. In *Innovations in Electronics and Communication Engineering*, pages 413–425. Springer, 2018.

[NTK13] Nhan Nguyen-Thanh and Insoo Koo. Optimal truncated ordered sequential cooperative spectrum sensing in cognitive radio. *IEEE sensors journal*, 13(11):4188–4195, 2013.

[NVD18] I. Ngomane, M. Velempini, and S. V. Dlamini. Trust-based system to defend against the spectrum sensing data falsification attack in cognitive radio ad hoc network. In *2018 International Conference on Advances in Big Data, Computing and Data Communication Systems (icABCD)*, pages 1–5, Aug 2018.

[PP02] A. Papoulis and S. U. Pillai. *Probability, Random Variables and Stochastic Processes*. McGraw Hill, fourth edition, 2002.

[PYLL13] Qingqi Pei, Beibei Yuan, Lei Li, and Hongning Li. A sensing and etiquette reputation-based trust management for centralized cognitive radio networks. *Neurocomputing*, 101:129–138, 2013.

[QGP18] Z. Qin, Y. Gao, and M. D. Plumbley. Malicious user detection based on low-rank matrix completion in wideband spectrum sensing. *IEEE Transactions on Signal Processing*, 66(1):5–17, Jan 2018.

[QH14] Xiaomin Qian and Li Hao. Spectrum sensing with energy detection in cognitive vehicular ad hoc networks. In *IEEE International Symposium on Wireless Vehicular Communications (WiVeC)*, pages 1–5, Sept 2014.

[QH15] Xiaomin Qian and Li Hao. On the performance of spectrum sensing in cognitive vehicular networks. In *Personal, Indoor, and Mobile Radio Communications (PIMRC), 2015 IEEE 26th Annual International Symposium on*, pages 1002–1006. IEEE, 2015.

[QHNT18] Xiaomin Qian, Li Hao, Dadong Ni, and Quang Thanh Tran. Hard fusion based spectrum sensing over mobile fading channels in cognitive vehicular networks. *Sensors*, 18(2), 2018.

[RACV10] Ankit Singh Rawat, Priyank Anand, Hao Chen, and Pramod K Varshney. Collaborative spectrum sensing in the presence of byzantine attacks in cognitive radio networks. *IEEE Transactions on Signal Processing*, 59(2):774–786, 2010.

[RNMT18] K. Rina, S. Nath, N. Marchang, and A. Taggu. Can clustering be used to detect intrusion during spectrum sensing in cognitive radio networks? *IEEE Systems Journal*, 12(1):938–947, March 2018.

[SA18] S. Sasipriya and A. Anusuya. Vehicle-to-vehicle communication using cognitive radio technology. In *2018 IEEE International Conference on Computational Intelligence and Computing Research (ICCIC)*, pages 1–5, Dec 2018.

[SAN+14] Lise Safatly, Babar Aziz, Amor Nafkha, Yves Louet, Youssef Nasser, Ali El-Hajj, and Karim Y Kabalan. Blind spectrum sensing using symmetry property of cyclic autocorrelation function: from theory to practice. *EURASIP Journal on Wireless Communications and Networking*, 2014(1):26, 2014.

[SBCA14] I. Souid, H. Ben Chikha, and R. Attia. Blind spectrum sensing in cognitive vehicular ad hoc networks over nakagami-m fading channels. In *International Conference on Electrical Sciences and Technologies in Maghreb (CISTEM)*, pages 1–5, Nov 2014.

[SJRB18] S. Shrivastava, S. John, A. Rajesh, and P. K. Bora. Preventing collusion attacks in cooperative spectrum sensing. In *2018 International Conference on Signal Processing and Communications (SPCOM)*, pages 90–94, July 2018.

[SN16] Abbas Ali Sharifi and Javad Musevi Niya. Securing collaborative spectrum sensing against malicious attackers in cognitive radio networks. *Wireless Personal Communications*, 90(1):75–91, 2016.

[SQC13] Zhihui Shu, Yi Qian, and Song Ci. On physical layer security for cognitive radio networks. *IEEE Network*, 27(3):28–33, May 2013.

[SRB14] KamalDeep Singh, Priyanka Rawat, and Jean-Marie Bonnin. Cognitive radio for vehicular ad hoc networks (cr-vanets): approaches and challenges. *EURASIP Journal on Wireless Communications and Networking*, 2014(1), 2014.

[SS08] Yeelin Shei and Yu T Su. A sequential test based cooperative spectrum sensing scheme for cognitive radios. In *Personal, Indoor and Mobile Radio Communications, 2008. PIMRC 2008. IEEE 19th International Symposium on*, pages 1–5. IEEE, 2008.

[SS10] S.S.Ikki and S.Aissa. Performance Analysis of Dual-Hop Relaying Systems in the Presence of Co-Channel Interference. In *IEEE Global Telecommunications Conference (GLOBECOM)*, pages 1–5, Dec. 2010.

[SSM19] Sundar Srinivasan, KB Shivakumar, and Muazzam Mohammad. Semi-supervised machine learning for primary user emulation attack detection and prevention through core-based analytics for cognitive radio networks. *International Journal of Distributed Sensor Networks*, 15(9):1550147719860365, 2019.

[STZ13] Fiky Y Suratman, Adrian Tetz, and Abdelhak M Zoubir. Collaborative spectrum sensing using sequential detections: Soft decision vs. hard decision. In *Information and Communication Technology (ICoICT), 2013 International Conference of*, pages 1–6. IEEE, 2013.

[SZ08] Hang Su and Xi Zhang. Cross-layer based opportunistic mac protocols for qos provisionings over cognitive radio wireless networks. *IEEE Journal on selected areas in communications*, 26(1), 2008.

[TJPM13] Kefeng Tan, Shraboni Jana, Parth H Pathak, and Prasant Mohapatra. On insider misbehavior detection in cognitive radio networks. *IEEE Network*, 27(3):4–9, 2013.

[TS10] Pablo Torio and Manuel Garcia Sanchez. Generating impulsive noise [wireless corner]. *IEEE Antennas and Propagation Magazine*, 52(4):168–173, 2010.

[TSC11] Pablo Torío, Manuel García Sanchez, and Íñigo Cuiñas. An algorithm to simulate impulsive noise. In *Software, Telecommunications and Computer Networks (SoftCOM), 2011 19th International Conference on*, pages 1–4. IEEE, 2011.

[TZWM12] Kefeng Tan, Kai Zeng, Daniel Wu, and Prasant Mohapatra. Detecting spectrum misuse in wireless networks. In *2012 IEEE 9th International Conference on Mobile Ad-Hoc and Sensor Systems (MASS 2012)*, pages 245–253. IEEE, 2012.

[VCM15] Aida Vosoughi, Joseph R Cavallaro, and Alan Marshall. Robust consensus-based cooperative spectrum sensing under insistent spectrum sensing data falsification attacks. In *2015 IEEE Global Communications Conference (GLOBECOM)*, pages 1–6. IEEE, 2015.

[WhH10] Xiao Yu Wang and Pin han Ho. A Novel Sensing Coordination Framework for CR-VANETs. *IEEE Transactions on Vehicular Technology*, 59(4):1936–1948, May 2010.

[WLK11] Mingwei Wu, Xuzheng Lin, and Pooi-Yuen Kam. New Exponential Lower Bounds on the Gaussian Q-Function via Jensen's Inequality. In *IEEE Vehicular Technology Conference (VTC Spring)*, pages 1–5, May 2011.

[WSW+17] Jun Wu, Tiecheng Song, Cong Wang, Yue Yu, Miao Liu, and Jing Hu. Robust cooperative spectrum sensing against probabilistic ssdf attack in cognitive radio networks. In *2017 IEEE 86th Vehicular Technology Conference (VTC-Fall)*, pages 1–6. IEEE, 2017.

[WSWH18] J. Wu, T. Song, C. Wang, and J. Hu. Reputation value ranking based sequential cooperative spectrum sensing against byzantine attack. In *2018 IEEE International Conference on Communications Workshops (ICC Workshops)*, pages 1–6, May 2018.

[WSY+18] J. Wu, T. Song, Y. Yu, C. Wang, and J. Hu. Generalized byzantine attack and defense in cooperative spectrum sensing for cognitive radio networks. *IEEE Access*, 6:53272–53286, Aug 2018.

[WYB15] Zhexiong Wei, F. Richard Yu, and Azzedine Boukerche. Cooperative Spectrum Sensing with Trust Assistance for Cognitive Radio Vehicular Ad Hoc Networks. In *Proceedings of the 5th ACM Symposium on Development and Analysis of Intelligent Vehicular Networks and Applications*, DIVANet '15, pages 27–33, New York, NY, USA, 2015. ACM.

[XHZG12] Xiaorong Xu, Aiping Huang, Jianwu Zhang, and Lanfen Gu. Cooperative wideband spectrum detection based on Maximum Likelihood Ratio for cognitive VANET. In *International Conference on Automatic Control and Artificial Intelligence (ACAI)*, pages 726–729, March 2012.

[XJLW13] Xu Xiaorong, Bao Jianrong, Yi Luo, and Huaxia Wang. Cooperative Wideband Spectrum Detection Based on Maximum Likelihood Ratio for CR Enhanced VANET. *Journal of Communications*, 8(12):814–821, Dec 2013.

[XZR09] Yan Xin, Honghai Zhang, and Sampath Rangarajan. Ssct: A simple sequential spectrum sensing scheme for cognitive radio. In *Global Telecommunications Conference, 2009. GLOBECOM 2009. IEEE*, pages 1–6. IEEE, 2009.

[YA09] T. Yucek and H. Arslan. A survey of spectrum sensing algorithms for cognitive radio applications. *Communications Surveys Tutorials, IEEE*, 11(1):116–130, First Quarter 2009.

[YHM+17] Ibrar Yaqoob, Ibrahim Abaker Targio Hashem, Yasir Mehmood, Abdullah Gani, Salimah Mokhtar, and Sghaier Guizani. Enabling communication technologies for smart cities. *IEEE Communications Magazine*, 55(1):112–120, 2017.

[YLC19] Shuai Yuan, Lei Li, and Chunxiao Chigan. On mmd-based secure fusion strategy for robust cooperative spectrum sensing. *IEEE Transactions on Cognitive Communications and Networking*, 2019.

[YWMF17] Tianyu Yuan, Ying Wang, Zhonyu Miao, and Zixuan Fei. Study on soft combination for spectrum sensing in cognitive vehicular ad hoc networks. In *Computer and Communications (ICCC), 2017 3rd IEEE International Conference on*, pages 701–706. IEEE, 2017.

[YYO12] Ming Yan, Yi Yang, and Stanley Osher. Robust 1-bit compressive sensing using adaptive outlier pursuit. *IEEE Transactions on Signal Processing*, 60(7):3868–3875, 2012.

[YYO13] Ming Yan, Yi Yang, and Stanley Osher. Exact low-rank matrix completion from sparsely corrupted entries via adaptive outlier pursuit. *Journal of Scientific Computing*, 56(3):433–449, 2013.

[ZFL+16] Haojin Zhu, Chenliaohui Fang, Yao Liu, Cailian Chen, Mengyuan Li, and Xuemin Sherman Shen. You can jam but you cannot hide: Defending against jamming attacks for geo-location database driven spectrum sharing. *IEEE Journal on Selected Areas in Communications*, 34(10):2723–2737, 2016.

[ZGFL16] Siting Zhu, Caili Guo, Chunyan Feng, and Xia Liu. Performance analysis of cooperative spectrum sensing in cognitive vehicular networks with dense traffic. In *Vehicular Technology Conference (VTC Spring), 2016 IEEE 83rd*, pages 1–6. IEEE, 2016.

[ZGL+15] W. Zhang, Y. Guo, H. Liu, Y. Chen, Z. Wang, and J. Mitola III. Distributed consensus-based weight design for cooperative spectrum sensing. *IEEE Transactions on Parallel and Distributed Systems*, 26(1):54–64, Jan 2015.

[ZL07] Yonghong Zeng and Ying-Chang Liang. Maximum-minimum eigenvalue detection for cognitive radio. In *Personal, Indoor and Mobile Radio Communications, 2007. PIMRC 2007. IEEE 18th International Symposium on*, pages 1–5. IEEE, 2007.

[ZLLZ10] R. Zhang, T. J. Lim, Y. Liang, and Y. Zeng. Multi-antenna based spectrum sensing for cognitive radios: A glrt approach. *IEEE Transactions on Communications*, 58(1):84–88, January 2010.

[ZPT14] Kun Zeng, QiHang Peng, and YouXi Tang. Mitigating spectrum sensing data falsification attacks in hard-decision combining cooperative spectrum sensing. *Science China Information Sciences*, 57(4):1–9, 2014.

[ZTSC07] Qing Zhao, Lang Tong, Ananthram Swami, and Yunxia Chen. Decentralized cognitive mac for opportunistic spectrum access in ad hoc networks: A pomdp framework. *IEEE Journal on selected areas in communications*, 25(3), 2007.

[ZXYY19] Yali Zeng, Li Xu, Xu Yang, and Xun Yi. An efficient privacy-preserving protocol for database-driven cognitive radio networks. *Ad Hoc Networks*, 90:101739, 2019. Recent advances on security and privacy in Intelligent Transportation Systems.

[ZXZY19] Rui Zhu, Li Xu, Yali Zeng, and Xun Yi. Lightweight privacy preservation for securing large-scale database-driven cognitive radio networks with location verification. *Security and Communication Networks*, 2019, 2019.

[ZZZZ13] Rui Zhang, Jinxue Zhang, Yanchao Zhang, and Chi Zhang. Secure crowdsourcing-based cooperative spectrum sensing. In *2013 Proceedings IEEE INFOCOM*, pages 2526–2534. IEEE, 2013.

Appendix A

Confidence Intervals

Simulated variables such as the overall probability of detection, Q_d, the overall probability of false alarm, Q_{fa}, as well as the average reporting time, $\overline{N}_{\mathcal{H}_j}$ are measured by averaging n successive runs or sessions. Each session, or run, use a random dispersion of SUs and the PU around the FC. To average the fading over SUs-FC and PU-SUs links, and to ensure the counters, $\{c_k\}_{k=1}^{K}$, follow the uniform distribution, each session is simulated for m simulation points. Therefore, after each session we obtain a sample mean for Q_d, Q_{fa}, and $\overline{N}_{\mathcal{H}_j}$, resulting in a distribution of means for all sessions. All n sessions are then averaged to obtain an overall sample mean for Q_d, Q_{fa}, and $\overline{N}_{\mathcal{H}_j}$. In this thesis, each graph or curve point represents 100×10^6 simulation points, divided into 10^4 sessions, i.e. $n = 10^4$, with 10^4 simulation points each, i.e. $m = 10^4$.

As we specified the number of simulation points beforehand, we need to verify that the resulting precision is satisfactory. Let $\bar{X}$ be the mean for a distribution of means, i.e. $\bar{X}$ can be Q_d, Q_{fa}, or $\overline{N}_{\mathcal{H}_j}$. The sample distribution mean $\bar{X}$ is obtained according to

$$\text{The mean } \bar{X} = \frac{1}{n} \sum_{i=1}^{n} X_i, \tag{A.1}$$

where X_i is the mean of session i. We can then use the Standard Error of the Mean (SEM) to make confidence intervals of the unknown population mean of $\bar{X}$. SEM is the standard deviation of the sampling distribution of the mean. SEM is an indication of the sample means' dispersion around the population mean and is given by

$$\sigma_{\bar{X}} = \frac{\sigma}{\sqrt{n}}, \tag{A.2}$$

where n is the number of observations (sessions) as mentioned above, and σ is the standard deviation of the sampling distribution given by

$$\sigma = \sqrt{\frac{1}{n-1}\sum_{i=1}^{n}(X_i - \bar{X})^2}. \tag{A.3}$$

Intuitively, sample means cluster more closely around the sampling distribution mean as the sample size, n, increases. The lower and upper limits of the β% confidence interval can then be calculated as follows

$$\begin{aligned} \text{Lower Limit: } L(X) &= \bar{X} - (\sigma_{\bar{X}} \times t[\beta\%; n-1]) \\ \text{Upper Limit: } U(X) &= \bar{X} + (\sigma_{\bar{X}} \times t[\beta\%; n-1]), \end{aligned} \tag{A.4}$$

where $t[\beta\%; n-1]$ is a value obtained from t-distribution tables. For example, let $\beta = 95$, then $t[\beta\%; n-1]$ for the 95% confidence interval and $n = 10^4$ would be 1.96. The β % confidence interval is a range $[L(X), U(X)]$ where we can be β % certain contains the true mean of the population, i.e. $E[X]$. If the number of samples is sufficient then the confidence interval is quite narrow and then we can be sure that our precision is satisfactory.